

OCEANIC DEEP-WATER CIRCULATION AND CLIMATE
DURING THE LATE NEOGENE

By

KATHRYN VENZ CURTIS

A DISSERTATION PRESENTED TO THE GRADUATE SCHOOL
OF THE UNIVERSITY OF FLORIDA IN PARTIAL FULFILLMENT
OF THE REQUIREMENTS FOR THE DEGREE OF
DOCTOR OF PHILOSOPHY

UNIVERSITY OF FLORIDA

2004

Copyright 2004

by

KATHRYN VENZ CURTIS

ACKNOWLEDGMENTS

I would like to thank Dr. David Hodell as my primary advisor for all his time and effort toward the completion of this dissertation. I also thank Dr. Ellen Martin and Dr. Jim Channell for their continued support in my effort to bring this dissertation to completion. I am also grateful to Dr. Paul Ciesielski and Dr. Joann Mossa for serving on my committee.

Friends and fellow students Natalia Hoyos, Jaime Escobar, Sarah Newell, Ellie Harrison-Buck, and David Buck have my gratitude for their generous friendship and time spent with my children. They made a huge difference in allowing me to devote large blocks of worry-free time to my dissertation. I am also grateful to Sharon Kanfoush for blazing the trail and to Mike Rosenmeier for camaraderie and friendship.

The unwavering support of my family has been crucial in the completion of this project. Joy and Bruce Curtis contributed much in emotional and financial support; they gently nudged me along with the occasional pep-talk, when required, and they kept me focused on completing my research. I owe my parents, Nancy and Don Venz, a huge debt of gratitude for their belief that I could do it, for their emotional and financial support, and for uncountable hours spent with their grandchildren so I could be free to work on this dissertation. I thank Sabrina, Julia, and Emma Curtis; it was, in part, because of them that I persevered. I reserve a special thank you to Jason Curtis for his unshakeable belief it could be done and his wholehearted support. Without Jason, it could not have been done.

TABLE OF CONTENTS

	<u>Page</u>
ACKNOWLEDGMENTS	iii
LIST OF TABLES	vi
LIST OF FIGURES	vii
CHAPTER	
1 INTRODUCTION	1
Statement of Objectives	1
The North Atlantic	5
The Southern Ocean	7
Late Neogene Evolution of Deep-Water Circulation	8
2. ODP SITE 982, NORTHEAST ATLANTIC	11
Background and Objectives	11
Materials and Methods	14
Sediments	14
Stable Isotopes	14
Sedimentology	15
Stratigraphy	16
Results	16
Oxygen Isotopes	16
Carbon Isotopes	17
Calcium Carbonate	19
Ice Rafted Debris	19
Discussion	20
Terminations	20
Northeast Atlantic Circulation During Terminations	23
Mechanism to Explain Long-Term Changes in IRD and Benthic $\delta^{13}\text{C}$	31
Conclusions	35
3. ODP SITE 1090, SOUTH ATLANTIC	37
Introduction	37

Materials and Methods.....	39
Hydrography.....	39
Sediments.....	43
Stable Isotopic Analyses.....	44
Stratigraphy.....	46
Results.....	46
Stable Isotopes – <i>Globigerina bulloides</i>	46
Stable Isotopes – <i>Cibicidoides wuellerstorfi</i>	50
Carbon Isotopic Gradients.....	53
Southern Ocean - Pacific $\delta^{13}\text{C}$ gradients.....	53
Atlantic basin $\delta^{13}\text{C}$ gradients.....	53
Discussion.....	58
Inter-Site Comparison of Benthic Carbon Isotopic Records.....	58
Late Pliocene / Early Pleistocene.....	61
Early Pleistocene Change in the Southern Ocean.....	64
The Mid-Pleistocene Transition.....	68
Ramifications of Using 1090 $\delta^{13}\text{C}$ to Compute %NCW.....	72
Conclusions.....	75
The Late Pliocene.....	75
The Early Pleistocene.....	75
The Mid-Pleistocene Transition.....	76
The Late Pleistocene.....	77
4. DEEP-WATER CIRCULATION CHANGES DURING THE LATE NEOGENE INFERRED FROM BENTHIC FORAMINIFER $\delta^{13}\text{C}$ IN THE SUBANTARCTIC SOUTH ATLANTIC.....	78
Introduction.....	78
Materials and Methods.....	79
Data Sources.....	79
Stratigraphy and Time Scales.....	80
Results.....	82
Carbon Isotopic Records.....	82
Oxygen Isotopic Records.....	91
Correlation Between Benthic Carbon and Oxygen Isotopic Records.....	92
Discussion.....	92
Deep-Water Circulation During the Late Miocene to Middle Pliocene.....	96
Deep-Water Formation During the Middle Pliocene and Pleistocene.....	100
Conclusions.....	104
5. SUMMARY.....	106
LIST OF REFERENCES.....	111
BIOGRAPHICAL SKETCH.....	124

LIST OF TABLES

<u>Table</u>	<u>page</u>
3-1. Core locations.....	41
3-2. Water mass properties.....	41
3-3. Age-Depth points for sites 1090 and 982.....	48
4-1. Sources of data used in this study.....	83
4-2. Sampling intervals for sites 982, 607, 704, 1090, 1092, and 849.....	83
4-3. Age-Depth points for sites 982 (3-5 Ma) and 704 (5-9 Ma).....	84
4-4. Results of statistical analysis of benthic carbon and oxygen isotopic data from sites 704 and 1090 during different deep-water circulation modes.....	94

3-12. Schematic representation of glacial-to-interglacial changes in deep-water mass boundaries in the North Atlantic	63
3-13. Calculation of percent NCW at site 607	74
4-1. (A) Location map.....	81
4-2. (A) Comparison of benthic carbon isotopic records.....	85
4-3. (A) Comparison of benthic oxygen isotopic records.....	86
4-4. Carbon isotopic records shown in 2A for the time periods (A) 0 to 2.0 Ma; (B) 2.0 to 5.5 Ma; and (C) 5.5 to 9.0 Ma.	87
4-5. Oxygen isotopic records shown in 2A for the time periods (A) 0 to 2.0 Ma; (B) 2.0 to 5.5 Ma; and (C) 5.5 to 9.0 Ma.....	88
4-6. $\delta^{13}\text{C}$ gradient calculated by resampling the data from sites 982, 1090/704, and 849.....	89
4-7. Scatter plots of the benthic carbon and oxygen isotopic data.....	93

Abstract of Dissertation Presented to the Graduate School
of the University of Florida in Partial Fulfillment of the
Requirements for the Degree of Doctor of Philosophy

OCEANIC DEEP-WATER CIRCULATION AND CLIMATE
DURING THE LATE NEOGENE

By

Kathryn Venz Curtis

August 2004

Chair: David A. Hodell

Major Department: Geological Sciences

Deep-water circulation was reconstructed for the late Neogene by comparing carbon isotopic records of benthic foraminifera from the North Atlantic (NA), Southern Ocean (SO), and deep Pacific basins. The history of NA intermediate water was studied using $\delta^{13}\text{C}$ at Ocean Drilling Program (ODP) site 982. Production of Glacial North Atlantic Intermediate Water (GNAIW) was enhanced during glacial periods of the late Pleistocene whereas production of lower North Atlantic Deep Water (NADW) was much reduced. During terminations, production of GNAIW ceased briefly until upper-NADW production resumed under full interglacial conditions. The magnitude of benthic $\delta^{13}\text{C}$ minima, ice-rafted debris maxima at site 982, and glacial suppression of NADW may be related to the spatial and seasonal extent of sea ice in the Nordic Seas.

The history of deep-water circulation in the Atlantic sector of the SO was examined using a $\delta^{13}\text{C}$ record from ODP site 1090 in the South Atlantic (SA). At 1.55 Ma, glacial $\delta^{13}\text{C}$ values in the SA sector of the SO became significantly lower than those

in the deep Pacific, establishing a pattern that persisted throughout the late Pleistocene. Lower $\delta^{13}\text{C}$ values in the SO may have resulted from expansion of sea ice and reduced ventilation of deep-water during glacial periods. Accompanying this change in SO deep-water circulation was enhanced interhemispheric coupling between the NA and SA. Calculation of %NADW using site 1090 indicates glacial reduction of NADW was less than suggested previously.

Carbon isotopic records from sites 982, 1090, and 849 (deep Pacific) were used to estimate inter-ocean $\delta^{13}\text{C}$ gradients for the last 9 myr. Through the late Neogene, benthic $\delta^{13}\text{C}$ (and inferred deep-water ventilation) of SO deep-water has decreased as sea ice cover and stratification of Antarctic surface waters increased. This reduced upwelling of deep-water to the surface, limited equilibration of surface water with the atmosphere, and altered deep-water formation. Changes in deep-water ventilation occurred in steps at 6.6, 2.7, and 1.5 Ma that likely represented threshold events resulting from gradual cooling of Antarctic surface waters. Each decrease in ventilation acted as positive feedback to ongoing climate cooling by increasing deep-ocean CO_2 content and lowering atmospheric pCO_2 .

CHAPTER 1 INTRODUCTION

Statement of Objectives

Vertical ocean circulation is driven by density differences among water masses that exist due to temperature and salinity variations within the ocean and is termed "thermohaline" circulation. Changes in the vertical temperature and salinity gradients in the polar ocean surface waters control the rate of deep-water formation and its chemistry. Since the middle Miocene, variation in the relative fluxes of the two primary deep-water masses, one formed in the high-latitude North Atlantic and another in the Weddell Sea, have had climatic consequences on a global scale through changes in oceanic heat transport and atmospheric greenhouse gases [Weyl, 1968; Raymo et al., 1990b; Crowley, 1992; Sigman et al., 2004; others].

The flow paths of deep-water and the mixing among different deep-water masses can be traced by examining the patterns of chemical distributions in the deep sea. One such tracer is the carbon isotopic composition of dissolved inorganic carbon (DIC) [Broecker and Peng, 1982; Kroopnick, 1985; Duplessy et al., 1988]. Each of the deep-water masses of the world's oceans has a characteristic carbon isotopic signature that is the result of the carbon isotopic value of its source waters, the length of time the deep-water has been isolated from the surface, the rate of organic matter accumulation, and the degree of mixing with other water masses. Kroopnick [1985] summarized the distribution of oceanic $\delta^{13}\text{C}$ data collected during the GEOSECS program. In addition to

changes deep water circulation, there are several processes that influence the $\delta^{13}\text{C}$ of sea water including global and regional changes in surface water productivity, gas exchange between the surface ocean and the atmosphere, and global exchanges between oceanic and terrestrial carbon reservoirs [Kroopnick, 1985].

Changes in surface water productivity affect the $\delta^{13}\text{C}$ of the ocean by changing the surface to deep carbon isotopic gradient. This gradient exists because phytoplankton preferentially uptake ^{12}C during photosynthesis. The removal of ^{12}C from the surface water in the photic zone leaves the DIC enriched in ^{13}C . The ^{13}C -depleted organic matter settles into deeper water where it is oxidized and released, thereby reducing the $\delta^{13}\text{C}$ of deep water relative to surface water. This results in $\delta^{13}\text{C}$ values of planktic foraminifers that are, on average, 1 ‰ heavier than the $\delta^{13}\text{C}$ of benthic foraminifera [Kroopnick, 1985]. Because the carbon isotopic gradient is produced by nutrient dependent biological productivity, abundant nutrients result in high productivity and increases the surface-to-deep carbon isotopic gradient. When nutrients are scarce, productivity and the carbon isotope gradient both decrease.

Gas exchange with the atmosphere is another important mechanism affecting the ^{13}C of ocean surface waters. If there is sufficient time for isotopic equilibration to occur, air-sea exchange of CO_2 leaves surface waters enriched in ^{13}C [Broecker and Peng, 1982]. Because deep water is isolated from the atmosphere after being formed, the ^{13}C of deep water is an indicator of the age of the water mass. As the deep water ages, organic matter is oxidized, which releases ^{12}C incorporated during photosynthesis and decreases the $\delta^{13}\text{C}$ of DIC along its flow path. Young water is O_2 -rich, CO_2 and

nutrient-poor, and has high $\delta^{13}\text{C}$ values, whereas old water is O_2 -poor, CO_2 and nutrient-rich, and has low $\delta^{13}\text{C}$ values.

Mean ocean $\delta^{13}\text{C}$ is influenced by exchanges of carbon between terrestrial and marine reservoirs. On glacial-to-interglacial timescales this involves the transfer of terrestrial carbon and carbon sequestered on continental shelves to marine reservoirs during times of sea level lowering and continental aridity (glacial periods) [Shackleton and Psias, 1985]. On longer timescales (millions of years), changes in tectonic uplift, continental weathering, and the isotopic composition of rivers also play a role [Raymo, 1994]. However, all of these processes affect all oceanic $\delta^{13}\text{C}$ records equally and should not influence the carbon isotopic gradients between ocean basins.

There are several assumptions implicit in using benthic $\delta^{13}\text{C}$ gradients to monitor changes in deep water circulation: 1) the benthic foraminiferal species chosen to analyze for $\delta^{13}\text{C}$ must accurately record the $\delta^{13}\text{C}$ of DIC of bottom water; 2) the $\delta^{13}\text{C}$ of benthic foraminiferal calcite must be precipitated in equilibrium with DIC or at a known constant offset from equilibrium that is not affected by other processes (e.g., carbonate ion concentration); 3) variations in $\delta^{13}\text{C}$ must reflect changes in the mixing ratio of water masses and not other factors such as changes in thermodynamic equilibrium in source areas of deep water formation; and 4) the cores chosen to represent the end member water masses must be suitably located to monitor end member $\delta^{13}\text{C}$ compositions. Paleocirculation studies using benthic $\delta^{13}\text{C}$ assume that the carbon isotopic composition of foraminifera reflect the isotopic composition of the DIC of the water in which the calcite is precipitated. However, most foraminifera display a species dependent non-equilibrium carbon isotopic fractionation, or "vital effect". Despite this isotopic

disequilibrium, a number of foraminiferal species have $\delta^{13}\text{C}$ values that are close to the $\delta^{13}\text{C}$ of total dissolved carbon in the ocean (or are offset by a constant value) [Williams et al., 1977]. Two commonly used benthic foraminiferal species that consistently record the $\delta^{13}\text{C}_{\text{DIC}}$ with no offset are *Cibicidoides wuellerstorfi* and *Cibicidoides kullenbergi* [Graham et al., 1981].

For the most part, variation in benthic foraminiferal $\delta^{13}\text{C}$ closely tracks variation in deep water nutrient concentrations in both glacial and interglacial reconstructions of deep-water circulation [Curry et al., 1988, Duplessy et al., 1988]. The exception is in the South Atlantic sector of the Southern Ocean where benthic $\delta^{13}\text{C}$ and other nutrient proxies such as Cd/Ca and Ba/Ca yield contradictory results [Oppo and Fairbanks, 1987; Oppo and Rosenthal, 1994; Lea, 1995]. Glacial $\delta^{13}\text{C}$ values in the South Atlantic were found to be lower than the deep Pacific, which led to the suggestion that benthic foraminifera may not be accurately recording $\delta^{13}\text{C}$ values of deep-waters [Mackensen et al., 1993]. Benthic foraminiferal Ba/Ca and Cd/Ca data do not support the high nutrient levels suggested by $\delta^{13}\text{C}$ values in the Southern Ocean during glacial intervals [Lea, 1995; Oppo and Rosenthal, 1994]. The accuracy of these tracers has been questioned and tested [Mackensen et al., 1993; McCorkle et al., 1995; Mackensen et al., 2001]; neither can be completely discounted. Both nutrient proxies and $\delta^{13}\text{C}$ may be reliable if $\delta^{13}\text{C}$ and nutrients were decoupled in the Southern Ocean through changes in deep-water production and ventilation that may be unique to the Atlantic sector [Broecker, 1993].

Today, North Atlantic Deep Water (NADW) has high $\delta^{13}\text{C}$ values ($\sim 1\%$) because it contains a large amount of upper ocean water that has become enriched in ^{13}C as a result of biologic uptake of ^{12}C during primary productivity [Broecker and Peng, 1982]. Within

the Atlantic, where the residence time of deep-water is short (~200 years; Broecker [1991]), the observed southward decrease of $\delta^{13}\text{C}$ is primarily caused by mixing of NADW with low $\delta^{13}\text{C}$ Southern Ocean water. Continuous oxidation of ^{13}C -poor organic matter falling from surface waters gradually reduces the $\delta^{13}\text{C}$ of deep-water along its flow path as it moves out of the Atlantic [Kroopnick, 1985]. Pacific Deep Water (PDW) is furthest from the NADW source region and has the lowest $\delta^{13}\text{C}$ values (0 to -0.5‰), whereas Circumpolar Deep Water (CPDW) has intermediate $\delta^{13}\text{C}$ values (~-0.4‰) as a result of mixing of NADW and recirculated Pacific water in the Southern Ocean [Kroopnick, 1985; Oppo and Fairbanks, 1987]. Modern deep-water circulation has been described as an oceanic "conveyor" where thermohaline circulation is driven by formation of NADW (with high- $\delta^{13}\text{C}$). NADW mixes with southern source waters in the Southern Ocean (intermediate- $\delta^{13}\text{C}$), and then continues flowing towards the North Pacific (low- $\delta^{13}\text{C}$) [Broecker, 1991]. In the Pacific, deep-water eventually mixes upward into intermediate depths with low $\delta^{13}\text{C}$ values. Return flow into the Atlantic occurs in the near surface either via the Drake Passage (cold water route) or the Agulhas retroflexion (warm water route) [Gordon, 1996].

The North Atlantic

Carbon isotopic records from the deep North Atlantic have been frequently used in studies of deep-water circulation [e.g., Raymo et al., 1990b; and many others]. Studies have shown that lower NADW production (water at greater than 2km depth) was much reduced or absent during glacial periods of the Pliocene-Pleistocene, whereas upper NADW (water above 2km depth) was enhanced during glaciations relative to interglacial stages [Boyle and Keigwin, 1987; Duplessy et al., 1988; deMenocal et al., 1992; Oppo et

al., 1995]. This pattern has been inferred from $\delta^{13}\text{C}$ records from many sites in the North Atlantic currently bathed by lower NADW. In contrast, intermediate depth sites bathed by upper NADW (water between 1000-2000m depth) show lower $\delta^{13}\text{C}$ values during interglacials relative to glacial periods [Oppo and Fairbanks, 1987; Oppo and Lehman, 1993; Bertram et al., 1995]. The fact that deep-water $\delta^{13}\text{C}$ values decreased at the same time as intermediate-water $\delta^{13}\text{C}$ values increased suggests a redistribution of nutrients in the glacial ocean from intermediate to deep water [Oppo and Fairbanks, 1987; Oppo and Lehman, 1993; Bertram et al., 1995]. This is consistent with reduced production of NADW at the same time as increased formation of a nutrient-depleted water mass at intermediate depths (upper-NADW or Glacial North Atlantic Intermediate Water, GNAIW). Therefore, $\delta^{13}\text{C}$ records from the deep North Atlantic may not reflect an end member composition because $\delta^{13}\text{C}$ values during glacial intervals are influenced by low- $\delta^{13}\text{C}$ water of southern origin. Records from intermediate-depths in the North Atlantic may serve as better monitors of deep water formed in the high-latitude North Atlantic during both glacial and interglacial periods.

Most Atlantic intermediate-depth cores are relatively short and span the last few glacial cycles only [Zahn et al., 1987; Oppo and Fairbanks, 1987]. Older records are limited to DSDP Site 502 in the Caribbean, which has a sill depth of 1600 to 1800 m and intersects intermediate waters [Oppo and Fairbanks, 1987; deMenocal et al., 1992; Oppo et al., 1995]. Until now, a long continuous record from an intermediate-depth site from the high-latitude North Atlantic has been lacking. Here I present a 3-Ma record from ODP Site 982, drilled in 1145 m of water on the Rockall Plateau during Leg 162, to

evaluate changes in surface and intermediate water mass circulation of the high-latitude North Atlantic

The Southern Ocean

Today, the Southern Ocean is considered to be an oceanic "junction box" where deep-water from the world's oceans (North Atlantic, Pacific, and Indian) mix to form CPDW [Broecker and Peng, 1982]. The traditional view has been that variation in Southern Ocean $\delta^{13}\text{C}$ is the result of changes in the proportion of NADW and PDW present in CPDW. Carbon isotopic values in the core of NADW in the North Atlantic are $\sim 1.0\text{‰}$ and $\delta^{13}\text{C}$ value of PDW range from 0 to -0.5‰ [Kroopnick, 1985]. Today, CPDW is very homogeneous with a $\delta^{13}\text{C}$ of $\sim 0.4\text{‰}$, reflecting an approximately equal proportion of NADW and PDW [Kroopnick, 1985]. Reconstructions of the late Pleistocene history of CPDW from South Atlantic cores suggest that the distribution of $\delta^{13}\text{C}$ was different than today. Carbon isotopic values during some glacial intervals of the late Pleistocene were lower in the Southern Ocean than values in the deep Pacific [Oppo and Fairbanks, 1987; Oppo et al., 1990; Raymo et al., 1990b; Hodell, 1993]. In this case, a two end member mixing model does not apply and the $\delta^{13}\text{C}$ of CPDW cannot be used to infer the relative proportion of NADW and PDW.

Recent studies have proposed a number of mechanisms that could decouple $\delta^{13}\text{C}$ and nutrients (i.e., change $\delta^{13}\text{C}$ of DIC without affecting nutrient levels) in the Southern Ocean. Air sea exchange of CO_2 between surface waters and the atmosphere can alter $\delta^{13}\text{C}$ values without changing nutrient concentrations. This process is important in the Southern Ocean today where only partial equilibration occurs between the ocean surface and atmosphere [Charles and Fairbanks, 1990]. Factors that limit the contact between

Antarctic surface waters and the atmosphere include changes in vertical water structure (stratification), and changes in sea ice extent [Toggweiler, 1999; Stephens and Keeling, 2000; Sigman and Boyle, 2000; Sigman et al., 2004]. Because Antarctic surface and near-surface waters are the source waters for CPDW formation, any changes in nutrient levels and CO₂ concentration will be transmitted to the deep ocean. Another mechanism capable of decoupling $\delta^{13}\text{C}$ and nutrients is the development of a vertical nutrient divide (decreased mixing between deep and intermediate depth water masses) during glacial periods [Toggweiler, 1999].

A new appreciation of the potential role of the Southern Ocean in deep-water ventilation has led to renewed efforts in developing improved records of deep-water circulation history from locations within the Southern Ocean. The available records from the Southern Ocean are inadequate for reconstructing long-term deep-water circulation history because they are either not ideally located or too short, have low sedimentation rates or coring gaps, or have poor age control. ODP site 1090 has many desirable characteristics for developing a long benthic $\delta^{13}\text{C}$ record for inferring past changes in CPDW variability. Here I used site 1090 to reconstruct the deep circulation history of the South Atlantic sector of the Southern Ocean for the past 3 myr.

Late Neogene Evolution of Deep-Water Circulation

Previous reconstructions of deep-water circulation have relied upon less-than-ideal carbon isotopic end member records from the deep North Atlantic and Pacific, often ignoring the Southern Ocean as a potential source of variability in deep-water circulation. The isotopic records from site 982 and site 1090 represent improved end member records that reliably monitor a high- $\delta^{13}\text{C}$ water mass in the North Atlantic and provide a history of CPDW variability from the Southern Ocean, respectively. These records were used in

conjunction with existing records from the same sites or nearby sites to create North Atlantic and Southern Ocean composites that span the interval from 0 to 9 Ma. However, in order to fully understand oceanic deep-water circulation, any changes that occur in the carbon isotopic gradient between the North Atlantic and the Southern Ocean must be compared to the deep Pacific. I generated a 4 myr record from site 849 to extend the existing 5 myr record of Mix et al. [1995] back to ~9 Ma. Based on the comparison carbon isotopic gradients between the North Atlantic, Southern Ocean, and the deep Pacific, I inferred changes in deep-water circulation patterns for the past 9 myr. The objective was to understand how deep-water circulation changed during the late Neogene including processes of deep-water formation on a regional scale, changes in whole ocean deep-water ventilation, and ultimately how these changes were related to the evolution of late Neogene climate.

This dissertation is presented in publishable paper format. Chapter 2 was published as "A 1.0 myr record of Glacial North Atlantic Intermediate Water variability from ODP site 982 in the northeast North Atlantic" in *Paleoceanography*, volume 14, pages 42-52. I was the primary author on this paper and generated the oxygen and carbon isotopic data and the percent carbonate data presented for site 982. The IRD (ice rafted debris) data was produced by Cathy Stanton and Detlef Warnke at California State University, Hayward. Chapter 3 was published as "New evidence for changes in Plio-Pleistocene deep water circulation from Southern Ocean ODP Leg 177 site 1090" in *Palaeogeography, Palaeoclimatology, Palaeoecology*, volume 182, pages 197-220. I was the primary author on this paper and generated the isotopic data presented for site 1090 from 0.6 to 2.8 Ma, and the isotopic data for site 982 from 1 to 3 Ma. Chapter 4 is titled "Deep-water circulation changes during the late Neogene inferred from benthic

foraminifer $\delta^{13}\text{C}$ in the subantarctic South Atlantic" and will be submitted to *Geochemistry, Geophysics, Geosystems*, an electronic journal for the earth sciences. I was the primary author and analyzed the data for site 849 from 5 to 9 Ma. Chapter 5 is a brief conclusion that summarizes the principal findings of the research presented in chapters 2 through 4.

CHAPTER 2
ODP SITE 982, NORTHEAST ATLANTIC

Background and Objectives

Large changes in deep and intermediate water circulation in the North Atlantic have occurred during glacial-to-interglacial cycles of the late Pleistocene. Production of lower North Atlantic Deep Water (NADW) was much reduced during the last glaciation, whereas production of Glacial North Atlantic Intermediate Water (GNAIW) was enhanced [Boyle and Keigwin, 1987; Oppo and Fairbanks, 1987; Duplessy et al., 1988; deMenocal et al., 1992; Oppo and Lehman, 1993]. The history of glacial reductions in lower NADW had an important effect on climate in the North Atlantic and Europe and may have impacted climate globally by altering deep-water circulation patterns [Broecker, 1991]. The switch from deep to intermediate water mass production during glaciations may also have influenced atmospheric CO₂ through the redistribution of nutrients and attendant changes in carbonate alkalinity [Boyle, 1988]. Knowledge of past variability in intermediate and deep-water circulation in the North Atlantic is important, therefore, for understanding glacial-to-interglacial changes in climate during the late Pleistocene.

In contrast to the history of deep-water circulation that is well known for the Plio-Pleistocene [Raymo et al., 1992], variations in the production of nutrient-depleted GNAIW are less well understood and have been inferred mainly from Deep Sea Drilling Project (DSDP) site 502. This site is located in the Caribbean Sea, which has a sill depth between 1600 and 1800 m and is filled by intermediate-depth waters from the North

Atlantic [deMenocal et al., 1992; Oppo et al., 1995]. Direct evidence of changes in GNAIW production from intermediate-depth piston cores in the North Atlantic extends only to MIS 6 [Oppo and Fairbanks, 1987; Zahn et al., 1987; Oppo and Lehman, 1993; Oppo et al., 1997]. Until now, a long continuous record from an intermediate-depth site in the North Atlantic has not been available to document the history of GNAIW near its source. Here I present isotopic and sedimentologic data from Ocean Drilling Program (ODP) site 982 (1145 m) on the Rockall Plateau to reconstruct changes in intermediate water circulation in the North Atlantic for the last 1.0 myr.

Site 982 ($57^{\circ}30.8'N$, $15^{\circ}52.5'W$) was the shallowest site drilled during ODP Leg 162 and is ideally situated to monitor the long-term history of intermediate water masses in the northeast Atlantic. Several studies have demonstrated the potential of the Rockall Plateau for producing high-resolution records of GNAIW variability, but previous work on piston cores has been limited to the last glacial cycle [Oppo and Lehman, 1993; Bertram et al., 1995]. Although this study focuses on the last million years at site 982, the potential exists for extending the record as far back as the Miocene [Jansen et al., 1996].

The thermohaline circulation of the modern ocean depends upon the formation of NADW in the northern North Atlantic by atmospheric cooling of warm, salty surface waters in the Nordic Seas and winter cooling of cold surface waters in the Labrador Sea [Broecker, 1991]. NADW may be divided into two main components: upper NADW (shallower than 2000 m) defined by a silicate minimum and salinity maximum; and lower NADW (deeper than 2000 m) composed of a deeper highly oxygenated core [Kawase and Sarmiento, 1986]. Lower NADW is composed of a mixture of the dense overflows

from the Nordic Seas and Labrador Sea Water (LSW), whereas upper NADW is a combination of LSW and other intermediate-depth water masses in the North Atlantic.

Intermediate depths in the North Atlantic today contain three principal water masses between ~800 and ~2000 m: Antarctic Intermediate Water (AAIW), Mediterranean Overflow Water (MOW), and LSW [Kawase and Sarmiento, 1986]. In the northeast Atlantic, near the Rockall Plateau and below the ventilated thermocline, AAIW occupies levels shallower than 800 m. MOW lies between ~800 and ~1000 m. LSW, the main constituent of upper NADW, occupies depths between ~1000 and ~1600 m [Kawase and Sarmiento, 1986]. Upper NADW consists of a mixture of LSW, MOW, and overflows from the Nordic Seas and is the densest of the intermediate water masses, occupying depths between ~1500 and ~1600 m in the interior ocean [Kawase and Sarmiento, 1986]. The primary water mass influencing site 982 today is LSW admixed with MOW.

Glacial-to-interglacial changes in benthic foraminiferal carbon isotopic and Cd/Ca signals of the intermediate North Atlantic have been used to infer changes in intermediate and deep circulation patterns [Boyle and Keigwin, 1987; Curry et al., 1988; Duplessy et al., 1988; deMenocal et al., 1992; Oppo and Lehman, 1993]. This evidence indicates that convection in the North Atlantic switched from a deep (NADW) mode in the Nordic Seas to an intermediate (GNAIW) mode in the northern North Atlantic during the last glacial cycle [Boyle and Keigwin, 1987; Oppo and Fairbanks, 1987; Bertram et al., 1995]. As the source area of convection moved south during the last glaciation, the lowered temperature of surface waters reduced evaporation rates and resulted in enhanced buoyancy of surface water north of the glacial polar front [Duplessy et al., 1988]. The density of the water mass formed was insufficient to sink into the deep North Atlantic

and, instead, intermediate water (GNAIW) was produced that bathed water depths between 1000 and 2000 m.

Materials and Methods

Sediments

Site 982 was drilled using the advanced piston coring (APC) system with four offset holes (A-D) to ensure complete recovery of the section. A spliced composite section was constructed using continuous multi sensor logging (density, magnetic susceptibility, p wave velocity) and spectral color reflectance data [Jansen et al., 1996]. All major chrons (Brunhes, Matuyama, Gauss) and subchrons (Jaramillo, Olduvai, Reunion) have been identified in the paleomagnetic inclination data [Channell and Lehman, 1999]. No hiatuses were detected at the resolution of the paleomagnetic and nannofossil stratigraphy, suggesting that the record is near complete [Channell and Lehman, 1999]. Site 982 was sampled at 5 cm intervals, resulting in a sampling frequency of one sample per 2000 years for the past 1.0 Myr.

Sedimentation rates in the Brunhes averaged 2.6 cm/1000 years with slightly lower sedimentation rates during glacial as compared to interglacial intervals. For example, rates during the Holocene (0-8 Ka) were ~5.9 cm/1000 years, compared to 2.75 cm/1000 years during the last glacial. A similar relationship holds for MIS 5e (3.21 cm/1000 years) and 6 (1.32 cm/1000 years). Manighetti and McCave [1995] attributed similar sedimentation rate changes in nearby piston cores to increased carbonate production during interglacial periods.

Stable Isotopes

Two benthic foraminifera, *Cibicidoides wuellerstorfi* and *Cibicidoides kullenbergi* (referred to collectively as *Cibicidoides*), and a planktic foraminifera (*Globigerina*

bulloides) were selected for stable isotopic analyses. These species of foraminifer occurred in sufficient abundance for stable isotopic measurement throughout the last 1.0 myr at site 982 and resulted in continuous signals. Tests of *Cibicidoides* (primarily *C. kullenbergi*) were picked from the >212 μm size fraction, and one to three individuals were used for isotopic analysis. Specimens of *G. bulloides* were picked from the >212 to <300 μm size fraction and ~10-15 individuals were used for measurement. Prior to isotopic analysis, foraminiferal tests were immersed in 15% H_2O_2 for 15 min to remove organic matter and cleaned by gentle sonication in methanol, and then dried overnight in an oven at 50°C.

Oxygen and carbon isotopic ratios were measured on carbon dioxide gas evolved using an automated preparation system consisting of a common acid bath of orthophosphoric acid (specific gravity 1.92) at 90°C. Isotopic ratios were measured on-line with a VG Isogas (Micromass) Precision Isotope Ratio Mass Spectrometer (PRISM). Isotopic ratios are expressed in standard delta notation relative to Vienna PDB (VPDB) [Coplen, 1996]. Analytical precision, estimated by the standard deviation (one sigma) of repeated analysis of a powdered carbonate standard (Carrara Marble-UF, n = 636), was $\pm 0.08\text{‰}$ for $\delta^{18}\text{O}$ and $\pm 0.05\text{‰}$ for $\delta^{13}\text{C}$. Sample reproducibility was estimated by the mean of the difference of 456 paired replicate analyses of *Cibicidoides* that resulted in a mean difference of 0.18‰ for $\delta^{18}\text{O}$ and 0.14‰ for $\delta^{13}\text{C}$. For *G. bulloides*, 176 paired analyses gave a mean difference of 0.16‰ for $\delta^{18}\text{O}$ and 0.18‰ for $\delta^{13}\text{C}$.

Sedimentology

Percent CaCO_3 by weight was determined by coulometric titration on a model 5011 carbon analyzer manufactured by Coulometrics (UIC) Inc. [Engleman et al., 1985].

Precision was estimated to be $\pm 0.7\%$ (1 standard deviation) on the basis of 241 measurements of reagent-grade (100%) CaCO_3 .

The volume percent of coarse-grained ice-rafted debris (IRD) was determined by examination of the 250 μm to 2 mm size fraction [Allen and Warnke, 1991]. The sample was split until about 500 grains remained, and point counting was carried out under a binocular microscope as described by Allen and Warnke [1991]. The IRD Index (%IRD) was defined by the ratio of the IRD grains to planktonic foraminifers and was calculated as $[\text{IRD} / (\text{IRD} + \text{Total planktic foraminifera})] \times 100$ [Poore and Berggen, 1975]. The IRD index is a closed sum and is therefore dependent upon the relative abundance of IRD and planktic foraminifers.

Stratigraphy

The middle-to-late Pleistocene stratigraphy of site 982 was derived by correlation of benthic and planktic foraminiferal oxygen isotopic records from site 982 to the astronomically tuned timescale of site 677 [Shackleton et al., 1990] using the program Analyseries [Paillard et al., 1996]. The Brunhes-Matuyama boundary (0.78 Ma) was identified at 20.03 meters composite depth (MCD) in site 982 [Channell and Lehman, 1999] and correlates to MIS 19 in the oxygen isotopic record. The top of the Jaramillo (0.99 Ma) was placed at 25.03 MCD and correlates with MIS 27. The correlations of the isotopic records from sites 982 and 677 are excellent at the stage level, but the relatively low resolution of the site 982 record precludes precise correlation of all substages.

Results

Oxygen Isotopes

The change in $\delta^{18}\text{O}$ values at site 982 between the last glacial maximum and the Holocene was 1.7‰ for *Cibicidoides* and 2.0‰ for *G. bulloides* (Figures 2-1a and 2-1b).

These results compare favorably with piston cores taken from the same region [Manighetti et al., 1995]. This range in glacial-to-interglacial $\delta^{18}\text{O}$ variability is fairly characteristic of the last 700 kyr in site 982 when the dominant period of climatic variability was 100 kyr (Figures 2-1a and 2-1b). Notable exceptions include glacial stages 12 and 16 when benthic $\delta^{18}\text{O}$ values exceeded those of the last glacial maximum. Interglacial $\delta^{18}\text{O}$ values are slightly less than Holocene values during MIS 5 and 11. Prior to 700 Ka (MIS 17-24) the amplitude of both the planktic and benthic $\delta^{18}\text{O}$ signals was reduced with an average range of glacial-to-interglacial values of 1.5‰. On the basis of oxygen isotope stratigraphy, the record from site 982 appears to be complete, although a brief hiatus may have occurred during MIS 12, as the glacial maximum appears attenuated.

Carbon Isotopes

Benthic foraminiferal $\delta^{13}\text{C}$ values at site 982 were greater during the last glaciation than during the Holocene (Figure 2-1c), similar to results from intermediate-depth piston cores in the northeast Atlantic [Oppo and Lehman, 1993; Manighetti et al., 1995]. The most prominent features of the benthic $\delta^{13}\text{C}$ record are carbon isotopic decreases found at most glacial terminations (Figure 2-1c). The largest carbon isotopic decreases (~1.0‰) occurred at Terminations IV (MIS 10/9) and X (MIS 22/21). Carbon isotopic lows also occurred at Terminations II (6/5), III (8/7), V (12/11), VII (16/15), VIII (18/17), and IX (20/19). A pronounced decrease in benthic $\delta^{13}\text{C}$ values did not occur, however, at Termination VI (13/14) or I (2/1). The benthic $\delta^{13}\text{C}$ signal also contains long-term variations (Figure 2-1c) with the greatest values occurring between 500 and 400 Ka (MIS

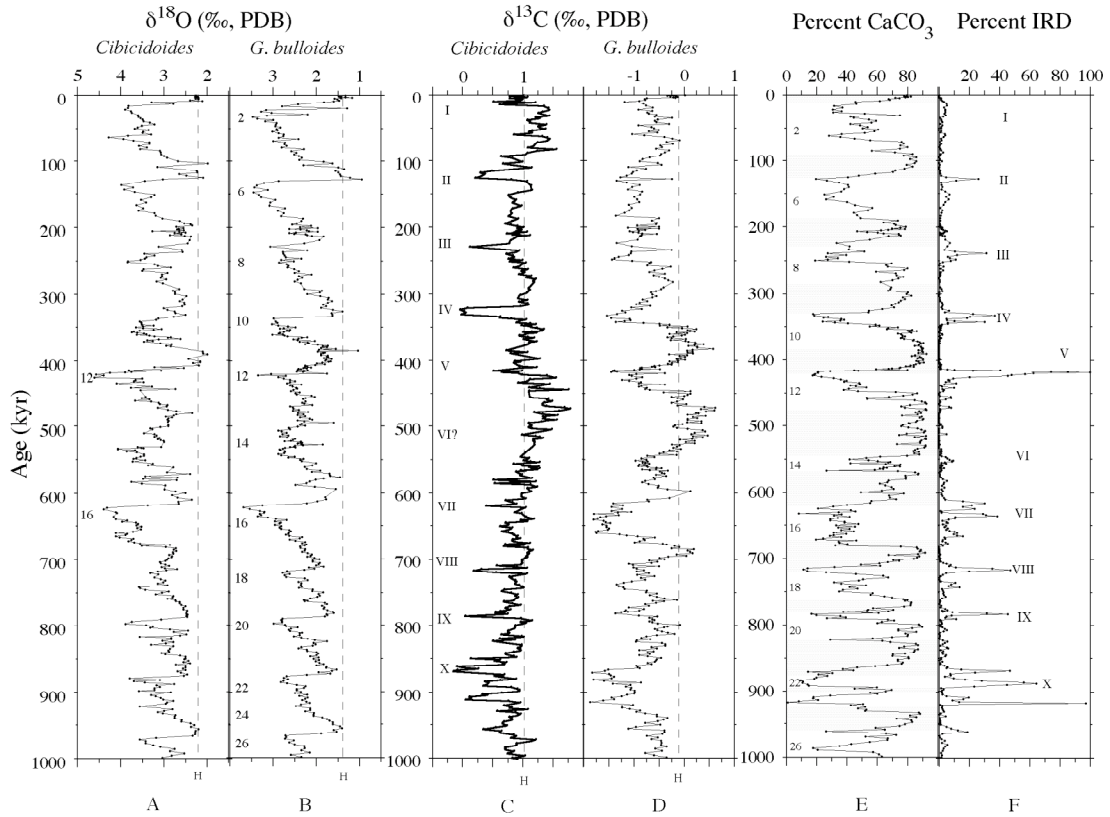


Figure 2-1. Oxygen isotopic records for the (a) benthic foraminifera *Cibicoides* and (b) planktic foraminifera *G. bulloides* and carbon isotopic records of (c) *Cibicoides* and (d) *G. bulloides* in site 982. The vertical line labeled "H" denotes Holocene $\delta^{13}\text{C}$ values in both records. Note the prominent $\delta^{13}\text{C}$ minima in the benthic record that occur at almost every termination of the past 1.0 myr. Terminations I-X are labeled. (e) Percent CaCO_3 record from site 982 is shown with interglacial stages shaded and labeled. (f) The ice-rafted debris index (%IRD) record from site 982 is shown with Terminations I-X labeled. The %IRD record displays two long-term trends with IRD maxima at ~ 920 and ~ 420 Ka and minima at ~ 500 and ~ 15 Ka.

14-12) and from 100 to 10 Ka (MIS 4-2). Planktic $\delta^{13}\text{C}$ values exceed those of the Holocene during the interval from 550 to 450 Ka and 400 to 350 Ka (Figure 2-1d).

Calcium Carbonate

Carbonate content of sediments at site 982 averaged 61.3% with higher values during interglacial periods and lower values during glacial intervals for the last 1.0 myr (Figure 2-1e). During Termination I, carbonate content increased from ~30% during the last glaciation to just over 80% in the Holocene. The typical glacial-to-interglacial change in carbonate percentage over the past 1.0 myr (from ~10 to ~90%) was slightly greater than that of the last climatic cycle. The lowest carbonate values occurred during glacial stages 16, 18, and 22, whereas the highest values occurred during interglacial stages 11, 13, 17, and 21.

Ice Rafted Debris

The percent IRD record from site 982 shows peaks at nearly all of the terminations during the last 1.0 myr (Figure 2-1f). I refer to these peaks as terminal ice rafting events (TIREs) because they tend to occur at the end of glacial cycles. The IRD record of the past 1.0 myr appears to be marked by two trends consisting of a maximum followed by smaller peaks. A pronounced IRD maximum occurs at Termination V (12/11) followed by smaller peaks associated with Terminations IV, III, and II. Termination I was marked by very little IRD deposition. Similarly, a major pulse of IRD occurred near 880 Ka (MIS 22/21) followed by smaller peaks associated with Terminations IX, VIII, and VII. A large IRD event also occurred at the MIS 24/23 boundary, but the IRD maximum is represented by a single point only. Termination VI was not marked by a strong TIRE, similar to Termination I.

Discussion

Terminations

In site 982, glacial terminations were marked by a sequence of events that included a decrease in oxygen isotopic values, an increase in IRD (a TIRE), a decrease in benthic carbon isotopic values, and an increase in %CaCO₃ (Figure 2-2). The relatively low and variable sedimentation rates at site 982 do not permit a detailed analysis of the relative timing of events at each termination, although some general patterns can be identified. For example, the sequence of events at Termination II is generally the same as found by Oppo et al. [1997] in a high sedimentation rate core (~8 cm/1000 years). Oppo et al. [1997] reported an IRD peak and transient planktic $\delta^{18}\text{O}$ low that immediately preceded Termination II and were followed by a decrease in benthic $\delta^{13}\text{C}$ values in both middepth and shallower cores in the northeast Atlantic.

Although the general pattern of events was similar at most terminations, there were differences in the timing and duration of IRD peaks and benthic foraminiferal $\delta^{13}\text{C}$ minima. Terminations I and VI (Type A) are marked by no TIRE and a minimal $\delta^{13}\text{C}$ depletion, and the preceding glacial has higher $\delta^{13}\text{C}$ values than the following interglacial (Figure 2-2). Terminations II, IV, and X (Type B) contain a prominent IRD peak and $\delta^{13}\text{C}$ minima that extend well into the subsequent interglacial. Terminations VIII and IX exhibit a third pattern (Type C) whereby $\delta^{13}\text{C}$ minima were coincident with IRD maxima. The remaining three terminations do not fall into any particular category. An IRD peak occurred during the MIS 7/8 transition; however, the $\delta^{13}\text{C}$ minimum postdated the IRD maximum and the termination (Termination III). Termination V is difficult to interpret because of a suspected hiatus during MIS 12, although it appears most similar to Type B.

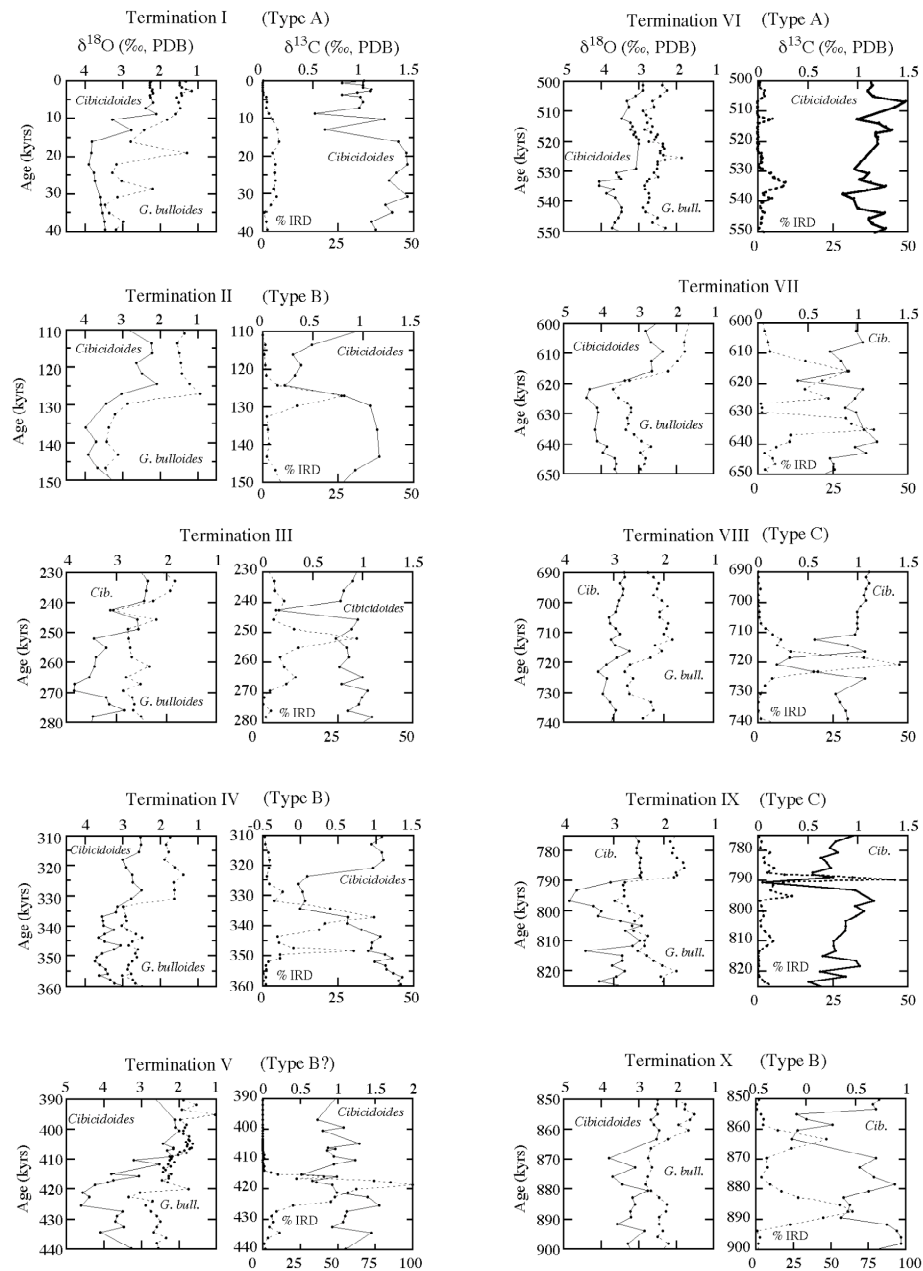


Figure 2-2. Changes in benthic foraminiferal $\delta^{13}\text{C}$ and $\delta^{18}\text{O}$ values, $\% \text{CaCO}_3$, and IRD deposition at site 982 during Terminations I-X. Terminations are grouped into "types." "Type A" terminations do not contain a TIRE and have minimal $\delta^{13}\text{C}$ depletions, and the preceding glacial has higher $\delta^{13}\text{C}$ values than the following interglacial. "Type B" terminations display a large peak in IRD and prolonged benthic $\delta^{13}\text{C}$ minima. "Type C" terminations contain coincident IRD peaks and $\delta^{13}\text{C}$ depletions. The remaining three terminations do not fall into any of these categories.

Termination VII contains a double IRD peak with a short $\delta^{13}\text{C}$ minimum during the second peak. Changes in sedimentation rate from low during glacial periods to high during interglacial intervals may explain some of the differences in the patterns observed at terminations in site 982.

At site 982, the intensity of benthic $\delta^{13}\text{C}$ minima and, to a lesser extent, the magnitude of IRD events also varied among terminations. The severity of the benthic $\delta^{13}\text{C}$ minima is related to the magnitude of TIREs, such that smaller benthic $\delta^{13}\text{C}$ minima (e.g., I and VI) are associated with little deposition of IRD. These terminations are usually preceded by glacial stages exhibiting high benthic $\delta^{13}\text{C}$ values (i.e., MIS 2, 4, and 14). In contrast, large benthic $\delta^{13}\text{C}$ decreases at terminations are associated with greater TIREs and are generally preceded by glacial stages with lower benthic $\delta^{13}\text{C}$ values (Figures 2-1c and 2-1f). Note that Termination V in site 982 does not show a strong benthic foraminiferal $\delta^{13}\text{C}$ minima, possibly owing to a short hiatus during late MIS 12.

Carbon isotopic depletions during Terminations I, II, and V have been reported in other cores from the northeast Atlantic [Oppo and Lehman, 1993; Oppo et al., 1997; Zahn et al., 1997; Oppo et al., 1998]. Similarly, Terminations I-VI were marked by low benthic $\delta^{13}\text{C}$ values in site 658, a middepth core (2263 m) off western Africa [Sarnthein and Tiedemann, 1990]. The $\delta^{13}\text{C}$ minima at terminations have been attributed to a reduction in the contribution of northern-source waters as a result of strong surface water stratification and increased influence of low- $\delta^{13}\text{C}$ waters of southern origin [Sarnthein and Tiedemann, 1990; Oppo and Lehman, 1993; Oppo et al., 1997, 1998]. Carbon isotopic minima are observed at nearly every termination at site 982 for the past 1.0 myr,

suggesting that this pattern of poorly ventilated intermediate waters was typical of terminations during the late Pleistocene.

Northeast Atlantic Circulation During Terminations

To reconstruct the relationship between intermediate and deep-water masses, the benthic foraminiferal $\delta^{13}\text{C}$ record of site 982 was compared with site 607 in the deep North Atlantic, which monitors lower NADW [Raymo et al., 1990b] (Figure 2-3). During interglacials, $\delta^{13}\text{C}$ values at sites 982 and 607 were both high ($\sim 1.0\text{‰}$), indicating a strong presence of upper and lower NADW at intermediate and lower depths. Benthic $\delta^{13}\text{C}$ values, however, differed markedly between the two sites during glacial periods. Glacial $\delta^{13}\text{C}$ values at site 607 were low, indicating reduced influence of lower NADW and greater contribution of Southern Ocean Water (SOW) [Raymo et al., 1990b]. In contrast, benthic $\delta^{13}\text{C}$ values at site 982 remained high during glaciations, indicating the presence of GNAIW [Duplessy et al., 1988, 1991; Oppo and Lehman, 1993]. The increase in the carbon isotopic gradient between sites 982 and 607 during glacials reflects the redistribution of nutrients from intermediate to deep-waters [Boyle, 1988]. At terminations, $\delta^{13}\text{C}$ values at site 607 increased by $\sim 1\text{‰}$ from low glacial values to high interglacial values, indicating increased production of lower NADW. In contrast, benthic $\delta^{13}\text{C}$ values at site 982 decreased at terminations by nearly 1.0‰ (Figure 2-3), indicating the cessation of GNAIW production. Only well after the terminations, during interglacial stages, did the $\delta^{13}\text{C}$ values of intermediate waters increase, indicating the resumption of upper NADW production that ventilated the middepth North Atlantic again.

The benthic foraminiferal carbon isotopic record from site 982 is compared to benthic $\delta^{13}\text{C}$ records from sites 502 and 552 that also monitor intermediate waters in the

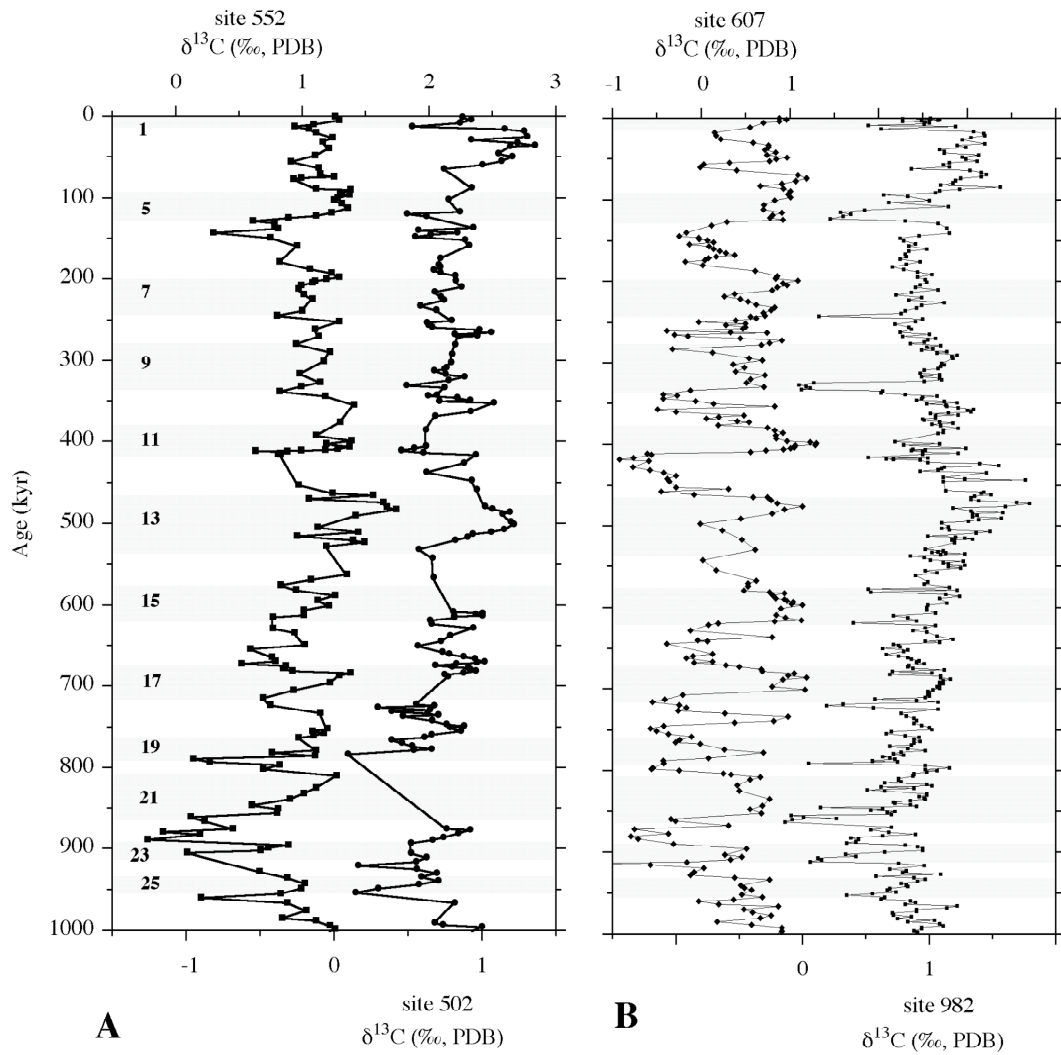


Figure 2-3. A comparison of the benthic foraminiferal $\delta^{13}\text{C}$ records from sites 982, 607, and 552 in the North Atlantic and site 502 in the Caribbean Sea. Carbon isotopic decreases during terminations at site 982 correlate with the $\delta^{13}\text{C}$ increases at site 607, indicating that as NADW production increased, GNAIW production ceased.

North Atlantic (Figure 2-3). Site 552 (56°N, 23°W, 2200 m) is located on the western edge of the Rockall Plateau near site 982 [Shackleton and Hall, 1984]. Site 502 (11°N, 80°W, 3051 m) is located in the Caribbean Sea, which has a sill depth between 1600 and 1800 m and is filled by intermediate-depth waters from the North Atlantic [deMenocal et al., 1992; Oppo et al., 1995]. During glacial intervals when GNAIW production was strong, carbon isotopic values at site 502 were equal to or slightly lower (0-0.5‰ lower) than those at site 982. Carbon isotopic values at site 552 during glacials varied from 0.2‰ higher (MIS 10) to almost 1‰ lower (MIS 2) than values at site 982. Site 552 had higher $\delta^{13}\text{C}$ values than 982 during MIS 8 and 10, suggesting that it may have been located closer to the core of GNAIW than site 982. At other times, site 552 was strongly influenced by SOW (e.g., MIS 2), whereas $\delta^{13}\text{C}$ values at sites 502 and 982 remained high. This indicates that during most glacials, the GNAIW-SOW boundary was near 2200 m, as suggested by previous studies [Oppo and Fairbanks, 1987; Zahn et al., 1987; Oppo and Lehman, 1993; Oppo et al., 1997]. During terminations, $\delta^{13}\text{C}$ values at site 982 decreased by nearly 1‰ when GNAIW production ceased. Carbon isotopic values at site 502 also show a slight decrease at terminations but not of the magnitude of the decrease measured at site 982. This suggests that poorly ventilated waters may have been present in a large portion of the intermediate depth North Atlantic during climate transitions. Carbon isotopic values at site 552, however, remained high during terminations, indicating renewed production of lower NADW that ventilated the northeast Atlantic below 2200 m.

A new, high-resolution, benthic foraminiferal $\delta^{13}\text{C}$ record from site 980/981 has been used with the records from sites 982 and 607 in a related paper by Flower et al.

[2000] to reconstruct the evolution of intermediate-to-deep carbon isotopic gradients in the North Atlantic during the past 1 myr. Site 980/981 (2200 m) is located on the Feni Drift (55°29'N, 14°42'W) near site 982 [Jansen et al., 1996]. Interglacial $\delta^{13}\text{C}$ values at all sites were similar; however, during glacial intervals, carbon isotopic values at site 980/981 were generally intermediate between sites 982 and 607. This suggests that site 980/981 was bathed by NADW during interglacial intervals and was probably within the mixing zone between GNAIW and SOW during glacial intervals [Flower et al., 2000]. Site 980/981 does exhibit some $\delta^{13}\text{C}$ depletions near terminations, but they are not as large in amplitude or duration as the depletions evident in the record from site 982, possibly because site 980/981 is deeper and was bathed by lower NADW when production resumed during glacial/interglacial transitions.

Long-term changes in the intermediate-to-deep carbon isotopic gradients are reflected by subtraction of the site 607 benthic foraminiferal $\delta^{13}\text{C}$ record from the site 982 record (Figure 2-4a). The $\delta^{13}\text{C}_{982-607}$ record is remarkably similar to the benthic foraminiferal $\delta^{18}\text{O}$ record (Figure 2-4b), and cross spectral analysis indicates strong covariance of changes in the intermediate-to-deep $\delta^{13}\text{C}$ gradient and benthic foraminiferal $\delta^{18}\text{O}$ during the past 1.0 myr [Flower et al., 2000]. The strong covariance of these signals supports a close relationship between NADW suppression, increased GNAIW production, and global ice volume. The covariance of intermediate-to-deep $\delta^{13}\text{C}$ gradients and benthic $\delta^{18}\text{O}$ also suggests that nutrient redistribution may be an important factor in glacial/interglacial climatic changes [e.g., Boyle, 1988].

On the basis of the carbon isotopic signals in the aforementioned sites, I present a generalized schematic view of the changes that may have occurred in circulation at

intermediate-to-deep depths in the North Atlantic from glacial-to-interglacial time during Type B terminations (Figure 2-5). During glacial periods (Figure 2-5a), SOW was the predominant water mass at depths >2200 m in the North Atlantic [Oppo and Fairbanks, 1987; Duplessy et al., 1988, 1991; Oppo and Lehman, 1993]. The intermediate-depth North Atlantic was well ventilated at this time by GNAIW, which formed north of the polar front in the northeast Atlantic [Duplessy et al., 1988; Oppo and Lehman, 1993], perhaps with a component produced in the Norwegian Sea [Veum et al., 1992]. During terminations (Figure 2-5b), production of lower NADW increased after the Nordic Seas became ice free and the North Atlantic Current transported warm salty surface waters into the Nordic Seas [Jones and Keigwin, 1988; Broecker and Denton, 1989; Lehman et al., 1991]. Benthic $\delta^{13}\text{C}$ values in the deep North Atlantic increased as newly formed lower NADW flooded the North Atlantic below ~2200 m and replaced SOW. As lower NADW formation increased at terminations, GNAIW production was halted as a result of iceberg and meltwater discharge into the Nordic Seas and northeast Atlantic, creating poorly ventilated intermediate waters above 2200 m (indicated by low benthic $\delta^{13}\text{C}$ values in site 982). During interglacial periods (Figure 2-5c) the intermediate-depth North Atlantic became ventilated again by upper NADW once conditions permitted renewed production of interglacial intermediate waters, such as LSW and MOW. Our results suggest that the intermediate North Atlantic was poorly ventilated during deglaciations of the past 1.0 myr, when circulation switched from intermediate convection in the North Atlantic to deep convection in the Nordic Seas.

Several lines of evidence suggest that formation of upper NADW did not commence until well after full interglacial conditions were established. The lag in resumption of upper NADW following some terminations must be related to

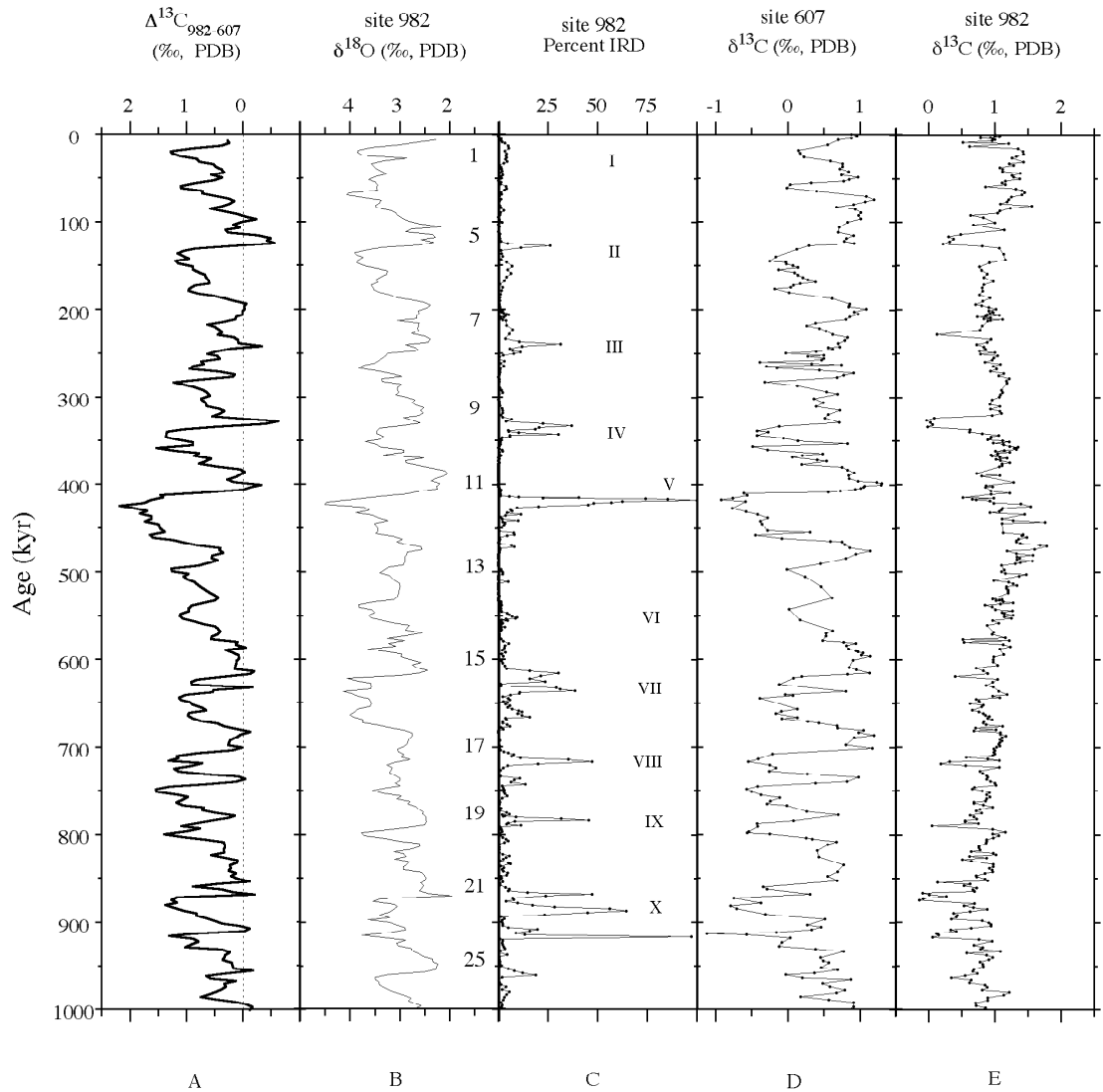


Figure 2-4. The intermediate-to-deep carbon isotopic gradient ($\Delta^{13}\text{C}_{982-607}$) (a) is remarkably similar to (b) the oxygen isotopic curve of the past 1.0 myr. (c) The IRD and (d) benthic foraminiferal $\delta^{13}\text{C}$ records from site 982 are compared with (e) the benthic $\delta^{13}\text{C}$ record at site 607. Maximum TIREs at site 982 correlate with minimum glacial $\delta^{13}\text{C}$ values at site 607 (maximum glacial suppression of NADW) at ~ 920 and ~ 400 Ka. As glacial $\delta^{13}\text{C}$ values at site 607 increase between ~ 920 and ~ 500 Ka (glacial suppression of NADW decreases), the magnitude of TIREs at site 982 is reduced. Minimal TIREs occur at 500 Ka (Termination VI) and 15 Ka (Termination I). Glacial $\delta^{13}\text{C}$ values are highest at both sites 607 and 982 during this interval.

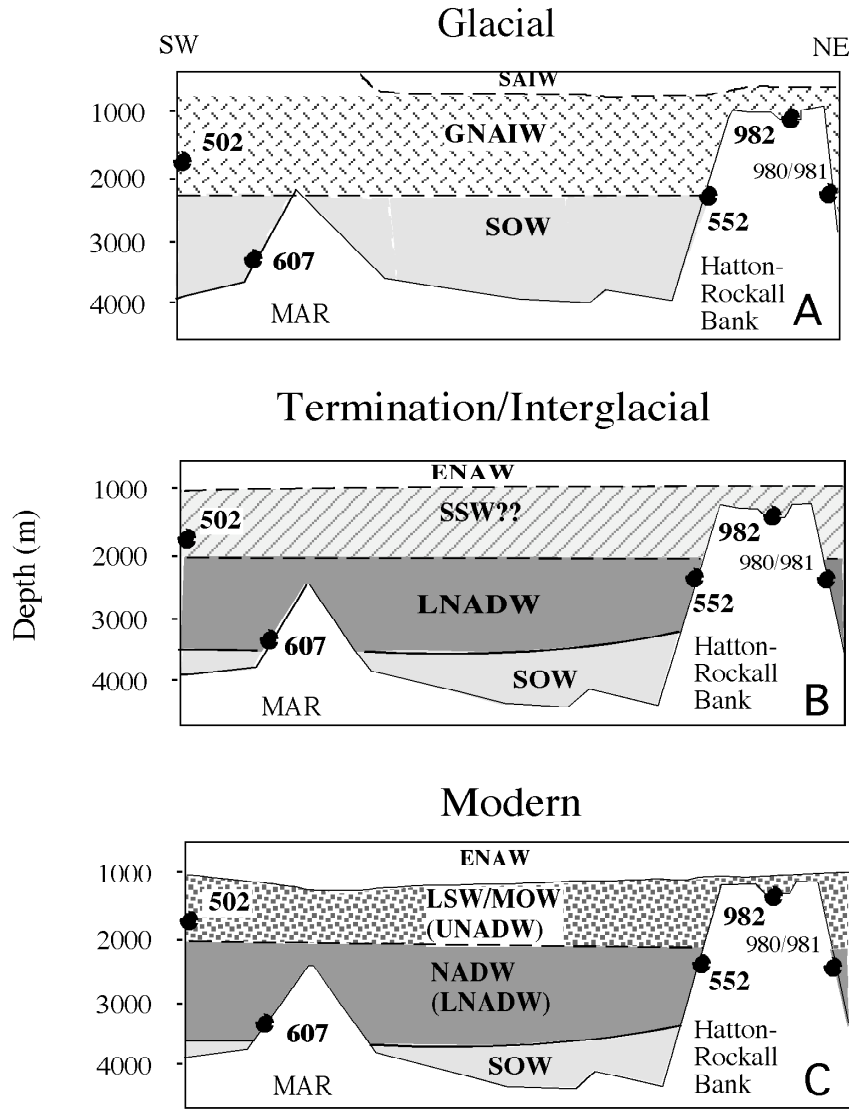


Figure 2-5. Schematic representation of glacial-to-interglacial changes in vertical watermass structure in the North Atlantic inferred from benthic $\delta^{13}\text{C}$ records from sites 982, 980/981, 552, 502, and 607. (a) Glacial configuration: GNAIW is on, NADW is reduced, and SOW influences the deep Atlantic below 2000 m. (b) A transitional mode during terminations: GNAIW is off, LSW and MOW are off (or reduced), and the intermediate-depth North Atlantic is poorly ventilated, possibly by waters of southern origin. Lower NADW is on. (c) Interglacial (modern) configuration: LSW and MOW are on, forming upper NADW, and lower NADW is on. Abbreviations for water masses are SAIW (Subarctic Intermediate Water), GNAIW (Glacial North Atlantic Intermediate Water), SOW (Southern Ocean Water), LSW (Labrador Sea Water), MOW (Mediterranean Overflow Water), SSW (Southern Source Water), and ENAW (Eastern North Atlantic Water).

conditions in source areas for either MOW or LSW. Stable isotopic evidence suggests that MOW was a source for the intermediate-depth Atlantic throughout the last 140,000 years, although production may have decreased during glaciations because lowered sea level decreased the outflow of MOW into the Atlantic [Zahn et al., 1987; Sarnthein et al., 1994; Zahn et al., 1997]. Conditions in the Labrador Sea affecting formation of LSW were more variable, however, resulting in greater glacial/interglacial changes in LSW production. Reconstructions by Climate: Long-Range Investigation, Mapping, and Prediction (CLIMAP) [1976] indicate that the polar front was located south of the Labrador Sea until late into the last deglaciation (~9000 years B.P.), resulting in unfavorable conditions for formation of LSW until the early Holocene. Floral and faunal evidence in the Labrador Sea and Baffin Bay suggests that extensive perennial sea ice persisted throughout the late glacial and during deglaciation, resulting in formation of a low-salinity surface layer that was maintained by a continuous meltwater supply from decaying ice sheets and a renewal of low-salinity waters via the Arctic Channel [Fillon and Duplessy, 1980; Fillon, 1985; Aksu et al., 1988]. Carbonate productivity in the Labrador Sea also peaked late in the Holocene and in stage 5e, suggesting that deep convection occurred only under full interglacial conditions [Hillaire-Marcel et al., 1994].

In summary, the intermediate-depth North Atlantic was generally well ventilated by upper NADW (a mixture of LSW and MOW) during full interglacials and by GNAIW during glacial intervals (Figures 2-5a and 2-5c). During terminations, however, the intermediate-depth North Atlantic was poorly ventilated when GNAIW production ceased because of iceberg and meltwater discharge into the Nordic Seas and northeast Atlantic (Figure 2-5b). Interglacial production of upper NADW following some terminations was not renewed until full interglacial conditions were established in the

Labrador Sea and LSW production resumed (Figure 2-5b). These results suggest that the intermediate North Atlantic was poorly ventilated during deglaciations, when circulation switched from intermediate convection in the North Atlantic to deep convection in the Nordic Seas.

Mechanism to Explain Long-Term Changes in IRD and Benthic $\delta^{13}\text{C}$

An ice-rafting event marks most of the glacial terminations in site 982 during the past 1.0 myr. The geographic distribution of IRD during the last glacial interval was greatest between 40° and 50°N in the belt of "maximal deposition" just north of the polar front [Ruddiman, 1977]. IRD distributions follow glacial surface circulation patterns in the North Atlantic, which consisted of a cyclonic gyre north of the polar front [Ruddiman, 1977; Fillon, 1985; Grousset et al., 1993; Robinson et al., 1995]. Site 982 is located on the northeastern edge of this recirculation gyre, north of the primary IRD belt, but still within the zone of IRD accumulation [McManus et al., 1994; Oppo and Lehman, 1995; Robinson et al., 1995, Vidal et al., 1997]. Potential source areas of IRD include North America, Greenland, Iceland, Scandinavia, Barents-Kara shelf, and possibly even the Rockall Plateau itself [Ruddiman, 1977; Jones and Keigwin, 1988; Bischof, 1994; McManus et al., 1994; Robinson et al., 1995]. However, the physical nature of the IRD (mainly quartz grains with mechanical breakage) and the paucity or absence of dolomite suggest Greenland as a "major supplier" of IRD [Stanton, 1997]. In addition, the ubiquitous presence of volcanogenic grains also implicates Iceland as a sediment source. This idea is in agreement with the findings of Lackschewitz and Wallrabe-Adams [1997] with respect to sediment cores from the Reykjanes Ridge investigated by them. However, for site 982, Scandinavian sources cannot be excluded [E. Jansen, personal communication to C.L. Stanton, 1997].

A comparison of the IRD and benthic foraminiferal $\delta^{13}\text{C}$ records from site 982 to the benthic $\delta^{13}\text{C}$ record from site 607 suggests a connection between site 982 and glacial conditions in the Nordic Seas (Figures 2-4c to 2-4e). The largest TIREs at site 982 occurred at ~ 920 and ~ 420 Ka, corresponding to the lowest glacial $\delta^{13}\text{C}$ values at site 607. At Terminations VI (~ 500 Ka) and I (15 Ka) when glacial $\delta^{13}\text{C}$ values at site 607 were highest, little IRD was deposited at site 982 and the low benthic $\delta^{13}\text{C}$ values, observed at other terminations, did not occur. This implies that the times of greatest suppression of NADW during glacials (lowest glacial $\delta^{13}\text{C}$ at site 607) coincide with the greatest delivery of IRD and lowest benthic $\delta^{13}\text{C}$ minima at site 982. In contrast, times of less suppression of NADW (higher glacial $\delta^{13}\text{C}$ at site 607) are marked by a small or absent benthic $\delta^{13}\text{C}$ minimum at site 982. This relationship suggests that glacial conditions with strong production of GNAIW and NADW resulted in relatively little IRD accumulation at site 982 and good ventilation of middepth waters in the North Atlantic during terminations. The relationship between inferred variations in NADW from site 607 and the benthic $\delta^{13}\text{C}$ and IRD records from site 982 suggests a link between glacial deep-water production in the Nordic Seas, GNAIW production, and IRD deposition on the Rockall Plateau during terminations.

Glacial deep-water production is dependent upon the extent of sea ice cover in the Nordic Seas [Kellogg, 1980; Raymo et al., 1990a]. Enhanced sea ice cover prevents the advection and atmospheric cooling of warm, salty Atlantic surface water in the Nordic Seas needed to form lower NADW; therefore, increased glacial suppression of NADW would be expected under conditions of perennial sea ice cover [Kellogg, 1980; Raymo et al., 1990a]. In contrast, ice-free conditions in the Nordic Seas during summer may have

allowed some deep-water convection and overflow to the Atlantic. Until recently, the Nordic Seas were thought to have remained continually ice covered throughout the last glacial cycle, or at least during the last glacial maximum (LGM) [CLIMAP, 1976]. New evidence now indicates that the Nordic Seas may have been seasonally ice-free during the LGM [Hebbeln et al., 1994; Rasmussen et al., 1996; Weinelt et al., 1996].

During the last glaciation some production of lower NADW may have occurred and leaked into the deep North Atlantic, as evidenced by relatively high glacial $\delta^{13}\text{C}$ values at site 607. At the same time, high benthic $\delta^{13}\text{C}$ values at site 982 indicate that intermediate depths were very well ventilated by GNAIW, and site 982 was probably close to the source area of GNAIW. Similar conditions may also have prevailed during stage 14 (Termination VI, ~500 Ka) when benthic $\delta^{13}\text{C}$ values at both sites 607 and 982 were relatively high, indicating reduced suppression of NADW and vigorous GNAIW production. At site 982, both Terminations I and VI were marked by negligible IRD and absence of strong benthic $\delta^{13}\text{C}$ minima. These observations can be explained by a relatively northerly position of the sea ice edge and locus of iceberg melting (and hence IRD deposition) relative to site 982 during glacial stages 2 and 14.

During those glaciations when the Nordic Seas were covered by perennial sea ice, glacial NADW production was at a minimum (e.g., stages 12 and 22) as evidenced by low benthic $\delta^{13}\text{C}$ at site 607 [Raymo et al., 1990b; Raymo, 1997]. Perennial sea ice cover of the Nordic Seas shifted the glacial polar front and intermediate water convective cell farther south into the North Atlantic beyond site 982. Although the glacial benthic $\delta^{13}\text{C}$ values were still high at site 982, they were not as high as glacial stages 2 or 14, indicating that intermediate water masses were not as well ventilated or that site 982 was

farther from the source area of GNAIW production. At site 982 a pronounced TIRE and benthic $\delta^{13}\text{C}$ minimum marked the terminations following glacial periods with strong glacial NADW suppression (Figures 2-4c to 2-4e). This suppression of NADW production may have resulted from a more southerly position of the glacial polar front, sea ice edge, and iceberg melting line that migrated over site 982 during the termination, resulting in increased deposition of IRD.

Although I have focused on the extreme states of sea ice cover in the Nordic Seas during glaciations and its effect on deep and intermediate water circulation, a continuum of glacial states probably existed in the Nordic Seas that gave rise to the varied responses observed in sites 607 and 982. Changes in the magnitude of glacial suppression of NADW production, terminal ice-rafting events, and ventilation of the middepth Atlantic during terminations may be related to varying extents of the spatial and temporal distribution of sea ice cover in the Nordic Seas. In addition, severe glacial cooling may also have given rise to the development of marine-based ice shelves in the Nordic and Labrador Seas whose breakup may have resulted in increased IRD delivery to the North Atlantic upon deglaciation [Hulbe, 1997]. Increased sea ice coverage and the development of marine ice shelves in the Nordic Seas during some glaciations would have a large impact on the locus and volume of deep and intermediate waters during glacial periods, but would have relatively little effect on benthic $\delta^{18}\text{O}$ values. This may explain the observed decoupling of global ice volume (as measured by benthic $\delta^{18}\text{O}$) and deep-water circulation (as measured by benthic $\delta^{13}\text{C}$) observed in site 607 during the late Pleistocene [Raymo et al., 1990b; Raymo, 1997].

Conclusions

The carbon isotopic record from site 982 indicates that the intermediate-depth circulation of the North Atlantic underwent major reorganization at the close of glacial periods during the last 1.0 myr. During most terminations of the late Pleistocene, melting of icebergs and production of low-salinity surface waters caused production of GNAIW to cease, resulting in decreased ventilation of the middepth North Atlantic. Poor ventilation of intermediate water masses lasted well into some interglacial stages, indicating a lag between the shutdown of GNAIW production at terminations and the renewed production of upper NADW (LSW and MOW) during full interglacial conditions. A comparison of the benthic $\delta^{13}\text{C}$ records from sites 982, 607, 552, and 502 reveals that as GNAIW production ceased during terminations, lower NADW production increased. The similarity between the magnitude of TIREs and benthic $\delta^{13}\text{C}$ minima at site 982 and glacial benthic $\delta^{13}\text{C}$ values at site 607 for the last 1.0 myr suggests a common mechanism relating variations in glacial production of lower NADW, the magnitude of IRD deposition, and the severity of the decrease in intermediate water ventilation during terminations. Variations in the spatial and seasonal extent of sea ice cover during glaciations in the Nordic Seas are one possible mechanism. Glaciations with perennial sea ice cover resulted in strong suppression of NADW formation (low $\delta^{13}\text{C}$ values at site 607), site 982 being farther from the source of GNAIW (lower $\delta^{13}\text{C}$ at site 982), large ice rafting events, and a strong decrease in intermediate ventilation on subsequent terminations. Glaciations characterized by seasonally ice-free conditions in the Nordic Seas resulted in greater production rates of glacial NADW (higher $\delta^{13}\text{C}$ values at site 607), site 982 being closer to the source of GNAIW (higher $\delta^{13}\text{C}$ at site 982), small

TIREs, and better ventilation of the middepth North Atlantic during subsequent terminations. I suggest that the spatial and temporal extent of sea ice coverage of the Nordic Seas may explain the observed decoupling of global ice volume and deep-water circulation during the late Pleistocene.

CHAPTER 3
ODP SITE 1090, SOUTH ATLANTIC

Introduction

Carbon isotopic gradients between benthic foraminifers from different locations in the ocean have been used to infer past changes in deep-water circulation, including estimates of changing production of Northern Component Water (NCW). Oppo and Fairbanks [1987] first suggested a quantitative index for estimating the relative proportion of NCW at a site (x) by using benthic $\delta^{13}\text{C}$ in Atlantic deep-sea cores (Equation 1):

$$\% \text{NCW} = \frac{\delta^{13}\text{C}_X - \delta^{13}\text{C}_{\text{SCW}}}{\delta^{13}\text{C}_{\text{NCW}} - \delta^{13}\text{C}_{\text{SCW}}} * 100$$

where $\delta^{13}\text{C}_{\text{NCW}}$ is the carbon isotopic value for Northern Component Water (NCW), $\delta^{13}\text{C}_{\text{SCW}}$ is the carbon isotopic value for Southern Component Water (SCW), and $\delta^{13}\text{C}_X$ is the carbon isotopic value of a core in the Atlantic basin located in the mixing zone between NCW and SCW.

There are several assumptions implicit in using benthic $\delta^{13}\text{C}$ gradients to monitor changes in deep-water circulation: 1) the benthic foraminiferal species chosen to analyze for $\delta^{13}\text{C}$ must accurately record the $\delta^{13}\text{C}$ of TCO_2 of bottom water; 2) the $\delta^{13}\text{C}$ of benthic foraminiferal calcite must be precipitated in equilibrium with TCO_2 or at a known constant offset from equilibrium that is not affected by other processes (e.g., carbonate ion concentration); 3) variations in $\delta^{13}\text{C}$ must reflect changes in the mixing ratio of water

masses and not other factors such as changes in thermodynamic equilibrium in source areas of deep-water formation; and 4) the cores chosen to represent the end member watermasses must be suitably located to monitor end member $\delta^{13}\text{C}$ compositions.

Traditionally, site 552 at 2301 m water depth in the North Atlantic has been used as the NCW end member, but Venz et al. [1999] produced a higher resolution and more continuous record using site 982 located in 1145 m of water on the Rockall Plateau. Here I extend the site 982 record and provide a continuous $\delta^{13}\text{C}$ signal of the NCW end member back to the late Pliocene (~ 3.2 Ma). In addition, I report a new benthic $\delta^{13}\text{C}$ record from ODP site 1090 in the subantarctic South Atlantic that provides a near-continuous record of SCW variability for the last 2.9 myr. Previously, Oppo et al. [1990] used piston core RC13-229 in the deep Cape Basin as the SCW end member for the late Pleistocene, but this record ends at ~ 750 Ka and has poor resolution beyond ~ 500 Ka. Hodell and Venz [1992] reported a Plio-Pleistocene record from site 704, but this record is discontinuous with a hiatus between ~ 2.8 and 2.4 Ma and a poor late Pleistocene record after ~ 1.1 Ma. Here, the benthic carbon isotopic signals from sites 982 and 1090 are compared to similar records from sites 607, 925, and 929 in the Atlantic in order to reconstruct changes in deep-water circulation during the Plio-Pleistocene.

In the absence of a suitably long record from the Southern Ocean, Raymo et al. [1990b; 1997] relied on carbon isotopic records from the deep Pacific to estimate past changes in NCW during the Plio-Pleistocene. This assumes that the history of deep-Pacific $\delta^{13}\text{C}$ was the same as SCW. Here I recalculated changes in NCW and SCW mixing ratios using site 1090 as the SCW end member and compare the results to previous estimates derived using a Pacific record [Raymo et al., 1990b; 1997].

Calculation of %NCW are made for site 607 in the deep North Atlantic and site 929 in the deep tropical Atlantic.

Materials and Methods

Hydrography

The core locations are shown relative to the modern distribution of deep-water $\delta^{13}\text{C}$ (Figure 3-1, Table 3-1) and temperature-salinity (Figure 3-2, Table 3-2) to illustrate their relation to end member water masses. Site 982, on the Rockall Plateau in the North Atlantic, is bathed primarily by upper NADW consisting of Labrador Sea Water (LSW) admixed with Mediterranean Overflow Water (MOW) [Kawase and Sarmiento, 1986; Venz et al, 1999]. It falls on a mixing line between LSW and MOW (Figure 3-2). Holocene $\delta^{13}\text{C}$ values at site 982 are similar to those of NCW at site 607 (Figure 3-1). Located south of site 982 in the North Atlantic is site 607, which has temperature and salinity characteristics nearly identical to NCW today (Figure 3-2). Further south, in the equatorial North Atlantic, are sites 925 (located within NCW) and 929 (in the mixing zone between NCW and SCW) on the Caera Rise [Bickert et al., 1997]. Site 929 is located near the interface between NCW and SCW as reflected by its Holocene $\delta^{13}\text{C}$ and temperature-salinity values, which are intermediate between NCW and CPDW values (Figures 3-1 and 3-2). Site 1090 is located on the Agulhas Ridge in the southeastern Atlantic within lower Circumpolar Deep Water (CPDW) near the lower boundary of NADW. Mixing ratios calculated on the basis of dissolved silicate concentrations suggest that site 1090 is bathed today by waters composed of ~60% CPDW and ~40% NADW [Hodell et al., 2002]. Holocene $\delta^{13}\text{C}$ and temperature and salinity values at site 1090 are similar to that of CPDW (Figures 3-1 and 3-2). In this study, I use site 1090 as

Table 3-1. Core locations.

Site	Location	Water Depth (m)	Watermass	Reference
982	57°31'N, 15°53'W	1145	upper NADW	Venz et al., 1999; This study
607	41°00'N, 33°37'W	3427	lower NADW	Raymo, 1990b
925	4°12'N, 43°29'W	3040	NADW	Bickert et al., 1997
929	5°58'N, 43°44'W	4369	NADW/CPDW boundary	Bickert et al., 1997
RC13-229	25°49'S, 111°31'W	4191	CPDW (80%CPDW, 20% NADW)	Oppo and Fairbanks, 1987; Oppo et al., 1990
704	46°53'S, 7°25'E	2532	NADW (50% CPDW, 50% NADW)	Hodell and Venz, 1992
1090	42°55'S, 8°54'E	3702	CPDW (60% CPDW, 40% NADW)	Hodell et al. 2000; this study
849	0°11'N, 110°31'W	3850	Pacific Deep Water	Mix et al., 1995

Table 3-2. Water mass properties.

Water Mass	Water Mass Properties	
	°C	S (‰)
Northern Component Water (NCW)	2.5	34.94
Labrador Sea Water (LSW)	3.3	34.86
Circumpolar Deep Water (CPDW)	0.62	34.71
Pacific Outflow Water (POW)	1.5	34.67
Mediterranean Overflow Water (MOW)	6.5	35.40

Potential temperatures are from Broecker and Peng [1982] and Broecker et al. [1985] (after Oppo and Fairbanks, [1987]).

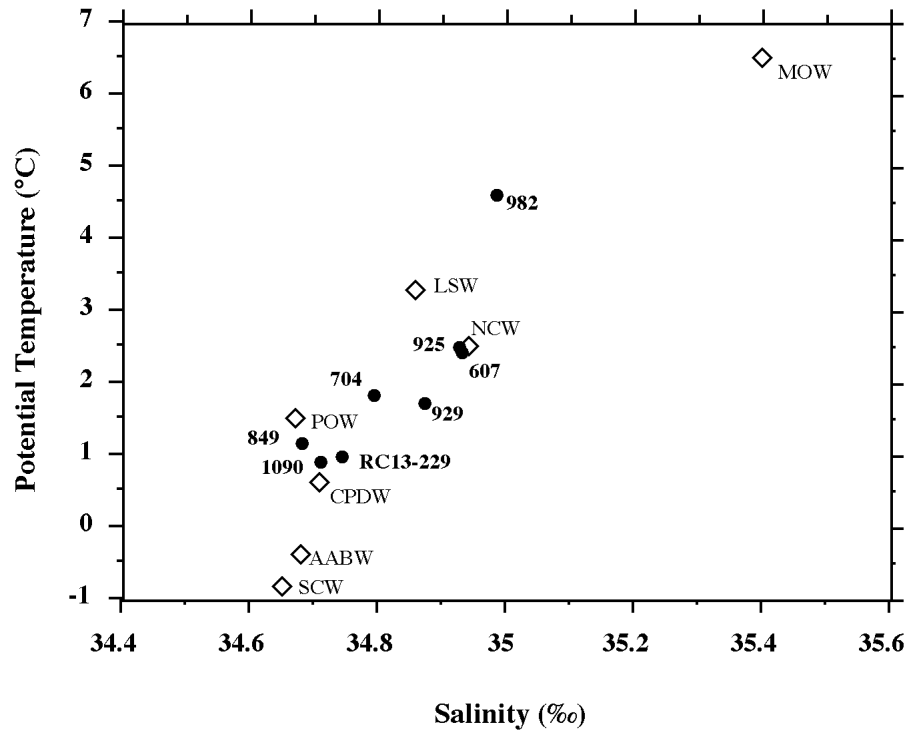


Figure 3-2. Positions of core locations (see also Table 3-1) are shown in potential temperature versus salinity space relative to the major deep-water masses in the world's oceans (after Oppo and Fairbanks, [1987]). Holocene $\delta^{13}\text{C}$ value at each site is noted in parentheses. MOW, Mediterranean Overflow Water; NCW, Northern Component Water; LSW, Labrador Sea Water; CPDW, Circumpolar Deep-water; POW, Pacific Outflow Water. Data for water mass properties are from Oppo and Fairbanks [1987] and Broecker and Peng [1982], summarized in Table 3-2.

the SCW end member and compare its $\delta^{13}\text{C}$ signal to two other cores (site 704 and piston core RC13-229) that have been used previously as monitors of SCW.

Sediments

I present new benthic isotopic data from two ODP sites (1090 and 982) and compare the results with other published records. At the location of ODP site 1090, a composite record was constructed using piston core TTN057-6-PC4 and site 1090 by splicing the two records together at ~ 400 Ka, or ~ 12.1 meters composite depth (mcd). The piston core was retrieved during the site survey cruise for Leg 177 and is located at the same position as site 1090. The 12.76-m piston core was recovered in 3751 m of water and has a complete record through marine isotope stage (MIS) 12 (~ 440 Ka) with sedimentation rates averaging 3 cm/1000 yrs [Hodell et al., 2000]. The core was sampled at an interval of every 3-cm over its length, yielding a temporal resolution of approximately one sample every 1000 years.

Site 1090 was drilled during Leg 177 using the advanced piston coring (APC) system with five offset holes (A-E) to ensure complete recovery of the section. A spliced composite section was constructed using continuous multi sensor core logging (density, magnetic susceptibility, p wave velocity) and spectral color reflectance data [Gersonde et al., 1999]. All major paleomagnetic chrons (Brunhes, Matuyama, Gauss) and subchrons (Jaramillo, Olduvai) were identified for the last 2.58 myr in the magnetic inclination data [Gersonde et al., 1999]. Site 1090 was sampled at 5 cm intervals (beginning at ~ 9 mcd to provide overlap with TTN057-6). Sedimentation rates average ~ 3 cm/1000 yrs in the Pleistocene (0 - 1.2 Ma), resulting in a temporal resolution of 1 sample every 2000 years. Sedimentation rates were lower (averaging ~ 1.2 cm/1000 yrs) prior to ~ 1.2 Ma, which yielded an average sampling frequency of 1 sample per 4000 years (Figure 3-3).

I also present new Plio-Pleistocene data from site 982 between 3.2 and 1.0 Ma. Stable isotope results for the last 1 myr were reported previously by Venz et al. [1999]. Site 982 was drilled during ODP Leg 162 using the advanced piston coring (APC) system with four offset holes (A - D) and a composite section was constructed to a depth of 255 mcd [Jansen et al., 1996]. The record from site 982 is relatively complete [Channell and Lehman, 1999] except for a short hiatus between 2.25-2.33 Ma (MIS 86, 87, and 88), which was identified by correlating the magnetic susceptibility signals between site 982 and nearby site 981 (55°28'N, 14°39'W, 2200 m) [Jansen et al., 1996]. Site 982 was sampled at 5-cm intervals resulting in a sampling frequency of one sample per 2500 years for the past 3.0 myr.

Stable Isotopic Analyses

Stable isotopic analyses from site 1090 were performed on the benthic foraminifera *Cibicidoides wuellerstorfi* and the planktic foraminifera *Globigerina bulloides*. Tests of *Cibicidoides* were picked from the >212 μm size fraction and 1 to 3 individuals were used for analysis. Specimens of *G. bulloides* were picked from the >212 to <300 μm size fraction, and 8 to 10 individuals were used for analysis. Prior to isotopic analysis, foraminiferal tests were immersed in 15% H_2O_2 for 15 minutes to remove organic matter and cleaned by gentle sonication in methanol, and then dried overnight in an oven at 50°C. Oxygen and carbon isotopic values from site 1090 were measured on a Finnigan MAT 252 mass spectrometer coupled to a Kiel III carbonate preparation device. Analytical precision of the site 1090 analyses, estimated by the standard deviation (one sigma) of repeated analysis of a powdered carbonate standard (NBS-19, n=371), was $\pm 0.06\text{‰}$ for $\delta^{18}\text{O}$ and $\pm 0.03\text{‰}$ for $\delta^{13}\text{C}$. Isotopic ratios are expressed in standard delta notation relative to VPDB [Coplen, 1996]. Stable isotopic methods and results for piston

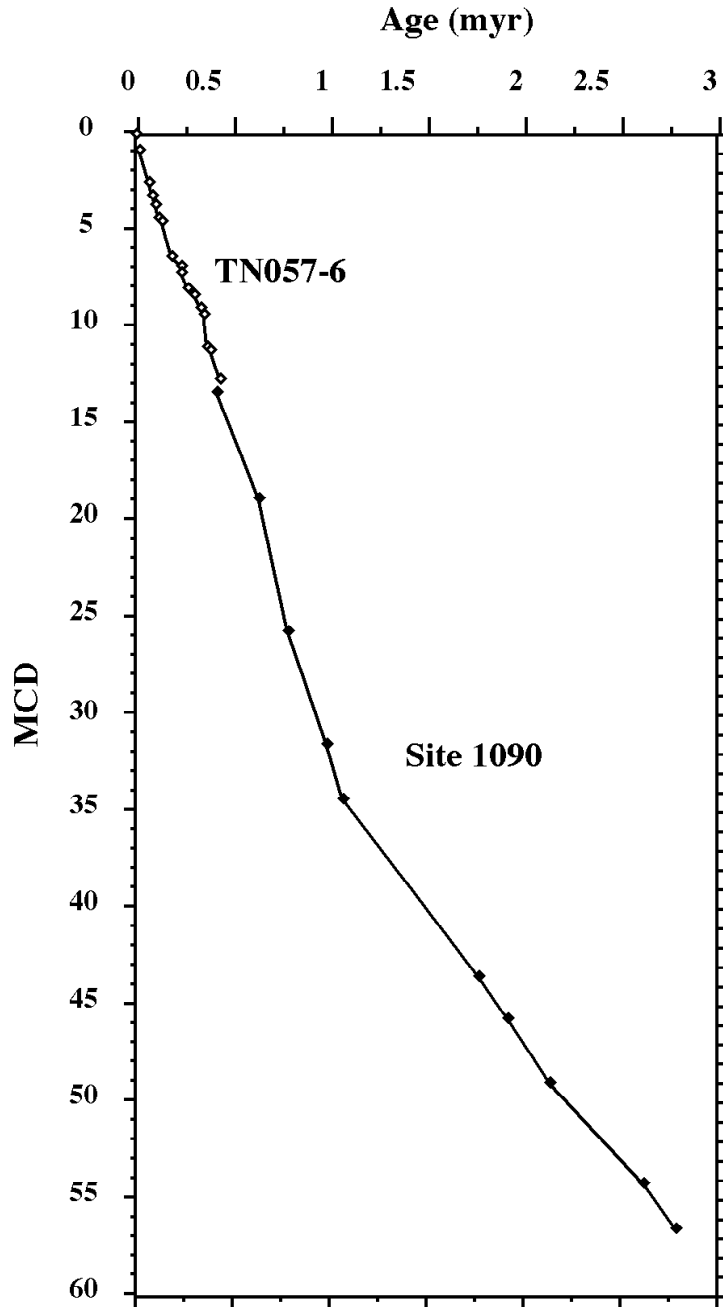


Figure 3-3. Age versus depth plot of isotopic and paleomagnetic control points. Note the change in sedimentation rates at ~35 mcd (1.1 Ma). Sedimentation rates average 3 cm/1000 years above 35 mcd (1.1 Ma) and 1.2 cm/1000 years below 35 mcd (1.1 Ma).

core TTN057-6-PC4 have been reported previously [Hodell et al., 2000]. Methods of stable isotopic analyses for site 982 follow those reported by Venz et al. [1999].

Stratigraphy

The chronologies of sites 1090 and 982 were derived by correlation of the benthic foraminiferal oxygen isotopic signals with ODP site 607 [Raymo et al., 1990b] using the program Analyseries [Paillard et al., 1996] (Figure 3-4). For site 607, I used the modified version of the age scale reported by Mix et al. [1995]. For site 1090, the correlation of the oxygen isotopic record to site 607 is excellent at the stage level to the bottom of the Olduvai (MIS 73), although small hiatuses occur in the Pleistocene (Table 3-3).

Correlations between ~2.0 and 2.9 Ma are not as strong owing to low sedimentation rates, gaps in the *Cibicidoides* data, and short hiatuses that were identified in site 1090 based on the benthic $\delta^{18}\text{O}$ stratigraphy (Figure 3-4, Tables 3-3 and 3-4). For site 982, correlation to site 607 was difficult in the middle Pleistocene to late Pliocene (1.5 - 2.1 Ma) because of the low-amplitude variation in the $\delta^{18}\text{O}$ signal (Figure 3-5, Table 3-3). The record contains a short hiatus between 2.25-2.33 Ma that removed MIS 86, 87, and 88. The time scale of site 929 was adjusted slightly to better match the $\delta^{18}\text{O}$ record of site 607 so that all Atlantic isotopic records would be tied to the same time scale.

Results

Stable Isotopes – *Globigerina bulloides*

The planktic oxygen isotopic record of site 1090 can be divided into three segments based on changes in signal variability (Figure 3-6a). During the late Pliocene and early Pleistocene (between 2.9 and 1.55 Ma), the $\delta^{18}\text{O}$ signal was marked by long-wavelength, low-amplitude fluctuations with values varying within a range of 0.5‰. At 1.55 Ma (MIS 52), the $\delta^{18}\text{O}$ variability increased to ~1‰ and remained within this range until

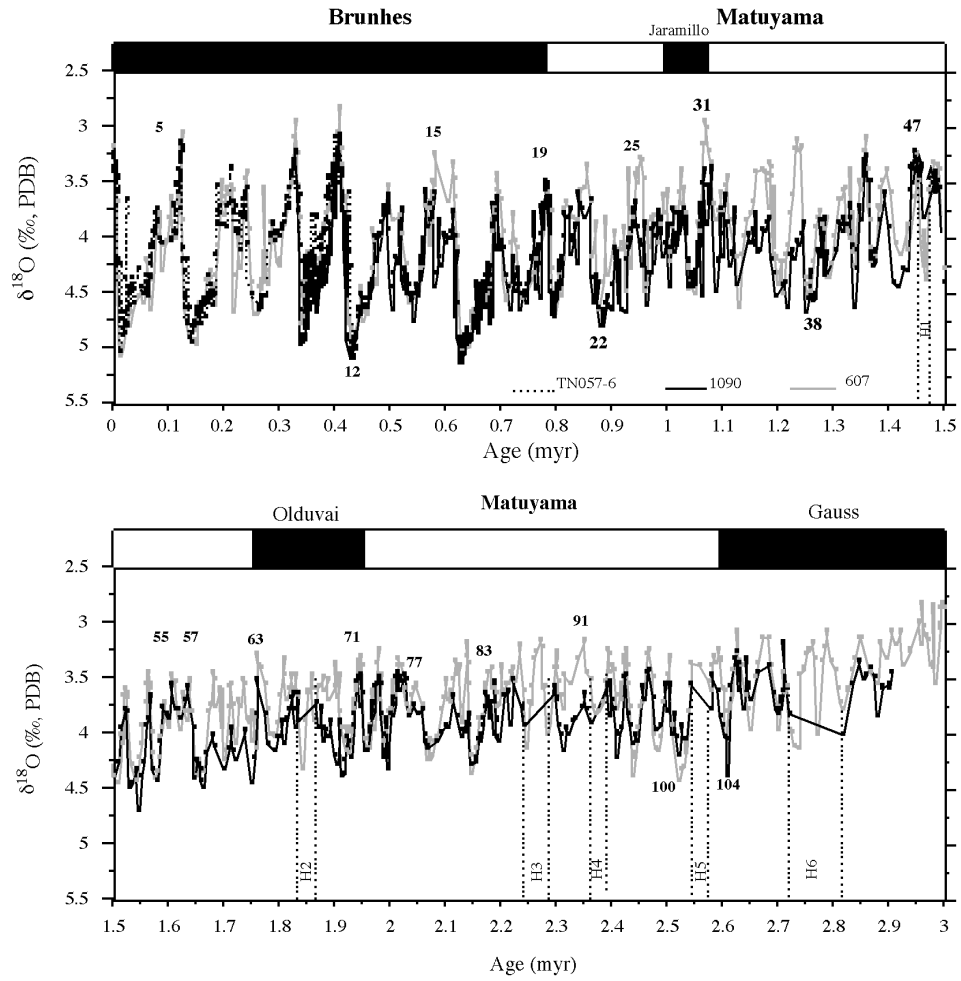


Figure 3-4. Oxygen isotopic records of benthic foraminifera (*Cibicoides wuellerstorfi*) from piston core TTN057-6-PC4 (dashed line; Hodell et al. [2000]), site 1090 (bold solid line; this study) and site 607 (gray solid line; Ruddiman et al. [1989]; Raymo et al., [1990b]) versus age with magnetic stratigraphy and selected isotopic stages labeled. Hiatuses in the record from site 1090 are noted by vertical dashed lines (Table 3-4).

Table 3-3. Age-Depth points for sites 1090 and 982.

Site 1090

Depth (mcd)	Age (Ka)	Depth (mcd)	Age (Ka)	Depth (mcd)	Age (Ka)
0.03	0	28.05	864.39	45.12	1915.1
0.75	20	31.38	986.6	45.77	1948.4
2.569	64	33.23	1048.8	46.52	1988.4
3.139	80	34.58	1088.5	47.54	2031.5
3.589	100	35.39	1123.2	47.69	2059.2
4.289	122	36.33	1192.8	47.99	2084.4
4.529	128	36.97	1249	48.94	2147.6
6.329	188	37.72	1288.6	50.24	2193
6.869	228	38.47	1336.6	50.74	2242.3
7.086	238	39.12	1372.7	50.94	2295.1
7.906	270	39.52	1419.7	51.84	2361.4
8.356	296	40.37	1457.9	51.89	2391.2
8.88	329.61	40.77	1490	52.58	2436.7
9.0031	338.71	41.02	1525.7	53.08	2487.9
13.227	425.23	41.47	1566.9	53.68	2543.6
16.21	522.97	42.47	1662.4	53.73	2577.1
17.16	560.84	43.12	1722.1	55.03	2650
18.11	616.08	43.42	1758.9	56.08	2720.2
21.81	682.8	43.67	1791.8	56.13	2817.8
24.96	782.9	44.37	1835.1	56.53	2879.8
27.01	811.3	44.42	1866.5	57.33	2903.5

Site 982

(mcd)	(Ka)	(mcd)	(Ka)	(mcd)	(Ka)
0.02	0	30.05	1208.9	49.45	2242.3
0.57	5.8474	30.45	1249	49.5	2284.6
3.02	131.4	31.1	1288.6	50.03	2310.7
3.62	183.58	31.9	1336.9	50.78	2370.5
4.97	245.56	32.35	1367.1	51.43	2410
6.92	339.55	33.45	1413.1	52.23	2436.7
10.09	422.98	33.6	1430.5	53.28	2481.8
11.64	476.67	34.1	1464.8	54.53	2521.5
14.14	528.95	34.55	1501.2	56.18	2577.1
16.1	629.2	35.25	1541.4	57.48	2603
17.63	682.8	37.73	1662.4	57.5	2604.6
18.73	707.4	39.08	1756.7	57.55	2618
20.03	782.9	39.7	1758.9	58.15	2650
20.63	810.04	40.4	1782.9	59.69	2701.6
22.48	862.18	40.5	1795.7	61.14	2736.4
23.53	926.37	41.1	1839.8	62.39	2770.5
24.58	959.15	42.45	1919.2	63.39	2817.8
25.28	1005.4	43.25	1948.4	64.64	2879.8
26.13	1037.3	44.15	1993	65.79	2983.5
29.15	1128.9	45.75	2065.7	68.17	3150.2
30	1194.8	47.8	2147.6	73.08	3299.8

Table 3-4. Hiatuses present in site 1090.

Hiatus	Depth (mcd)	Age (Ka)	missing Marine Isotopic Stage (MIS)
H1	40.37	1458-1476	48
H2	44.37	1835-1867	66-67
H3	50.79	2256-2295	86-88
H4	51.84	2361-2391	90/91
H5	53.68	2543-2577	101
H6	56.08	2720-2820	110-114

~0.9 Ma. Beginning at ~0.9 Ma, the variability of the $\delta^{18}\text{O}$ signal increased again, exhibiting a range of 1.5‰ and occasionally greater difference in glacial-to-interglacial values. For example, the planktic $\delta^{18}\text{O}$ difference between interglacial MIS 11 and glacial MIS 12 was >2.0‰.

Isotopic variation in the planktic $\delta^{13}\text{C}$ record is relatively constant between 2.9 to ~0.9 Ma with values similar to the Holocene (Figure 3-6b). A decrease of ~0.3‰ occurred between ~0.9 and 0.6 Ma, followed by a >1‰ increase that culminated during MIS 11 and 13 in the mid-Brunhes [Hodell et al., 2003b]. Planktic carbon isotopic values decreased again after MIS 11 to mean values of ~0‰.

Stable Isotopes – *Cibicidoides wuellerstorfi*

The benthic oxygen isotopic records of sites 1090 and 982 (Figures 3-5 and 3-6c) are similar to standard records and will not be described. Benthic $\delta^{18}\text{O}$ is used as the primary correlation tool to synchronize the records among sites in order to calculate inter-site $\delta^{13}\text{C}$ gradients. From the base of the record at 2.9 Ma to 1.55 Ma, the benthic $\delta^{13}\text{C}$ signal at site 1090 varies between -0.5 to 0.5‰ (Figure 3-6d). During this interval, three glacial stages (MIS 82, 72, and 70) exhibit unusually strong $\delta^{13}\text{C}$ depletions when values drop below -1‰. A major change in the character of the benthic $\delta^{13}\text{C}$ signal occurs at ~1.55 Ma (MIS 52). Thereafter, minimum $\delta^{13}\text{C}$ values during glacial periods are almost always less than -1‰. With few exceptions, mean interglacial $\delta^{13}\text{C}$ values between ~1.6 and 0.9 Ma were lower than those in the periods preceding and following this interval. At ~0.9 Ma, the amplitude of the glacial-to-interglacial $\delta^{13}\text{C}$ signal increases and values generally vary between 0.3 and -1.3‰ for the remainder of the late Pleistocene. Two periods of exceptionally high benthic $\delta^{13}\text{C}$ values are associated with MIS 11 and 13.

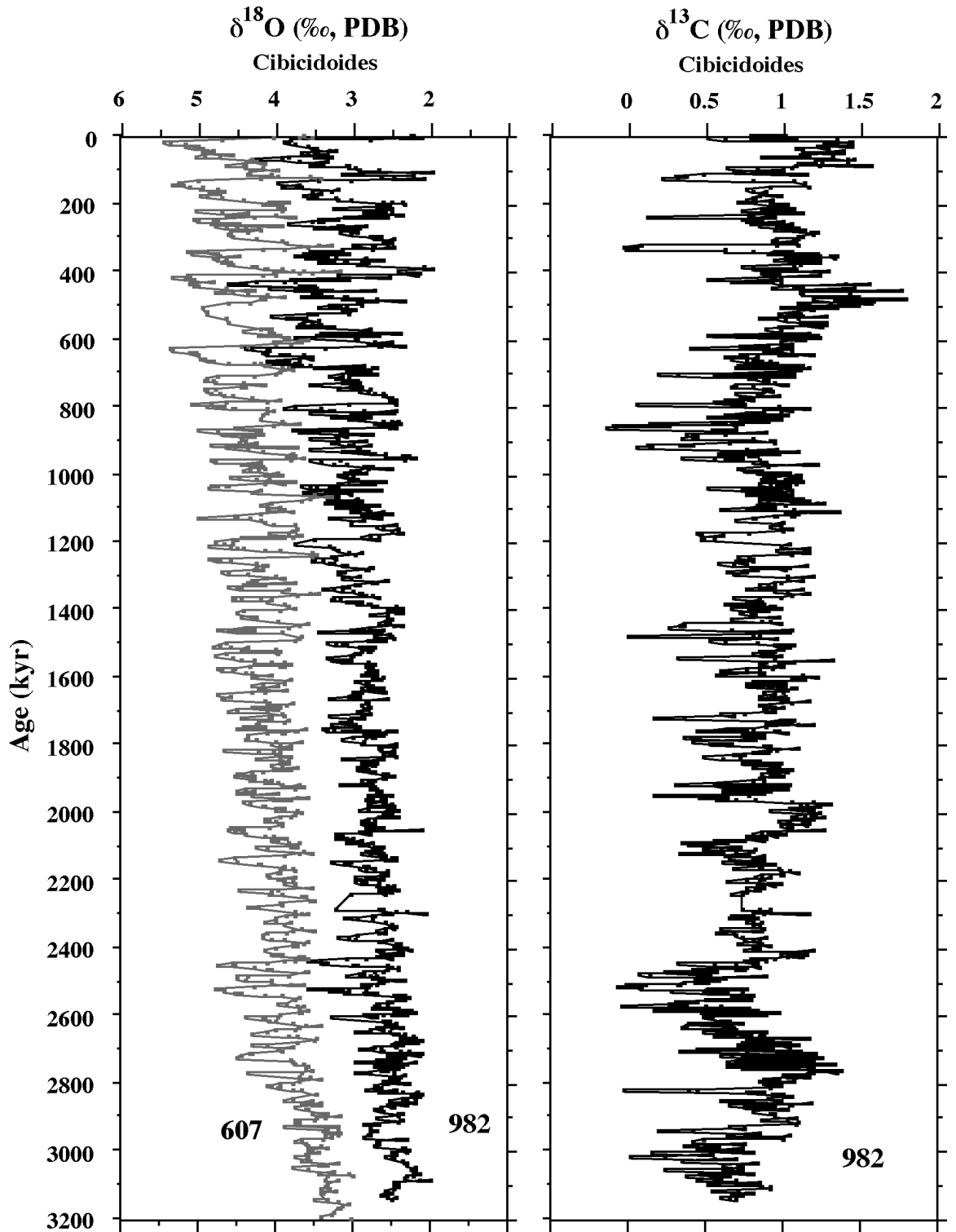


Figure 3-5. Oxygen (A) isotopic records of benthic foraminifera (*Cibicoides wuellerstorfi*) from site 982 and site 607 versus age. Plots have been offset for clarity by adding 1‰ to the site 607 data. (B) Carbon isotopic record of benthic foraminifera (*Cibicoides wuellerstorfi*) from site 982 versus age.

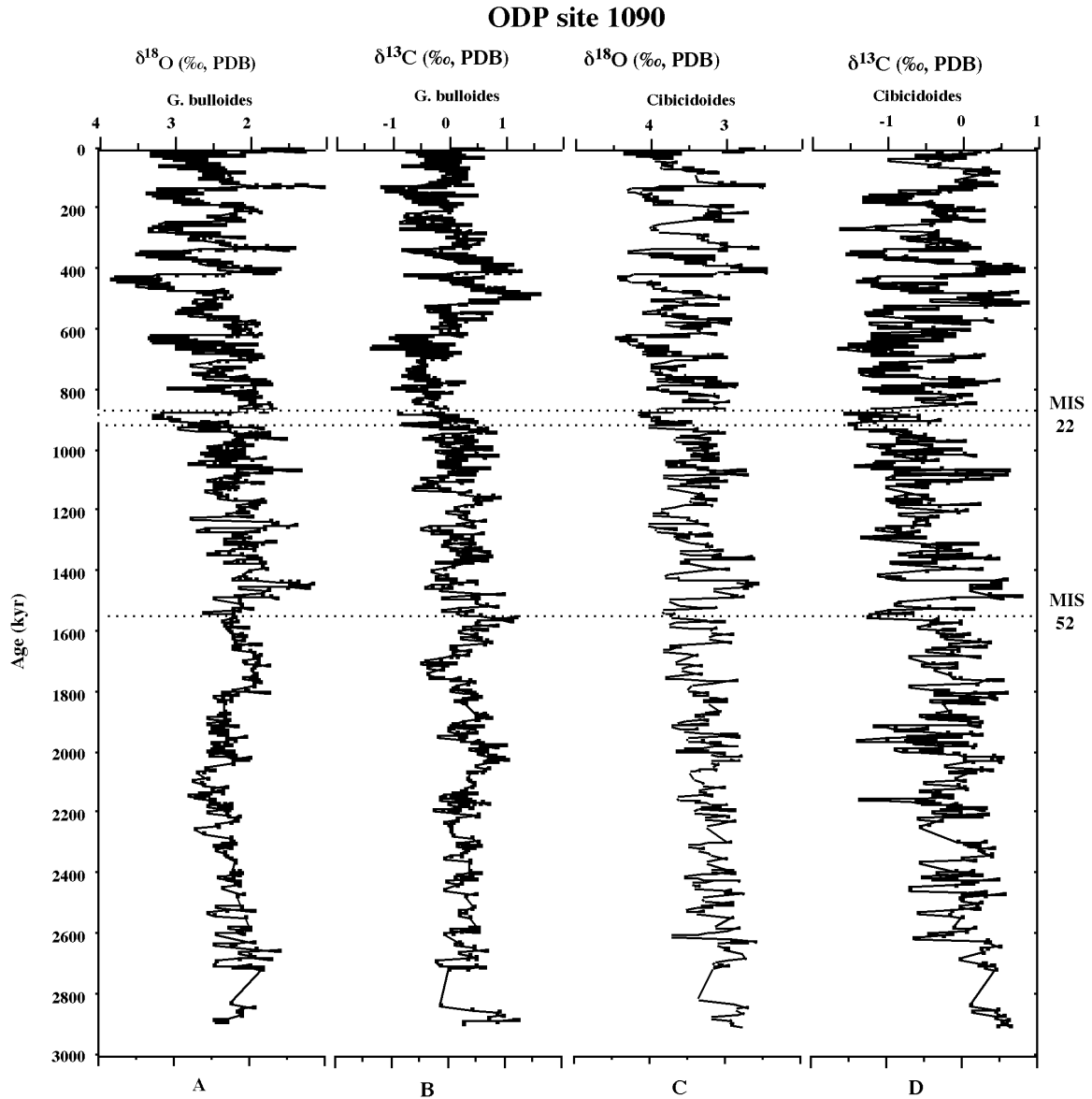


Figure 3-6. Oxygen isotopic (A) and carbon isotopic (B) records for the planktic foraminifera *G. bulloides* in site 1090. Oxygen isotopic (C) and carbon isotopic (D) records of *Cibicidoides* in site 1090. The dashed line represents long-term change in mean values of the *Cibicidoides* $\delta^{13}\text{C}$ record. The curve was calculated using the Least Squared error method with a smoothing factor that considered 20% of the data when smoothing. The horizontal lines denote MIS 52 and MIS 22 in all records.

Carbon Isotopic Gradients

I calculated benthic carbon isotopic gradients between the Southern Ocean (site 1090) and the Pacific (site 849), and among site 1090 and Atlantic sites 982, 607, 925, and 929 (Figure 3-7, Table 3-1 for references). Each of these records was constructed using the benthic foraminifera *Cibicidoides* and has been tied to the common time scale of site 607. All records were interpolated to a constant 3 kyr interval before subtraction. Because the calculation of carbon isotopic gradients may introduce a bias to the records due to slight time scale mismatches and interpolation of data, the original carbon isotopic records from sites 982, 607, 929, 1090, and 849 are plotted in Figures 3-8 and 3-9.

Southern Ocean - Pacific $\delta^{13}\text{C}$ gradients

From ~ 2.6 to 1.55 Ma, mean $\delta^{13}\text{C}_{849-1090}$ values were low with a mean of $\sim 0\text{‰}$ (Figure 3-7a). In this interval, site 1090 benthic $\delta^{13}\text{C}$ values decrease briefly to values significantly lower than the Pacific during glacial stages 82, 72, and 70, which are thought to be particularly strong glaciations [Raymo et al., 1989; Hodell and Venz, 1992] (Figure 3-8). At ~ 1.55 Ma (MIS 52), glacial $\delta^{13}\text{C}$ values at site 1090 decreased markedly (Figure 3-8) and were then always lower than deep Pacific values with a gradient as high as 1‰ (Figure 3-7a). Interglacial $\delta^{13}\text{C}$ gradients between the Southern Ocean and the deep Pacific remained near zero, although occasionally interglacial $\delta^{13}\text{C}$ values in the Southern Ocean were more than 0.5‰ higher than those in the Pacific.

Atlantic basin $\delta^{13}\text{C}$ gradients

607-1090 / 925-1090 (deep North Atlantic - South Atlantic). Because the carbon isotopic records from sites 925 and 607 are similar, the gradients between these sites and 1090 ($\delta^{13}\text{C}_{925-1090}$ and $\delta^{13}\text{C}_{607-1090}$) are described simultaneously (Figure 3-7b). From 2.6 to 1.55 Ma, the mean carbon isotopic gradient between the deep North Atlantic (site

607/925) and the Southern Ocean (site 1090) was relatively constant at $\sim 1\text{‰}$ (Figure 3-7b). At 1.55 Ma, glacial $\delta^{13}\text{C}$ values in the Southern Ocean became strongly depleted relative to values in the North Atlantic (Figure 3-9), resulting in an increase in the $\delta^{13}\text{C}_{607-1090}$ gradients (to $\sim 1.5\text{‰}$) during glacials between 1.55 and 1.25 Ma (Figure 3-7b). At 1.25 Ma, glacial $\delta^{13}\text{C}$ values in the North Atlantic decreased to near Southern Ocean values (Figure 3-9) resulting in low $\delta^{13}\text{C}_{607-1090}$ ($\sim 0\text{‰}$) during glacials and higher gradients during interglacials (Figure 3-7b). A shift toward lower mean $\delta^{13}\text{C}_{607-1090}$ and greater glacial/interglacial variability began at ~ 0.9 Ma (MIS 22) and continued throughout the late Pleistocene.

982-607 (intermediate North Atlantic - deep North Atlantic). Between 2.6 and 1.55 Ma, the gradient between the intermediate and deep North Atlantic ($\delta^{13}\text{C}_{982-607}$) was near zero (Figure 3-7c). Glacial $\delta^{13}\text{C}_{982-607}$ increased between 1.55 and 1.25 Ma when glacial $\delta^{13}\text{C}$ values at site 607 in the deep North Atlantic decreased relative to intermediate depth site 982 (Figures 3-7c and 3-8). During glacial periods after 1.25 Ma, the gradient between intermediate and deep $\delta^{13}\text{C}$ values strengthened (to $>1\text{‰}$), whereas the interglacial gradients remained near zero. At 0.9 Ma, glacial $\delta^{13}\text{C}_{982-607}$ increased further and large gradients persisted throughout the late Pleistocene (Figure 3-7c).

929-1090 (deep tropical Atlantic - Southern Ocean). Between 2.6 and 1.8 Ma, carbon isotopic values in the deep tropical North Atlantic (site 929) were similar to those in the Southern Ocean (site 1090) resulting in $\delta^{13}\text{C}_{929-1090}$ values varying between 0 and 1‰ (Figures 3-7d and 3-9). From 1.8 to 1.55 Ma, $\delta^{13}\text{C}_{929-1090}$ increased owing to an increase in carbon isotopic values at site 929. At 1.25 Ma, glacial gradients between sites 929 and 1090 again approached zero, as $\delta^{13}\text{C}$ values in the North Atlantic

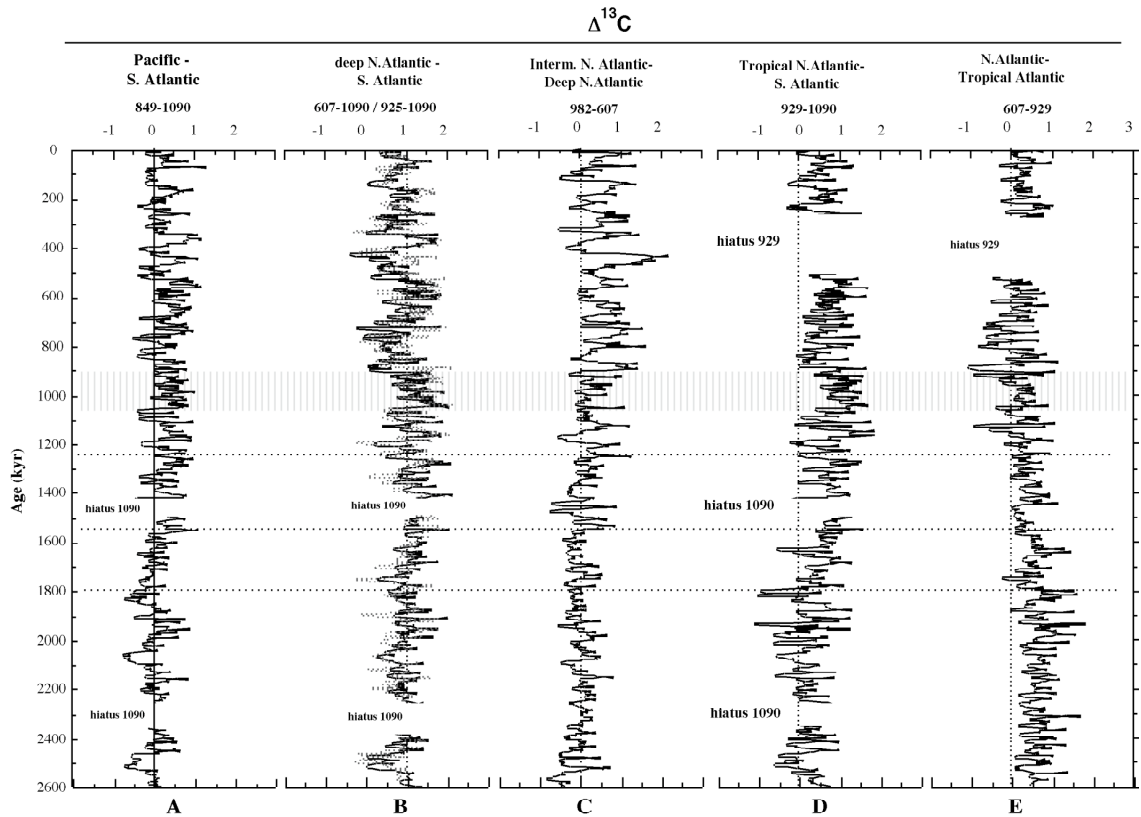


Figure 3-7. Calculated benthic carbon isotopic gradients between the Southern Ocean (site 1090) and the Pacific (site 849) and among a latitudinal and depth transect of the Atlantic including sites 982, 607, 925, 929, and 1090.

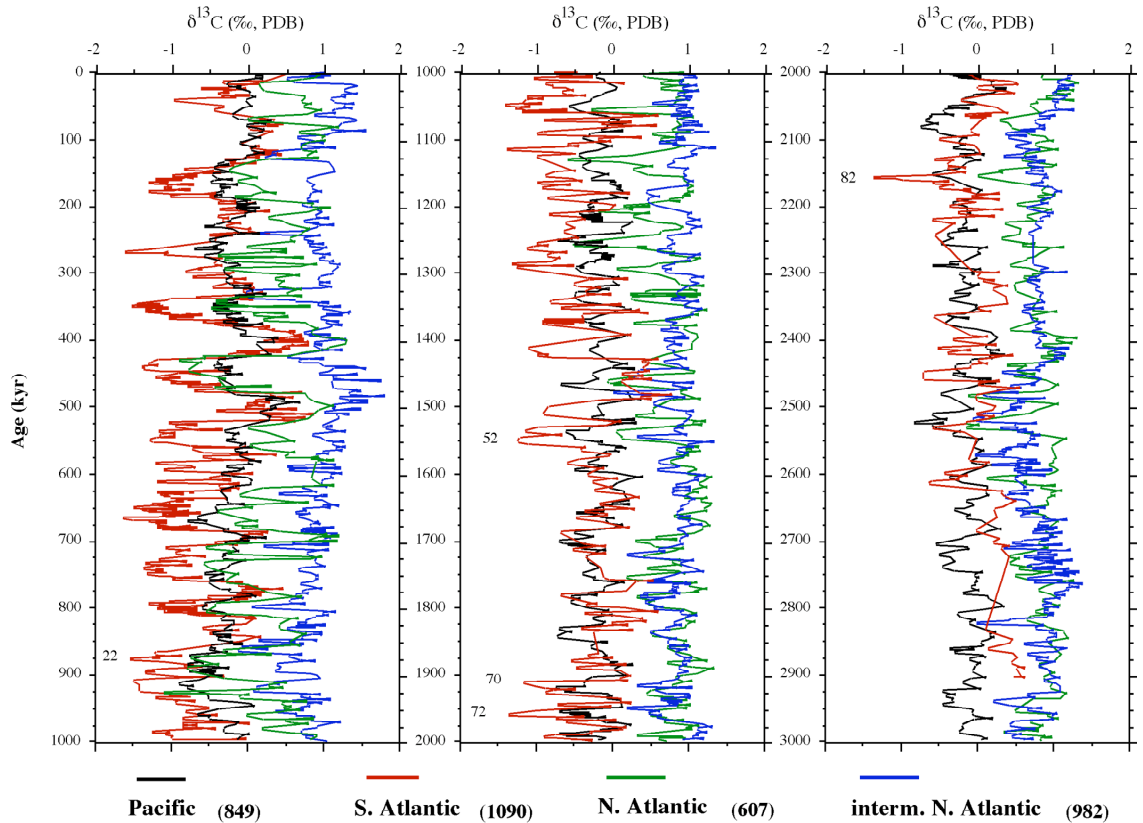


Figure 3-8. Comparison of the Southern Ocean benthic $\delta^{13}\text{C}$ record from site 1090 (red) with similar records from cores located within other deep-water end member locations: site 982 (mid-depth North Atlantic; blue), site 607 (deep North Atlantic; green), and site 849 (deep Pacific; black). Refer to Table 3-1 for core locations and references.

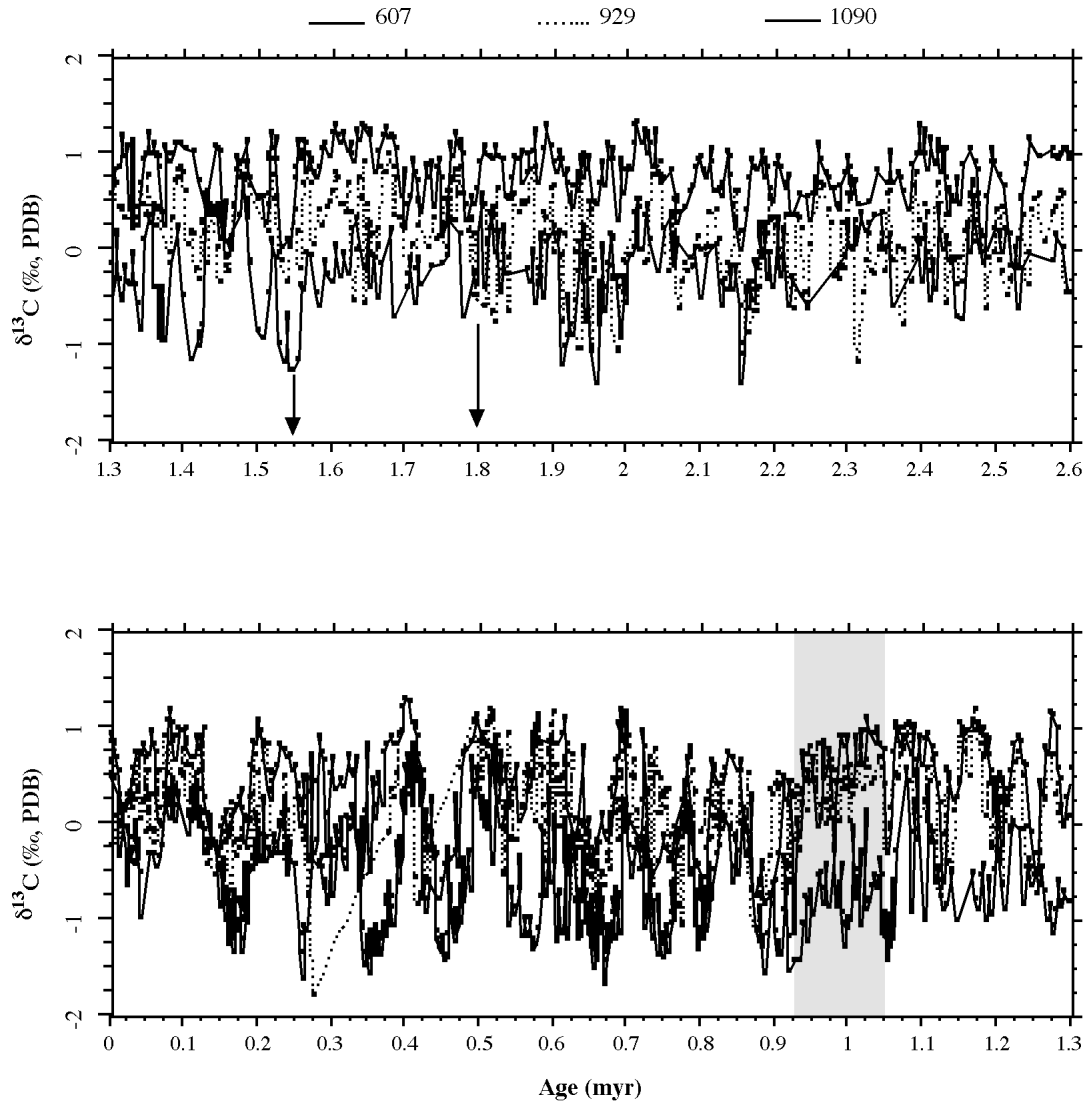


Figure 3-9. Comparison of the Southern Ocean benthic $\delta^{13}\text{C}$ record from site 1090 (heavy dark line) with similar records from site 929 (deep equatorial North Atlantic; dashed line) and site 607 (deep North Atlantic; thin dark line). Refer to Table 3-1 for core locations and references.

began to undergo strong glacial decreases (Figure 3-9). Between 1.05 and 0.90 Ma, mean $\delta^{13}\text{C}_{929-1090}$ was high with little glacial/interglacial variation compared to the intervals before and after this period (Figure 3-7d). The deep tropical Atlantic and the Southern Ocean maintained a uniformly high $\delta^{13}\text{C}$ gradient during this time (Figure 3-9). After ~ 0.9 Ma, mean $\delta^{13}\text{C}_{929-1090}$ decreased as carbon isotopic values in both the North and South Atlantic underwent large glacial/interglacial change (Figures 3-7 and 3-9).

607-929 (deep North Atlantic - deep tropical Atlantic). Between 2.6 and 1.8 Ma, the deep North Atlantic (site 607) and the deep tropical Atlantic (site 929) generally maintained a carbon isotopic gradient between 0.2 and 1.2‰ (Figure 3-7e). During the interval from 1.8 to 1.55 Ma, $\delta^{13}\text{C}_{607-929}$ varied between 0 and 1‰ as carbon isotopic values at site 929 became more similar to those at site 607 (Figures 3-7e and 3-9). Mean $\delta^{13}\text{C}_{607-929}$ decreased further after 0.9 Ma, to ~ 0 ‰, and the variability of the $\delta^{13}\text{C}$ gradient increased between sites 929 and 607.

Discussion

Inter-Site Comparison of Benthic Carbon Isotopic Records

Although the Southern Ocean is an ideal location for recording SCW $\delta^{13}\text{C}$ variability, the reliability of benthic $\delta^{13}\text{C}$ as a tracer of deepwater circulation has been questioned because benthic $\delta^{13}\text{C}$ values during glacial periods in the Southern Ocean were less than those in the deep Pacific [Mackensen et al., 1993; Mackensen and Bickert, 1999]. Glacial benthic $\delta^{13}\text{C}$ in the Southern Ocean may suffer from productivity overprints to a greater extent than in other ocean basins (for review see Mackensen and Bickert [1999]). Variations in Cd/Ca of benthic foraminifera suggest little or no change in nutrient concentrations of SCW during glaciations [Boyle, 1988; Oppo and Rosenthal,

1994; Lea 1995; Rosenthal et al., 1997], thereby contradicting glacial benthic $\delta^{13}\text{C}$ results indicating large increases in TCO_2 and inferred nutrients. Ca/Cd data are not completely without complicating factors, however, and interpretation can be ambiguous because of depth-dependent and dissolution effects [McCorkle et al., 1995].

To assess the reliability of the site 1090 benthic $\delta^{13}\text{C}$ signal as a monitor of SCW, I compare it with similar records from piston core RC13-229 [Oppo et al., 1990] and ODP site 704 [Hodell and Venz, 1992], which have been used previously to monitor the $\delta^{13}\text{C}$ history of SCW in the late Pleistocene and Plio-Pleistocene, respectively (Table 3-2, Figure 3-10). Despite the pronounced differences in the geographic and surface oceanographic settings of these sites, the benthic $\delta^{13}\text{C}$ record of site 1090 is remarkably similar to those at RC13-229 and site 704 (Figure 3-10). The common denominator among all three records is they are all influenced by SCW, which suggests that the combined benthic $\delta^{13}\text{C}$ signals accurately reflect the carbon isotopic history of SCW. Further evidence that local or regional productivity changes did not significantly influence the benthic $\delta^{13}\text{C}$ record at site 1090 is provided by planktic (*G. bulloides*) $\delta^{13}\text{C}$ and organic carbon accumulation rates. Planktic $\delta^{13}\text{C}$ values at site 1090 were lower during glacial intervals which is contrary to the trend predicted for enhanced surface water productivity (Figure 3-6). In addition, organic carbon accumulation at site 1090 shows no change at 1.5 Ma as would be expected if productivity increased at this time [Diekmann and Kuhn, 2002]. The similarity of the $\delta^{13}\text{C}$ records from RC13-229, site 704, and site 1090, plus the additional proxy evidence from site 1090 argues against a significant productivity overprint (i.e. "Mackensen Effect"), and suggests that the benthic $\delta^{13}\text{C}$ record at site 1090 accurately reflects changes in the $\delta^{13}\text{C}$ of SCW. Consequently,

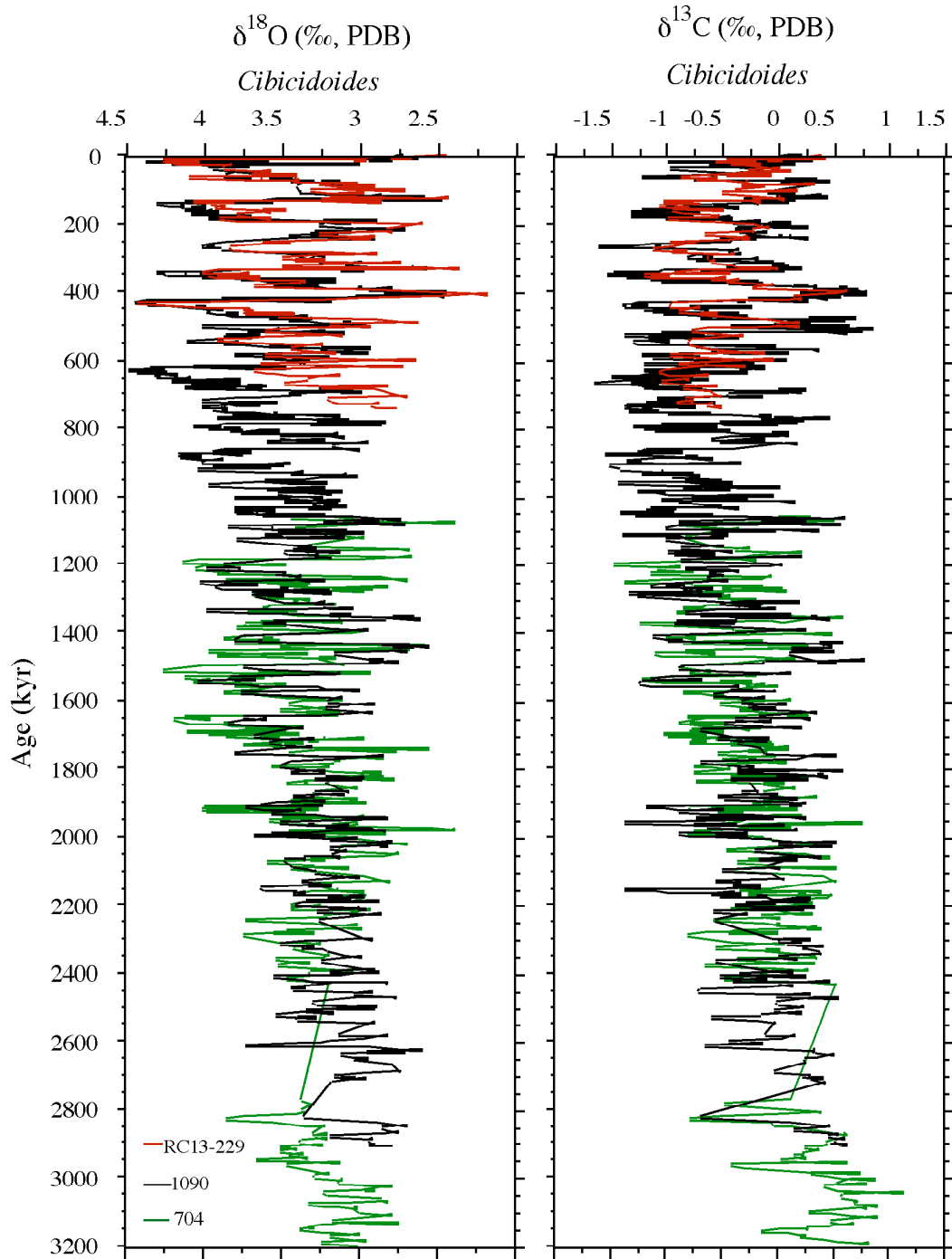


Figure 3-10. Oxygen (A) and carbon (B) isotopic records of benthic foraminifera from site 1090 (black; this study), site 704 (green; Hodell and Venz [1992]), and piston core RC13-229 (red; Oppo et al. [1990]). Note the similarity of $\delta^{13}\text{C}$ values in the interval of overlap between sites 1090 and 704 from 2.9 to 1.1 Ma and the overlap between site 1090 and piston core RC13-229 from 0.8 to 0 Ma.

I used the $\delta^{13}\text{C}$ record at site 1090 as the SCW end member in the calculation of the mixing ratios of NCW and SCW in the deep Atlantic during the Plio-Pleistocene (Figure 3-11).

Late Pliocene / Early Pleistocene

During the late Pliocene (2.6 to 1.8 Ma), %NCW in the deep North Atlantic at site 607 was high, whereas site 929 to the south was dominated by SCW (Figure 3-11). This suggests that the NCW/SCW boundary was located further north and/or at shallower depth than today (Figure 3-12). The upper limit of SCW, however, remained deeper than ~3000 m because carbon isotopic values at site 925 are similar to site 607 throughout this interval [Bickert et al., 1997]. The large carbon isotopic gradient between sites 607 and 1090 in the late Pliocene suggests relatively strong NCW production, and therefore, the dominance of SCW at site 929 is unlikely due to reduced NCW [Raymo et al., 1990b; Raymo et al., 1992; Mix et al., 1995]. Alternatively, if NCW was less dense in the late Pliocene then the NCW/SCW interface would be found at shallower depth. Indeed, Sikes et al. [1991] interpreted low carbon isotopic values in the deep eastern equatorial Atlantic as indicating a greater influence of southern source water at nearly all times in the late Pliocene (2.6 to 2.1 Ma).

At ~1.8 Ma, carbon isotopic values at site 929 increased to values mid-way between the deep North Atlantic and the Southern Ocean. Calculated %NCW at site 929 indicates the proportion of NCW increased significantly between 1.8 and 1.6 Ma (Figure 3-11). This change suggests the boundary between SCW and NCW shifted deeper and/or further south in the deep equatorial Atlantic after ~1.8 Ma (Figure 3-12). Calculated %NCW values at site 607 were high, indicating continued strong NCW influence in the deep North Atlantic during the early Pleistocene, particularly in the interval between ~1.8

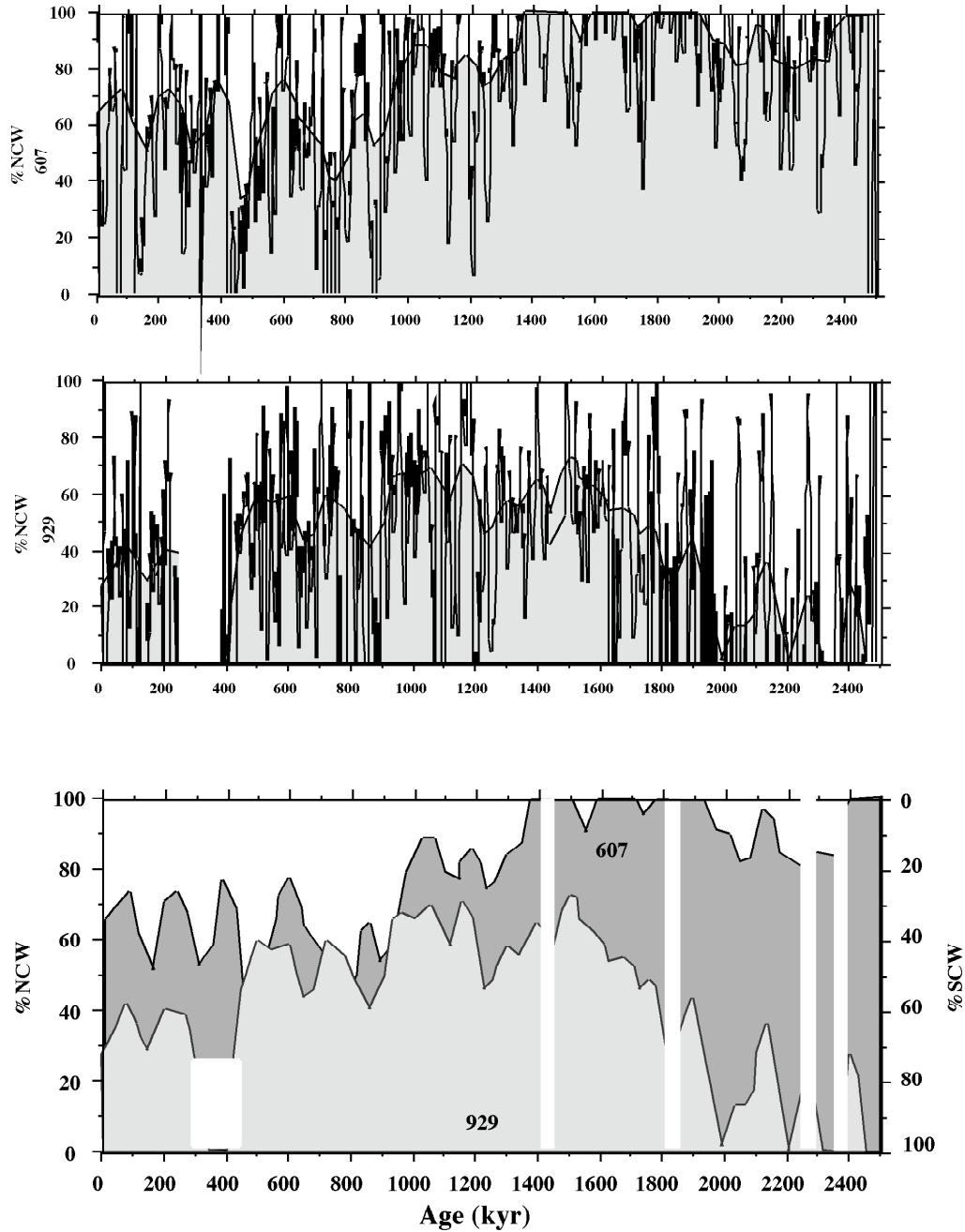


Figure 3-11. Calculation of percent NCW at site 607 (A) and site 929 (B) using Equation 1 with site 982 as the NCW end member and site 1090 as the SCW end member (solid line). The line drawn through the plot is a curve calculated using the weighted Least Squared error method with a smoothing factor that considers 3% of the data when smoothing. Variation in the long-term mean %NCW at site 607 and 929 represented by the weighted curves in (A) and (B) is shown without large glacial/interglacial variation in (C).

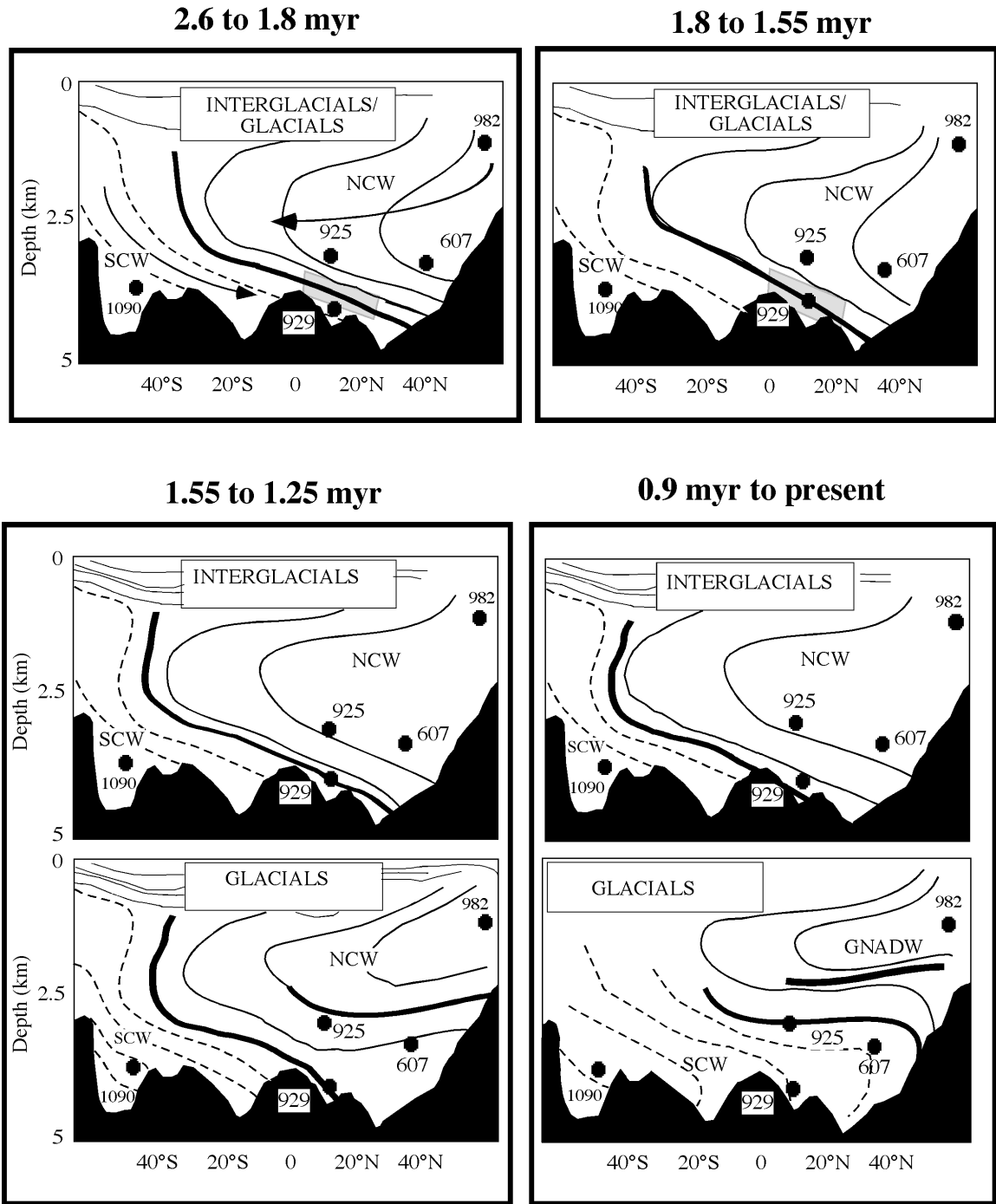


Figure 3-12. Schematic representation of glacial-to-interglacial changes in deep-water mass boundaries in the North Atlantic inferred from benthic $\delta^{13}\text{C}$ records and $\delta^{13}\text{C}$ gradients from sites 982, 607, 925, 929, and 1090.

to ~1.3 Ma (Figure 3-11). Mix et al. [1995] estimated the period between 2.1 and 1.3 Ma to be the time of greatest NCW production of the past 3.0 myr.

I suggest that the increased %NCW at site 929 between 1.8 and 1.6 Ma was due to an increase in the density of NCW and a deepening of the NCW/SCW interface. This interpretation is supported by evidence from the Norwegian-Greenland Sea (NGS) at that time. Prior to ~1.8 Ma, NCW was not forming in the NGS as it was during interglacials of the late Pleistocene, but instead, deep-water formation was occurring in the high latitude North Atlantic south of the Greenland-Scotland Ridge [Jansen et al., 2000]. The NGS was dominated by stable polar conditions that inhibited deep-water production prior to ~1.8 Ma [Henrich, 1989; Thiede et al., 1998; Jansen et al., 2000; Henrich et al., 2002]. Between ~1.9 and 1.7 Ma, the first intrusions of a Proto-Norwegian Current into the southeastern NGS initiated NCW formation in this area. This change in the source area of deep-water formation may have resulted in a cooling of NCW, which increased its density and deepened the NCW/SCW boundary in the equatorial Atlantic.

Early Pleistocene Change in the Southern Ocean

At 1.55 Ma a strong depletion of glacial $\delta^{13}\text{C}$ values occurred in the Southern Ocean and in the deep North Atlantic. Low glacial $\delta^{13}\text{C}$ values at site 607 have been attributed to the first significant glacial reduction in NCW production [Raymo et al., 1990b], whereas formation of a carbon isotopic gradient between 3000 and 3500 m (site 925 and 607) in the North Atlantic suggests the formation of a shallow glacial NCW [Duplessy et al., 1988; Oppo and Fairbanks 1987; Oppo and Lehman, 1993; Bickert et al., 1997].

The shift in glacial benthic foraminiferal $\delta^{13}\text{C}$ values at site 1090 during MIS 52 (~1.55 Ma) marks the beginning of the late Pleistocene pattern whereby glacial $\delta^{13}\text{C}$

values in the Southern Ocean are less than those in the Pacific (Figure 3-8). Several processes may account for the “lower-than-Pacific” glacial benthic $\delta^{13}\text{C}$ values beginning at ~ 1.55 Ma. Hodell and Venz [1992] attributed it to enhanced reduction of NADW during glacials. However, variations in the relative flux of NADW to the South Atlantic by itself can not explain carbon isotopic values in the Southern Ocean that are up to 1‰ lower than those in the deep Pacific. If NADW production ceased completely, then the $\delta^{13}\text{C}$ of SCW would fall to the Pacific value, but would not decrease further. The lower $\delta^{13}\text{C}$ values in the Southern Ocean might be explained by formation of deep-water in the north Pacific, but evidence for such a deep-water source is lacking or too limited to explain the observed $\delta^{13}\text{C}$ values of SCW [Keigwin, 1987; Keigwin, 1998; Lund and Mix, 1998].

Clay mineral ratios (kaolinite/chlorite and quartz/feldspar) measured at site 1090 indicate that the strongly depleted $\delta^{13}\text{C}$ values in the Southern Ocean were not accompanied by a change in deep-water transport patterns [Diekmann and Kuhn, 2002]. If production of NCW or SCW did not change at 1.55 Ma, then the low glacial $\delta^{13}\text{C}$ values must be related to changes in the chemistry of the source waters for SCW. For example, decreased nutrient utilization and/or gas exchange with the atmosphere in high-latitude surface water may account for the lower glacial $\delta^{13}\text{C}$ values of SCW.

At 1.55 Ma, pronounced changes occurred in the $\delta^{13}\text{C}$ of *N. pachyderma* and in opal percentages at site 704 (47°S) in the Polar Frontal Zone (PFZ). An increase in nutrient concentrations or surface stratification at this time favored diatom production in the subantarctic South Atlantic during glacial periods [Hodell and Venz, 1992]. Increased biogenic silica fluxes and lower planktic $\delta^{13}\text{C}$ during glacials at site 704

beginning at 1.55 Ma may signify increased cross-frontal transport of dissolved silica and nutrients as diatoms south of the PFZ were unable to utilize these biolimiting elements due to expanded sea ice cover [Charles et al., 1991]. Sea ice cover and increased stratification of the ocean surface beginning with MIS 52 would have limited gas exchange with the atmosphere, thus preventing loss of oceanic CO₂ and lowering $\delta^{13}\text{C}$. Expansion of sea ice and the resulting decrease in the thermodynamic imprint of air-sea exchange on $\delta^{13}\text{C}$ of δCO_2 has been proposed previously to explain the low $\delta^{13}\text{C}$ values of benthic foraminifera in glacial-aged sediments in the Southern Ocean [Broecker, 1993]. Alternatively, a box model by Toggweiler [1999] suggested that it is possible to reduce $\delta^{13}\text{C}$ in the Southern Ocean to very low values without a substantial change in the nutrient content of glacial bottom water by limiting mixing between deep and mid-depth water in the Southern Ocean and by decreasing deep-water ventilation. Surface stratification and sea ice have also been implicated in a number of recent studies linking glacial lowering of atmospheric CO₂ to reduced deep-water ventilation in the Southern Ocean and [Francois et al., 1997; Elderfield and Rickaby, 2000; Sigman and Boyle, 2000; Stephens and Keeling, 2000].

The ventilation of SCW may also have been affected by the northward migration of high latitude wind fields in the Southern Ocean, similar to that observed for the Last Glacial Maximum. Toggweiler and Samuels [1993a, 1995] argued that modern export of Atlantic deep-waters into the circumpolar Antarctic is controlled by the wind stress at the latitude band of the Drake Passage. During warm periods when the wind axis is further south the regional Eckman divergence and northward Eckman drift draws Atlantic deep-water into the Antarctic region below the level of deep topographic ridges, NADW is drawn southward into the Southern Ocean. As the wind axis migrated north during

glacial periods, the geostrophic “pull” that draws Atlantic deep-water into the Antarctic region would diminish and the deep-waters of the Antarctic would become more isolated. Deepwater circulation in the South Atlantic sector of the Southern Ocean may have become restricted during glaciations, allowing the accumulation of metabolic CO₂ from the oxidation of ¹³C-depleted organic matter [Imbrie et al., 1992; Toggweiler and Samuels, 1993a, 1995]. Rhamstorf and England [1997], however, reported that the influence of Southern Ocean winds on NADW flow is not as strong as previously suggested by Toggweiler and Samuels [1993a, 1995]. Keeling and Stephens [2001] suggested that while westerly winds on the ACC ultimately drive northward Eckman drift and deep upwelling [Toggweiler and Samuels, 1993b, 1995], the magnitude of the northward drift and deep-water ventilation in the Atlantic is more dependent on freshwater forcing due to glacial/interglacial variation of Antarctic sea ice cover and associated changes in the oceans' salinity structure.

I propose that increased glacial severity at 1.55 Ma in the Southern Ocean permitted a northward expansion of sea ice that reduced productivity south of the PFZ, and decreased gas exchange and SCW ventilation. The increase in sea ice cover changed the chemistry of southern component source water resulting in increased nutrients, increased \square CO₂, and lowered \square ¹³C. The northerly migration of the westerlies at the Drake Passage during glacials may have weakened the magnitude of NCW export from the North Atlantic into the Southern Ocean and contributed to the reduction in SCW ventilation [Imbrie et al., 1992; Toggweiler and Samuels, 1993a, 1995]. Alternatively, loss of freshwater input to Antarctic waters due to expanded sea ice cover may have upset the salinity contrast between the North and South Atlantic, weakening global thermohaline circulation and reducing SCW ventilation [Keeling and Stephens, 2001].

In addition to the changes in deep-water circulation and surface hydrography in the Southern Ocean at 1.55 Ma [Raymo et al., 1990b; Hodell and Venz, 1992; Bickert et al., 1997; this study], other paleoclimatic records also indicate a change in climate at ~1.6 Ma. Rutherford and D'Hondt [2000] suggested enhanced heat transport from low to high latitude began at 1.5 Ma, based on the propagation of tropical semiprecessional cycles (with a period of ~11.5 kyr) to higher latitudes. Also at 1.5 Ma, rates of loess deposition in China increased and glacial/interglacial variation began to strongly correlate with the marine ice volume record [Bloemendal et al., 1995]. Increased African aridity and enhanced 41-kyr climate variability occurred at ~1.6 Ma, which approximately coincided with a change in the timing of Asian monsoon maxima in the precession and obliquity bands relative to the timing of maximum ice volume [deMenocal, 1995; Clemens et al., 1996]. These events do not appear to be linked to an obvious change in ice volume, but are rather related to strengthened interhemispheric coupling through thermohaline circulation.

The Mid-Pleistocene Transition

Beginning at ~1.2 Ma, the Mid-Pleistocene Transition (MPT) marks a shift from a climate system dominated by variation at a period of 41 kyr to one dominated by the 100-kyr cycle [Ruddiman et al., 1989; Berger and Jansen, 1994; Chen et al., 1995; Weber and Piasias, 1999; Diekmann and Kuhn, 2002]. The MPT represents a change in climate variability that included an increase in the strength of the 100-kyr cycle at 1.2 Ma, a rapid increase in global ice volume at ~0.9 Ma (MIS 22) with a shift to dominance of the 100-kyr cycle, and a further increase in the amplitude of the 100-kyr cycle at ~0.6 Ma [Berger and Jansen, 1994; Mudelsee and Schulz, 1997].

Some of these changes in the climate system during the MPT correlate with variations in deep-water circulation. Early in the MPT, deep-water circulation changes were centered in the North Atlantic. At 1.2 Ma, an increase in the carbon isotopic gradient between site 982 and site 607 indicates increased glacial suppression of NCW, which permitted penetration of SCW into the deep North Atlantic (Figure 3-7b). The large $\delta^{13}\text{C}$ gradient between sites 607 and 982 suggests strong differences in nutrient concentrations between the intermediate and deep-waters in the North Atlantic (Figure 3-7c) during glacial periods, similar to those observed in the late Pleistocene.

The carbon isotopic record from site 1090 does not indicate any marked changes in Southern Ocean deep-water circulation at 1.2 Ma (Figure 3-6d). However, other proxies at site 1090 show changes in both the time and frequency domains. Diekmann and Kuhn [2002] reported an increase in both the strength of the 100-kyr cycle and the glacial/interglacial variation in clay mineral ratios at 1.2 Ma, indicating a shift in the periodicity of deep-water transport into the Southern Ocean. The 100-kyr cycle gained strength in the site 1090 carbonate record at this time [Diekmann and Kuhn, 2002] and the SSST signal also contains a small increase in the 100-kyr power at 1.2 Ma that continued to build throughout the MPT [Becquey and Gersonde, 2002].

Between ~ 1.1 and 0.9 Ma, North Atlantic $\delta^{13}\text{C}$ records exhibited very low glacial-to-interglacial variability, which is similar to the early Pleistocene signal (Figures 3-7 and 3-9). Glacial $\delta^{13}\text{C}$ values at North Atlantic sites 607 and 929 remained persistently high and never approached Southern Ocean values, suggesting strong NCW throughout this interval during both glacial and interglacial periods. The Southern Ocean, however, maintained generally low carbon isotopic values with only two brief intervals where

interglacial $\delta^{13}\text{C}$ of SCW approached North Atlantic values, suggesting that the influence of NCW in the Southern Ocean was generally weak throughout this period. An interval of reduced variability in the clay mineral ratios at site 1090 between ~ 1.05 and 0.9 Ma lends support to this conclusion [Diekmann and Kuhn, 2002]. This period of reduced variability in Atlantic $\delta^{13}\text{C}$ records is similar in timing to a temporary decrease in the strength of the 100-kyr cycle between 1.1 and 0.9 Ma recorded in a $\delta^{18}\text{O}$ record from the tropical Indian Ocean [Chen et al., 1995]. Weak orbital forcing during this interval may explain the damped variability in Atlantic thermohaline circulation at this time.

At 0.9 Ma, a significant change occurred in the character of both surface and deep-water proxy signals in the Southern Ocean. At ~ 0.9 Ma, the range of glacial-to-interglacial variation in planktic $\delta^{18}\text{O}$ values (Figure 3-6) and SSTs [Becquey and Gersonde, 2002] increased markedly after 0.9 Ma. Interestingly, the bulk sediment data and clay mineral ratios do not show any significant changes at ~ 0.9 Ma in neither the time nor frequency domain [Diekmann and Kuhn, 2002].

Previous studies of changes in carbon isotopic records over the MPT indicate three main events occurred at 0.9 Ma [Raymo et al., 1990b, 1997]: 1) a global decrease in oceanic $\delta^{13}\text{C}$ values of $\sim 0.3\text{‰}$ that lasted until ~ 0.4 Ma; 2) an increase in the glacial suppression of NCW in the North Atlantic; and 3) an increase in the vertical nutrient gradient between the intermediate and deep Atlantic. Carbon isotopic results from site 1090 generally support these findings. A decrease in $\delta^{13}\text{C}$ values between 0.9 and 0.6 Ma is clearly present in the planktic record (Figure 6b), and supports the conclusion of Raymo et al. [1997] that the abrupt decrease in oceanic $\delta^{13}\text{C}$ resulted from a one-time addition of ^{13}C depleted terrestrial biomass due to global aridification. Benthic $\delta^{13}\text{C}$

values in the Southern Ocean, however, began to decline much earlier, at ~ 1.5 Ma, and reached minimum values (the lowest values of late Pleistocene glaciations) between ~ 0.9 Ma and 0.6 Ma (Figure 3-6d). Interglacial benthic $\delta^{13}\text{C}$ values were higher after 0.9 Ma, resulting in an increase in the range of glacial-to-interglacial variability of benthic $\delta^{13}\text{C}$ values after the MPT at 0.9 Ma. Large glacial-to-interglacial changes in benthic $\delta^{13}\text{C}$ began in both the Southern Ocean and the deep North Atlantic at ~ 0.9 Ma, indicating that ice volume and deep-water circulation became tightly coupled (Figure 3-9).

Raymo et al. [1997] noted increased severity of glacial NCW reductions at 0.9 Ma based on a comparison of the $\delta^{13}\text{C}$ record from site 607 with site 849 in the deep Pacific. Comparison of $\delta^{13}\text{C}$ gradients between site 607 and 1090 supports this conclusion (Figures 3-7 and 3-9). I disagree, however, with the explanation for why $\delta^{13}\text{C}$ values at site 607 are lower than those of the Pacific between 0.92 and 0.40 Ma. Raymo et al. [1997] suggested that lower-than-Pacific $\delta^{13}\text{C}$ values at site 607 indicated severe glacial suppression of NADW plus an additional aging effect, possibly a re-circulation gyre in the deep North Atlantic. Comparison of the record from site 607 to the new record from site 1090 suggests that low glacial $\delta^{13}\text{C}$ values at site 607 can be attributed to suppression of NCW plus mixing with SCW that had a highly depleted $\delta^{13}\text{C}$ composition.

Finally, strong glacial depletion of $\delta^{13}\text{C}$ values in the North Atlantic after 0.9 Ma reduced glacial $\delta^{13}\text{C}$ gradients between the deep North Atlantic and the Southern Ocean, and increased the vertical nutrient gradient between site 982 in the intermediate depth North Atlantic and site 607, which is consistent with previous results [Raymo et al., 1990b, 1997]. However, benthic $\delta^{13}\text{C}$ values at intermediate site 982 also began to increase slightly during glacials after 0.9 Ma, suggesting formation of a glacial North

Atlantic Intermediate Water that furthered strengthened the glacial vertical nutrient gradient in the North Atlantic [Venz et al., 1999] (Figures 3-7c and 3-12).

Ramifications of Using 1090 $\delta^{13}\text{C}$ to Compute %NCW

The new benthic $\delta^{13}\text{C}$ record from site 1090 indicates that the $\delta^{13}\text{C}$ of SCW had a different carbon isotopic history than the deep Pacific, particularly after 1.5 Ma (Figure 3-8). In previous studies, changes in the mixing ratio between NCW and SCW have been calculated using a deep Pacific $\delta^{13}\text{C}$ record due to the lack of an appropriate record from the Southern Ocean [Raymo et al., 1990b; Mix et al., 1995; Raymo et al., 1997]. As a result, previous calculations of %NCW (Equation 1) in the Atlantic using Pacific benthic $\delta^{13}\text{C}$ records to monitor SCW may have overestimated the degree of NADW suppression during glacial intervals. Here I recalculate %NCW for site 607 in the deep North Atlantic using site 982 as the NCW end member and site 1090 as the SCW end member (Figure 3-13). These results are compared with the same calculation using the Pacific record (site 849) as the Southern Ocean end member. Before recalculation of %NCW, all isotopic records (sites 982, 607, 1090, and 849) were interpolated to a constant 3.0 kyr sample spacing.

Although the general pattern remains the same (Figure 3-13), glacial reductions of NADW in the Pleistocene using site 1090 were not as severe as suggested by %NCW calculations using deep Pacific $\delta^{13}\text{C}$ values. This is not surprising because glacial $\delta^{13}\text{C}$ values in the Southern Ocean are generally lower than in the deep Pacific. For example, %NCW during MIS 12 never reach zero using site 1090. The differences between using site 1090 versus a Pacific record to calculate %NCW are as small as 10% and range to more than 20-30% during some glaciations, whereas the interglacial estimates of %NCW

are essentially the same because interglacial values at site 1090 are similar to the deep Pacific.

Raymo et al. [1990b, 1997] reported that increased glacial suppression of NADW occurred after ~0.9 Ma and that glacial %NADW began gradually increasing toward the present after ~0.4 Ma (Figure 3-13). Because these inferred changes in the relative strength of NADW suppression after 0.4 Ma do not correspond to changes in glacial severity (ice volume) as indicated by the benthic $\delta^{18}\text{O}$ record, Raymo et al. [1990b] suggested a decoupling between ocean circulation and ice volume. Our new %NCW index, however, does not indicate such a trend in the relative suppression of NADW during glacial intervals during the past 0.9 Ma (Figure 3-13). A reduction in %NCW occurred at the MPT (0.9 Ma), similar to the result of Raymo et al. [1997], but the reductions in %NCW during glacial periods between 0.9 and 0.5 Ma were generally similar in magnitude to those from 0.4 Ma to present, when calculated using the record from site 1090 (Figure 3-13). This is similar to calculated %NCW results from site 664, located in the South Atlantic on the eastern edge of the Romanche Fracture Zone [Raymo et al., 1997]. The apparent decoupling of deepwater circulation and global ice volume during the interval after 0.4 Ma may have been an artifact caused by using a carbon isotopic record from the deep Pacific rather than the Southern Ocean to represent SCW. There is, however, an amplitude mismatch between ice volume ($\delta^{18}\text{O}$) and %NCW even when calculated using site 1090. For example, a comparison of MIS 16 (a strong glacial with high $\delta^{18}\text{O}$ values) versus MIS 14 and 18 (lower maximum $\delta^{18}\text{O}$) reveals that the reduction of %NCW during MIS 16 was less than during weaker glacial stages 14 and 18 (Figure 3-13).

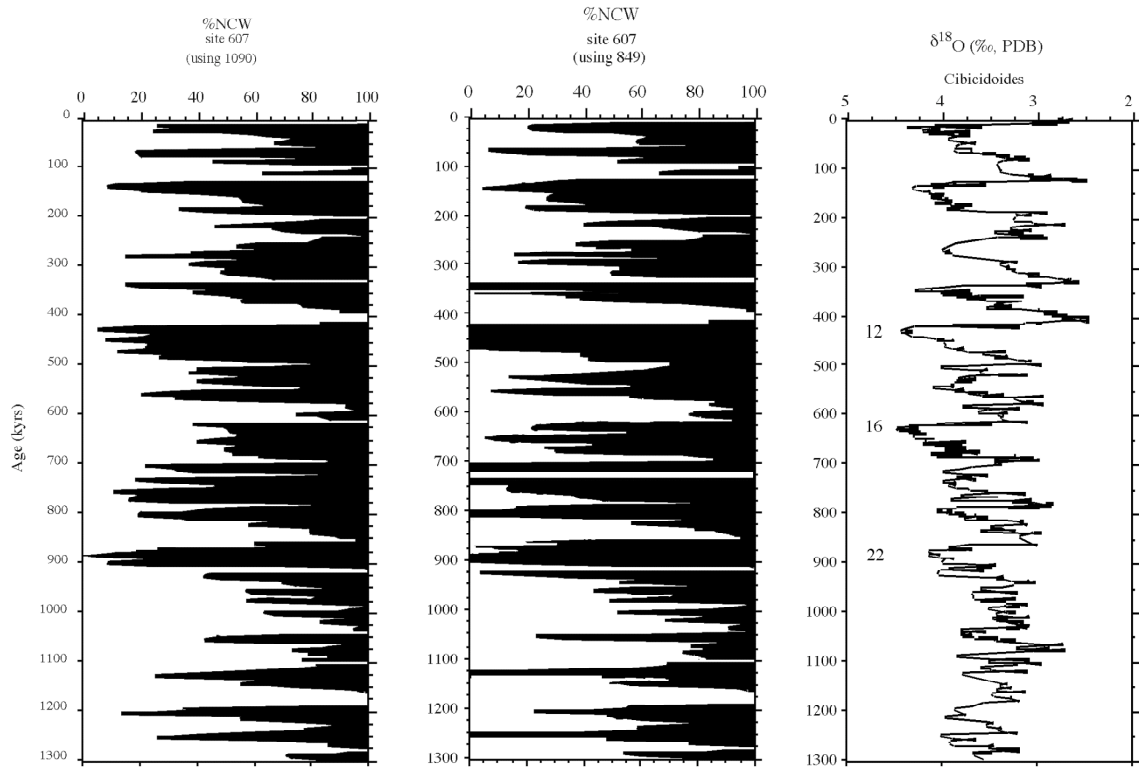


Figure 3-13. Calculation of percent NCW at site 607 using Equation 1 with site 982 as the NCW end member and site 1090 as the SCW end member (solid line) (A). The calculation was repeated using Pacific site 849 (dashed line) as the SCW end member in place of the record from site 1090 (B). The benthic $\delta^{18}\text{O}$ record from site 1090 is also shown (C). Gaps in the %NCW proxy represent gaps or hiatuses in the site 1090 and site 929 records.

Conclusions

The benthic $\delta^{13}\text{C}$ record from site 1090 provides a near-continuous record of changes in Southern Ocean deep-water circulation for the last 2.9 myr. Comparison of carbon isotopic gradients among site 1090 and other records from the deep North Atlantic enables reconstruction of deep-water circulation during the Plio-Pleistocene. Some of the major transitions in Atlantic deep-water circulation occur at the same time as climatic changes recorded in the marine oxygen isotopic record, but others do not. The main deep-water circulation "events" are as follows:

The Late Pliocene

During the late Pliocene between 2.6 and 1.8 Ma, $\delta^{13}\text{C}_{\text{NCW}}$ at site 929 was low, indicating the deep equatorial Atlantic was dominated by SCW. Production of NCW, however, was strong at this time, as indicated by similar $\delta^{13}\text{C}$ values at sites 607 and 982 in the North Atlantic. The simplest way to reconcile strong NCW at site 607 and dominance of SCW at site 929 is through production of a less dense NCW during the late Pliocene whereby the interface between NCW and SCW was shallower than today in the North Atlantic at site 929. An increase in the density of NCW and a deepening of the NCW/SCW boundary occurred after ~ 1.8 Ma as recorded by increased percentage of NCW at site 929.

The Early Pleistocene

The pattern of strongly depleted glacial $\delta^{13}\text{C}$ values in the Southern Ocean, typical of the late Pleistocene, began at 1.55 Ma. Glacial $\delta^{13}\text{C}$ values at site 1090 since MIS 52 have been as much as 1‰ lower than those in the deep Pacific, consistent with previous results from site 704 [Hodell and Venz, 1992]. Such depleted $\delta^{13}\text{C}$ values in the Southern Ocean cannot be attributed solely to glacial reduction of NADW. I suggest low

$\delta^{13}\text{C}$ values in the Southern Ocean after 1.55 Ma was related to sea ice expansion, which limited air/sea exchange of CO_2 and reduced deep-water ventilation. Raymo et al. [1990b, 1997] attributed depleted $\delta^{13}\text{C}$ values at site 607 during MIS 52 to strong glacial suppression of NCW; however, low $\delta^{13}\text{C}$ values at site 607 could also be explained by mixing with SCW with reduced $\delta^{13}\text{C}$ values. Calculated %NCW at 1.55 Ma using the record from site 1090 supports and increase in glacial suppression of NCW but it is not as severe as previously calculated using a Pacific end member.

The change in benthic $\delta^{13}\text{C}$ at site 1090 at 1.55 Ma is indicative of a fundamental change in Southern Ocean deep-water circulation. Migration of wind fields [Imbrie et al., 1992; Toggweiler and Samuels, 1993, 1995a] or alteration of the salinity structure in the South Atlantic [Keeling and Stephens, 2001] during glacials after 1.55 Ma may have also strongly affected the density characteristics and/or export of NCW out of the North Atlantic. This teleconnective linkage of deep-water circulation between the North and South Atlantic may have led to tighter interhemispheric coupling observed between site 704 and North Atlantic records after 1.5 Ma [Hodell and Venz, 1992]. There is little evidence in marine proxy records that the changes in Southern Ocean deep-water circulation and SCW chemistry beginning at 1.55 Ma were tied to climatic in global ice volume [Shackleton et al., 1990].

The Mid-Pleistocene Transition

Between 1.2 and 0.9 Ma, changes in deep-water circulation occurred that correlate with climatic events associated with the MPT. At 1.2 Ma, deep-water circulation changes were focused in the North Atlantic with a strong reduction in %NCW at site 607 (Figure

3-11) as evidenced by an increased $\delta^{13}\text{C}$ gradient between site 982 (intermediate depth North Atlantic) and site 607 (deep North Atlantic) (Figure 3-7c).

At 0.9 Ma (MIS 22) a shift in dominance from the 41-kyr to 100-kyr frequency occurred in climate records accompanied by an increase in global ice volume that initiated "excess" ice growth of the late Pleistocene [Berger and Jansen, 1994; Mudelsee and Schulz, 1997]. The magnitude and pacing of variation in deep-water circulation changed throughout the Atlantic after 0.9 Ma in unison with increased strength of the 100-kyr cycle in ice volume change. At this time, an increase occurred in the range of $\delta^{13}\text{C}$ values in the Southern Ocean. The late Pleistocene after 0.9 Ma was marked by increased variability of deep-water circulation that included well-ventilated interglacials and poorly-ventilated glacials. Estimates of extremely low %NCW at site 607 after 0.9 Ma indicate increased glacial suppression of NCW and support increased variation in deep-water circulation at this time [Raymo et al., 1990b, 1997].

The Late Pleistocene

The general pattern of glacial-to-interglacial change in %NCW in the deep North Atlantic at site 607 calculated using site 1090 as the SCW end member is similar to that calculated using a Pacific end member. The primary difference between the two calculations is that a trend toward reduced glacial suppression of NADW during the past 400 kyr, relative to the interval between 0.9 and 0.5 Ma, is not evident in the new calculation. This suggests that the apparent decoupling of ice volume and deepwater circulation may be an artifact of using a Pacific, rather than a Southern Ocean, carbon isotopic record to calculate past mixing ratios of NCW and SCW.

CHAPTER 4
DEEP-WATER CIRCULATION CHANGES DURING THE LATE NEOGENE
INFERRED FROM BENTHIC FORAMINIFER $\delta^{13}\text{C}$ IN THE SUBANTARCTIC
SOUTH ATLANTIC

Introduction

The Southern Ocean plays an important role in coupling the atmosphere to the deep sea. Gas exchange with the atmosphere determines, in part, the geochemical fingerprint of Antarctic surface water, which is transmitted to the deep sea through the process of deep-water formation. Bottom water produced in the Southern Ocean is the most widespread deep-water mass in the world and ventilates all the deep ocean basins [Gordon, 1971]. Deep-water formation begins with upwelling of Circumpolar Deep-water (CPDW) to the surface where it liberates heat and acquires surface characteristics (i.e., it becomes colder, fresher, and undergoes partial air-sea gas exchange) as it is exposed to the atmosphere [Broecker and Peng, 1982]. Surface waters in the Weddell Sea are transformed into deep-water as they are cooled (by the atmosphere and by contact with sea ice), become saltier (through brine rejection during sea ice formation), and mix with warmer, denser (i.e., more saline) CPDW to form Antarctic Bottom Water [Broecker, 1982; Mantyla and Reid, 1983; Gordon, 1988]. The overturning of water in the Antarctic ventilates the deep ocean by drawing water to the surface, allowing it to approach the composition of the atmosphere, and then forcing it back downward to the deep ocean [Gordon, 1988].

Recent studies have emphasized the importance of Antarctic surface water processes in affecting deep-water ventilation rates and ultimately the CO_2 composition of

the atmosphere. These processes include variation in sea ice extent [Stephens and Keeling, 2000; Keeling and Stephens, 2001; Gildor and Tziperman, 2002] and surface stratification [Toggweiler, 1999; Sigman and Boyle, 2000; Sigman et al., 2004]. Long-term changes in Antarctic surface conditions and deep-water ventilation may have been a forcing mechanism for late Neogene climate cooling through the carbon cycle [Shackleton, 2000]. This mechanism underscores the importance of reconstructing deep-water ventilation in the Southern Ocean and examining potential linkages with late Neogene climate change.

To this end, three benthic foraminiferal stable isotopic records are presented for the past 9 myr from locations in the North Atlantic (ODP site 982), the subantarctic South Atlantic (piston core TN057-6 and ODP sites 1090, and 704), and the deep Pacific (ODP site 849). Changes in deep-water circulation and ventilation during the late Neogene were inferred by comparing benthic $\delta^{13}\text{C}$ records among ocean basins. To assess potential relationships between deep-water ventilation and late Neogene climate change the covariance of Southern Ocean benthic $\delta^{13}\text{C}$ and $\delta^{18}\text{O}$ records were compared statistically.

Materials and Methods

Data Sources

Carbon isotopic records were selected to represent endmember water masses from the North Atlantic, Southern Ocean, and deep Pacific (Figure 4-1). The record from site 982, which is located at intermediate water depths (1100 m) in the high-latitude North Atlantic, monitors the upper levels of North Atlantic Deep Water (NADW). The record from deep Atlantic site 607 (3400 m) is within the core of lower NADW and was compared to site 982 for the interval between 0 and 5 Ma. The composite record of site

1090/704 (3700/2500 m) in the subantarctic South Atlantic monitors Circumpolar Deep Water (CPDW) and represents the deep Southern Ocean endmember. The record from nearby subantarctic South Atlantic site 1092 (2000 m) was used to compare with the record from site 704 for the interval between 2.6 and 4.4 Ma. The record from Pacific site 849 (3850 m) is located within Pacific Deep Water (PDW) and represents the deep Pacific endmember. For detailed information on preparation techniques, isotopic analyses, and data sources consult the references cited in Table 4-1.

The record from ODP site 1090 is a composite record that includes piston core TN057-6 and ODP site 1090. The piston core was retrieved during the site survey cruise for ODP Leg 177 and is located at the same position as site 1090. A Plio-Pleistocene composite record was constructed by splicing the TN057-6 and ODP site 1090 records together at ~400 kyr [Hodell et al., 2000; Venz and Hodell, 2002]. The benthic isotopic records from sites 1090 and 704 were spliced at 2.6 Ma to create a continuous benthic $\delta^{18}\text{O}$ and $\delta^{13}\text{C}$ record from the Southern Ocean for the late Neogene (0 - 9 Ma). Only 5° of latitude separate sites 1090 and 704 in the subantarctic South Atlantic (Figure 4-1) and the benthic $\delta^{13}\text{C}$ records are similar in the intervals of overlap, indicating they both sample CPDW [Venz and Hodell, 2002].

Stratigraphy and Time Scales

Sampling frequencies range from 1 kyr to 22 kyr and are listed in Table 4-2. Sampling details can be found in the references cited in Table 4-1. All of the cores (ODP sites 982, 704, 1090, 849 and piston core TN057-6) examined have low-to-moderate sedimentation rates between 1 and 3 cm/1000 years. The chronologies for these sites were mostly based on oxygen isotopic correlation to the Shackleton et al. [1995] time scale (Table 4-1), except for the 5-9 Ma portion of the records from sites 982 and 704.

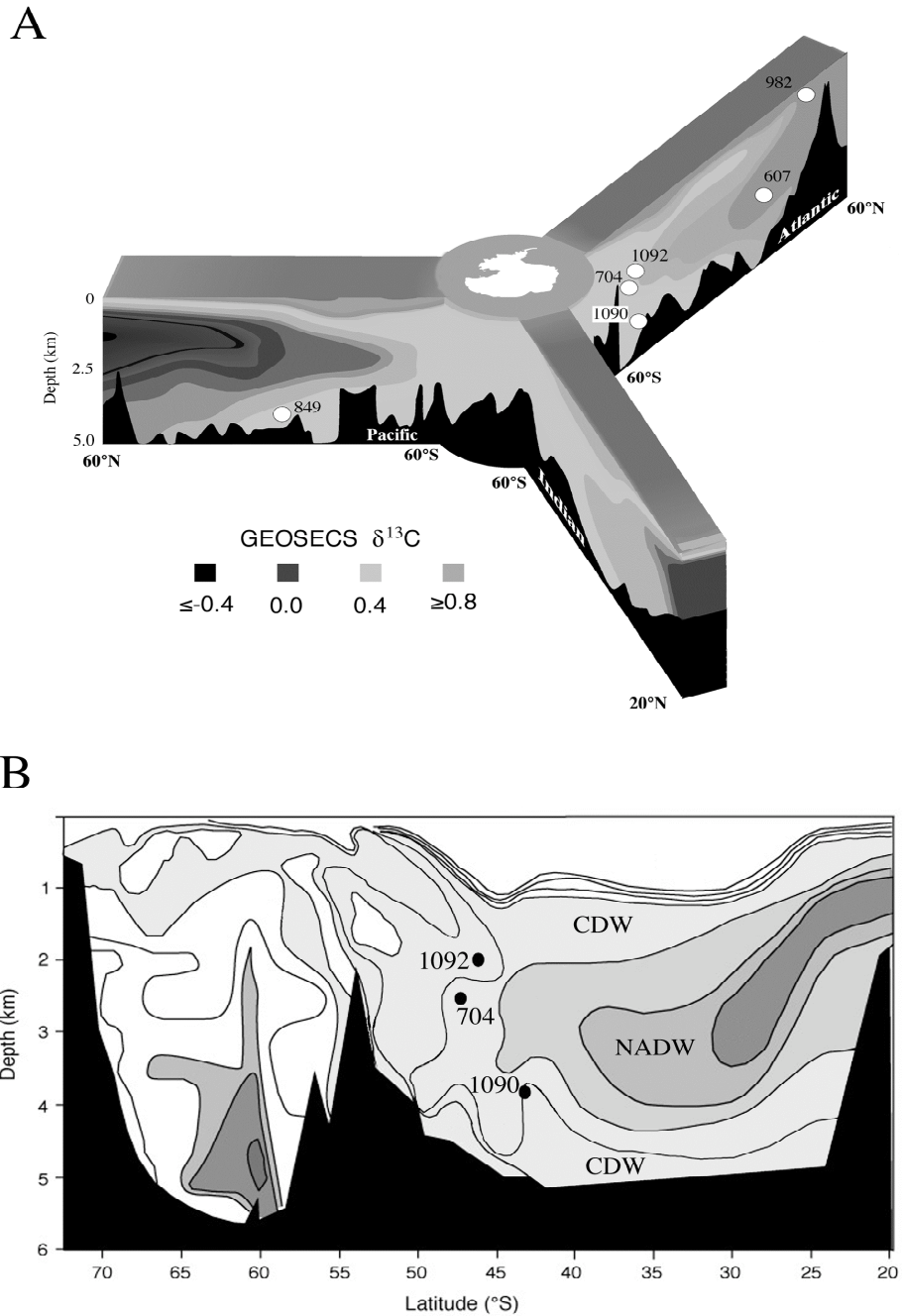


Figure 4-1. (A) Location map displaying the relative positions and depths of North Atlantic sites 982 and 607, South Atlantic sites 704, 1090, and 1092, and deep Pacific site 849. (B) A detail map of the subantarctic South Atlantic displaying the locations of sites 704, 1090, and 1092 relative to the deep-water masses of the Southern Ocean. Modified from Hodell et al., 2003a.

Site 982 was astronomically tuned [Hodell et al., 2002] and the late Miocene portion of the record from site 704 was converted to age by assuming constant sedimentation rate between polarity reversal boundaries [Muller et al., 1991] using the timescale of Shackleton et al. [1995] (Table 4-3).

Results

In Figures 4-2 and 4-3, unprocessed stable isotopic records are shown in the top panel and smoothed signals are presented in the lower panels to emphasize changes in long-term mean isotopic values. The data sets were resampled to a constant 10 kyr interval and were smoothed using a 50 point running mean (Figures 4-2b and 4-3b). The unprocessed 9 myr isotopic records were broken into shorter segments so that details of the changes during specific intervals could be observed (Figures 4-4 and 4-5). Inter-ocean $\delta^{13}\text{C}$ gradients were calculated for each 10 kyr interval (Figure 4-6a and 4-6b) and signals were then smoothed using a 50 point running mean (Figure 4-6c).

Carbon Isotopic Records

Carbon isotopic values in the North Atlantic and South Atlantic were similar between 9 and 6.6 Ma (Figures 4-2 and 4-4), resulting in a low gradient throughout this interval (Figure 4-6). Carbon isotopic values decreased simultaneously in the North Atlantic and South Atlantic between ~ 7.6 and 6.65 Ma, marking the Late Miocene Carbon Shift (LMCS) [Keigwin, 1979] (Figures 4-2 and 4-4). The North-South Atlantic gradient remained near zero throughout the LMCS. Only after the LMCS did the gradient increase (Figure 4-6). After ~ 6.6 Ma, carbon isotopic values in the South Atlantic fell mid-way between North Atlantic and Pacific values (Figures 4-2 and 4-4). The North-South Atlantic gradient increased to $\sim 0.5\%$ after ~ 6.6 Ma because the decrease in South Atlantic $\delta^{13}\text{C}$ values was $\sim 0.2\%$ greater than in the North Atlantic

Table 4-1. Sources of data used in this study

Site	Interval (Ma)	Reference	Chronology
982	0-1	Venz et al., 1999	$\delta^{18}\text{O}$ correlation to site 607 [Raymo et al., 1992; Mix et al., 1995]
	0-3	Venz and Hodell, 2002	$\delta^{18}\text{O}$ correlation to site 607 [Raymo et al., 1992; Mix et al., 1995]
	3-5	Raymo, unpublished data	$\delta^{18}\text{O}$ correlation to site 607 [Raymo et al., 1992; Mix et al., 1995]
	5-9	Hodell et al., 2001	Astronomically tuned
607	0-5	Raymo et al., 1992	Paleomagnetic reversal boundaries, modified by Mix et al., 1995
704	0-0.45	Hodell, 1993	$\delta^{18}\text{O}$ correlation [Martinson et al., 1987; Imbrie et al., 1984]
	0-0.45	Hodell et al., 2000 (new data)	$\delta^{18}\text{O}$ correlation [Martinson et al., 1987; Imbrie et al., 1984]
	1.1-4.8	Hodell and Venz, 1992	$\delta^{18}\text{O}$ correlation to site 607 [Raymo et al., 1992; Mix et al., 1995]
	5.0-9.0	Mueller et al., 1991	Paleomagnetic reversal boundaries aged using Shackleton et al. [1995]
TN057-6	0-0.6	Hodell et al., 2000	$\delta^{18}\text{O}$ correlation [Martinson et al., 1987; Imbrie et al., 1984]
1090	0-2.8	Venz and Hodell, 2002	$\delta^{18}\text{O}$ correlation to site 607 [Raymo et al., 1992; Mix et al., 1995]
1092	2.6-4.4	Andersson, 2002	Paleomagnetic reversal boundaries aged using Shackleton et al., 1995
849	0-5	Mix et al., 1995	[Shackleton et al., 1995]
	5-9	This study	[Shackleton et al., 1995]

Table 4-2. Sampling intervals for sites 982, 607, 704, 1090, 1092, and 849.

Site	Interval (Ma)	Sample Frequency Kyrs (average)
982	9	~2.5
607	5	~4
704	0-2.4	~3-4
	2.8-3.5	~5
	3.5-5	~10
	5.0-9.0	~15
1090	0-0.4	~1
	0.4-1.2	~2
	1.2-3.0	~4
1092	2.6-4.4	~4-5
849	0-5	~4
	5-9	~22

Table 4-3. Age-Depth points for sites 982 (3-5 Ma) and 704 (5-9 Ma)

Site 982

	<u>Depth (mcd)</u>	<u>Age (Ma)</u>
	52.23	2.440
	54.58	2.521
	57.48	2.609
	73.08	3.303
	120.74	4.606
	128.09	4.693
	139.35	4.895
	143.23	4.940
	147.21	5.022
	154.53	5.133

Site 704B

<u>Datum</u>	<u>Depth (mcd)</u>	<u>Age (Ma)</u>
Sidufjall	209.02	4.878
Thvera (t)	213.09	4.977
Thvera (o)	215.24	5.232
C3An.1n (t) (Gilbert)	220.69	5.875
C3An.1n (o)	226.84	6.122
C3An.2n (t)	229.64	6.256
C3An.2n (o)	237.42	6.555
C3Bn (t)	248.00	6.919
C3Bn (o)	253.30	7.072
C4n.1n (t)	255.30	7.406
C4n.1n (o)	260.30	7.533
C4n.2n (t)	261.30	7.618
C4n.2n (o)	263.30	8.027
C4r.1n (t)	266.00	8.174
C4r.1n (o)	271.00	8.205
C4An (t)	285.80	8.631
C4An (o)	314.30	8.945
C4Ar.1n (t)	319.90	9.142
C4Ar.1n (o)	322.85	9.218
C4Ar.2n (t)	334.35	9.482

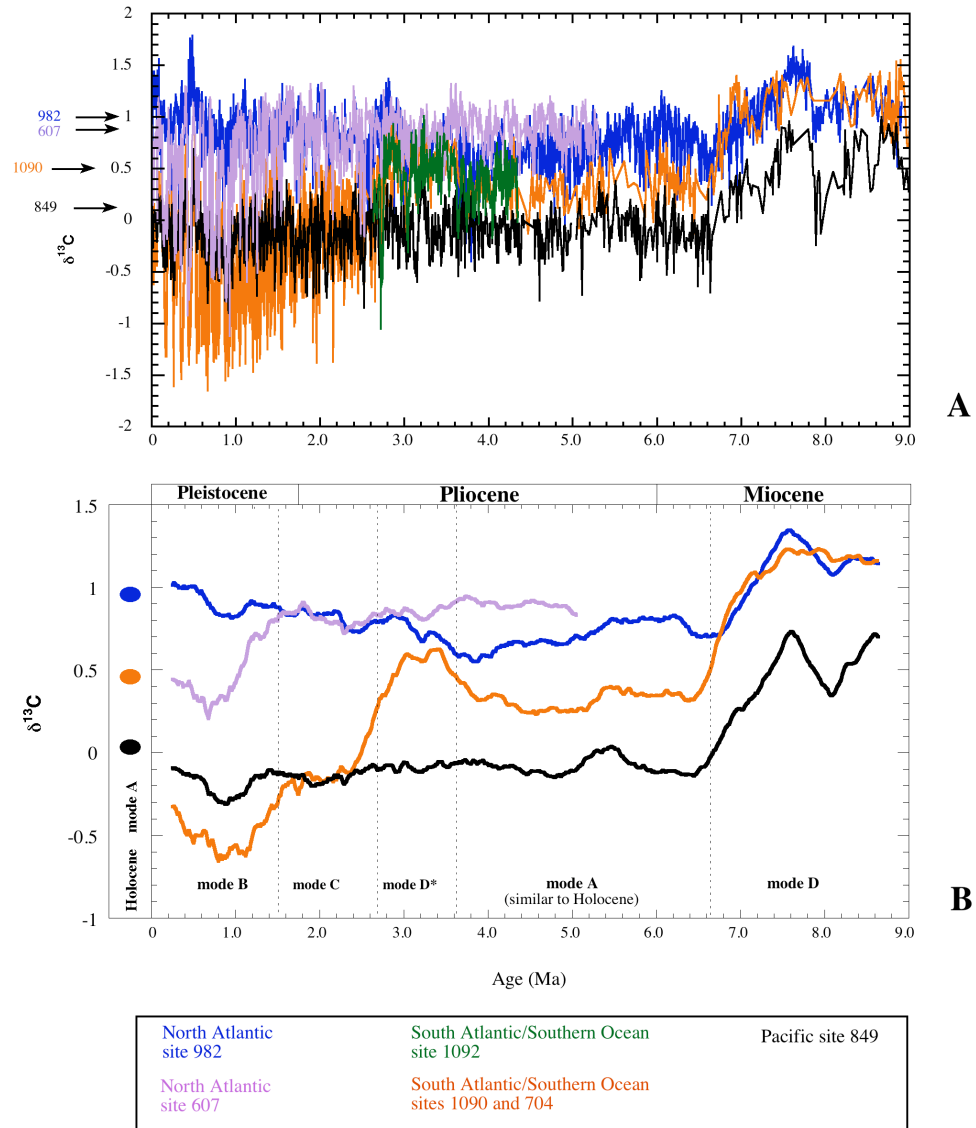


Figure 4-2. (A) Comparison of benthic carbon isotopic records from site 982 (blue) in the North Atlantic, sites 704/1090 (orange) subantarctic South Atlantic, and site 849 (black) in the deep Pacific for the last 9 myr. The record from subantarctic site 1092 [Andersson, 2002] (green) is plotted for comparison to site 704 during the interval from ~ 4.4 to 2.6 Ma. (B) The same records resampled at 10 kyr increments and smoothed with a 50-point running mean. Holocene $\delta^{13}\text{C}$ values are noted along Y axis by arrows and colored ovals.

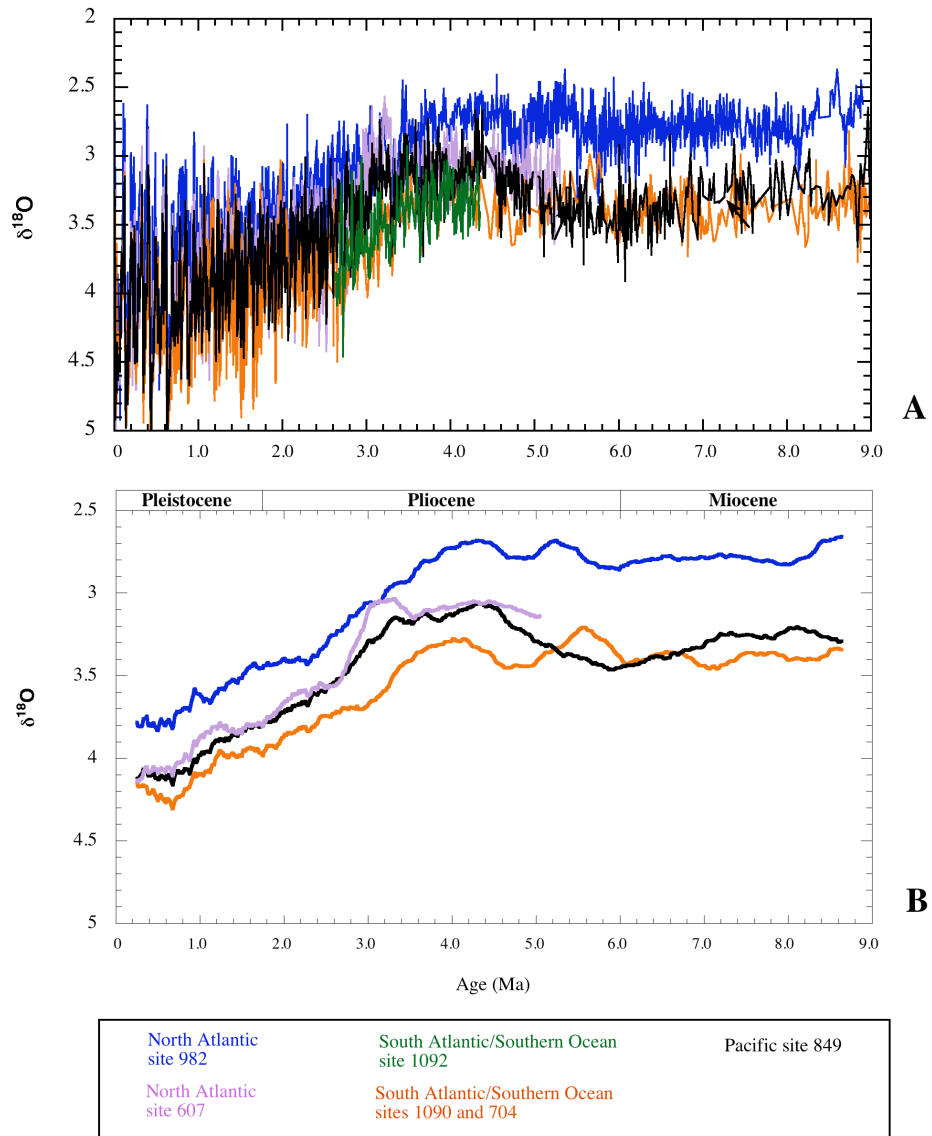


Figure 4-3. (A) Comparison of benthic oxygen isotopic records from site 982 (blue) in the North Atlantic, sites 704/1090 (orange) subantarctic South Atlantic, and site 849 (black) in the deep Pacific for the last 9 myr. The record from subantarctic site 1092 [Andersson, 2002] (green) is plotted for comparison to site 704 during the interval from ~4.4 to 2.6 Ma. (B) The same records resampled at 10 kyr increments and smoothed with a 50-point running mean.

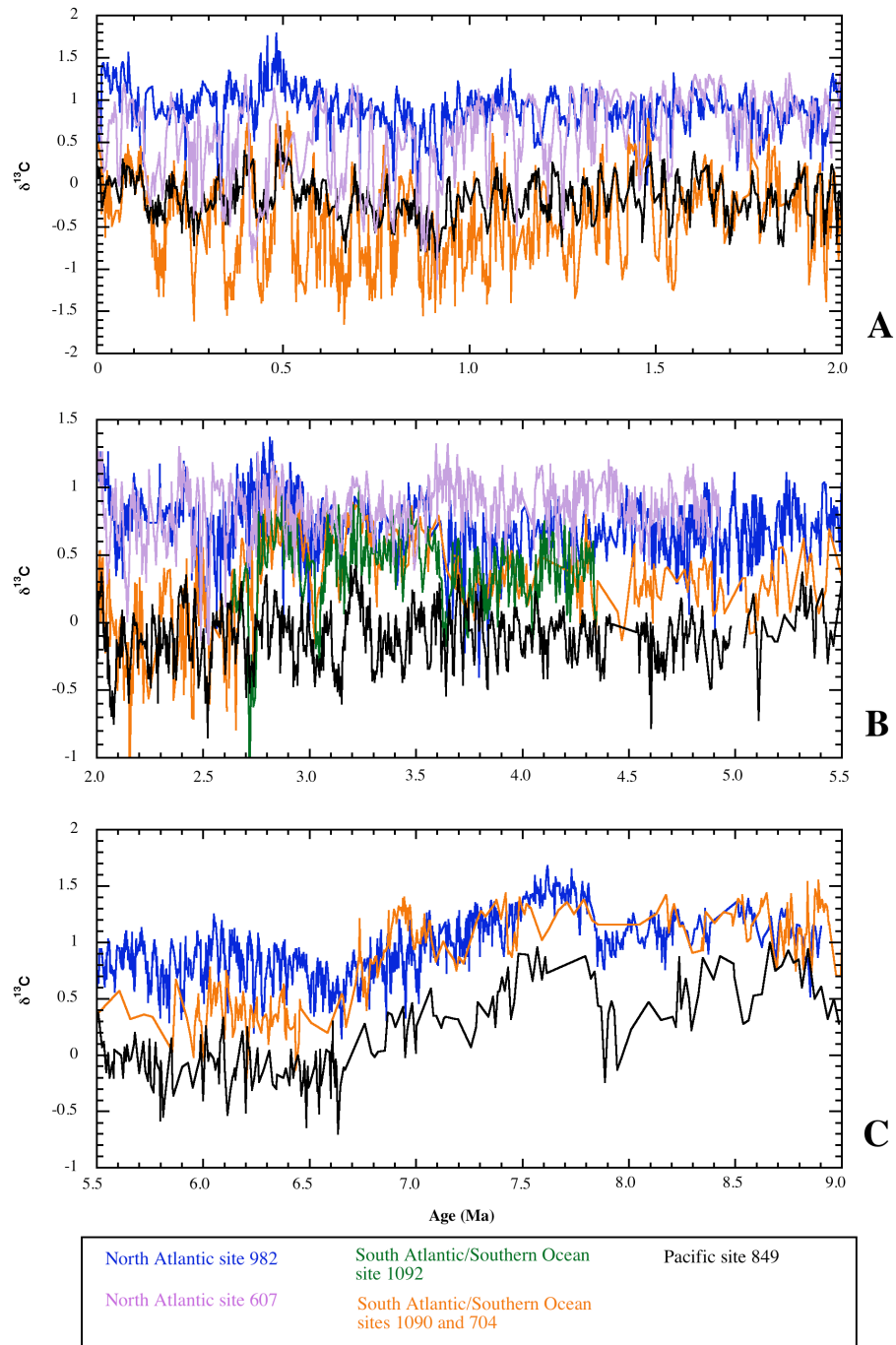


Figure 4-4. Carbon isotopic records shown in Figure 2A for the time periods (A) 0 to 2.0 Ma; (B) 2.0 to 5.5 Ma; and (C) 5.5 to 9.0 Ma.

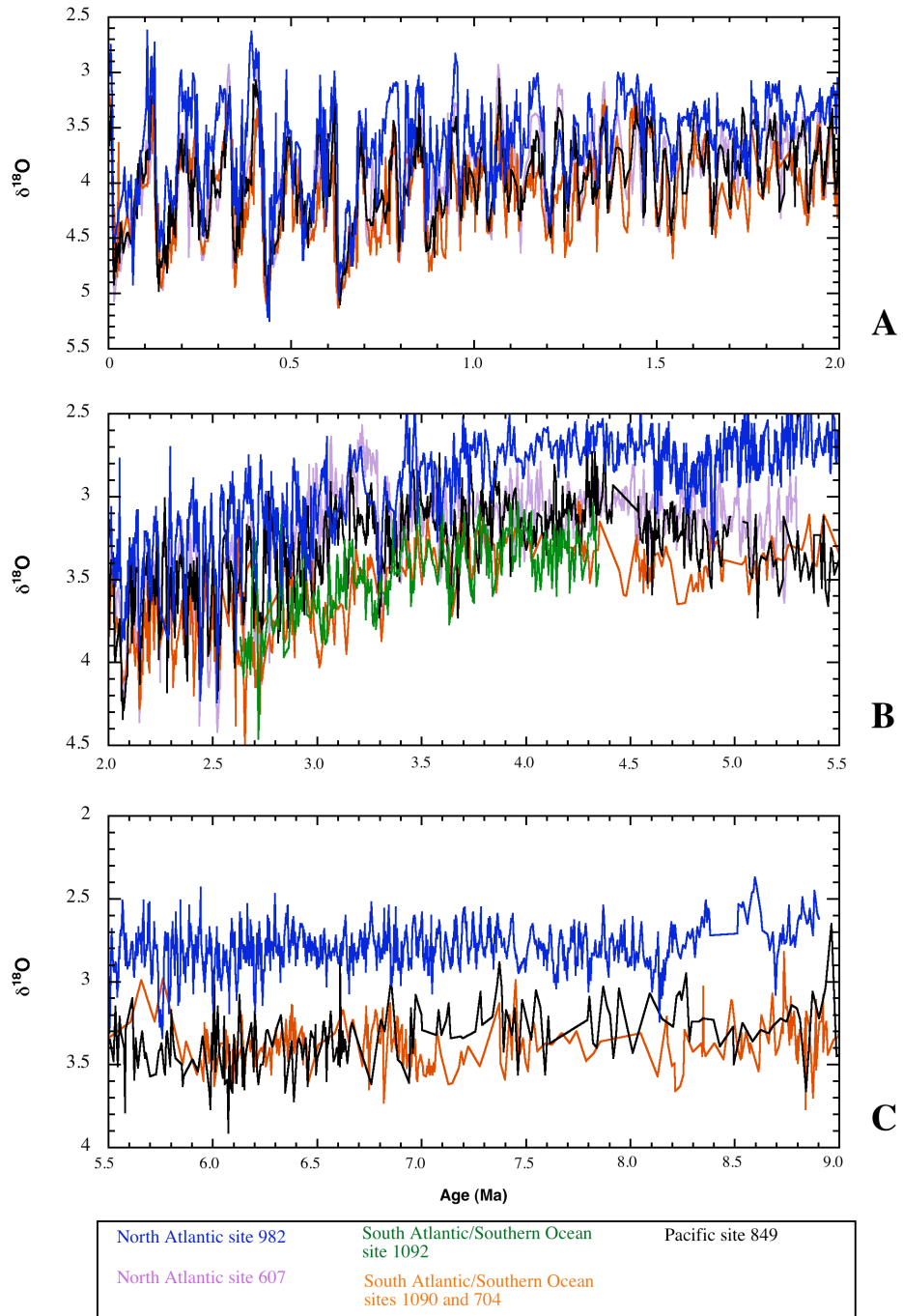


Figure 4-5. Oxygen isotopic records shown in Figure 2A for the time periods (A) 0 to 2.0 Ma; (B) 2.0 to 5.5 Ma; and (C) 5.5 to 9.0 Ma.

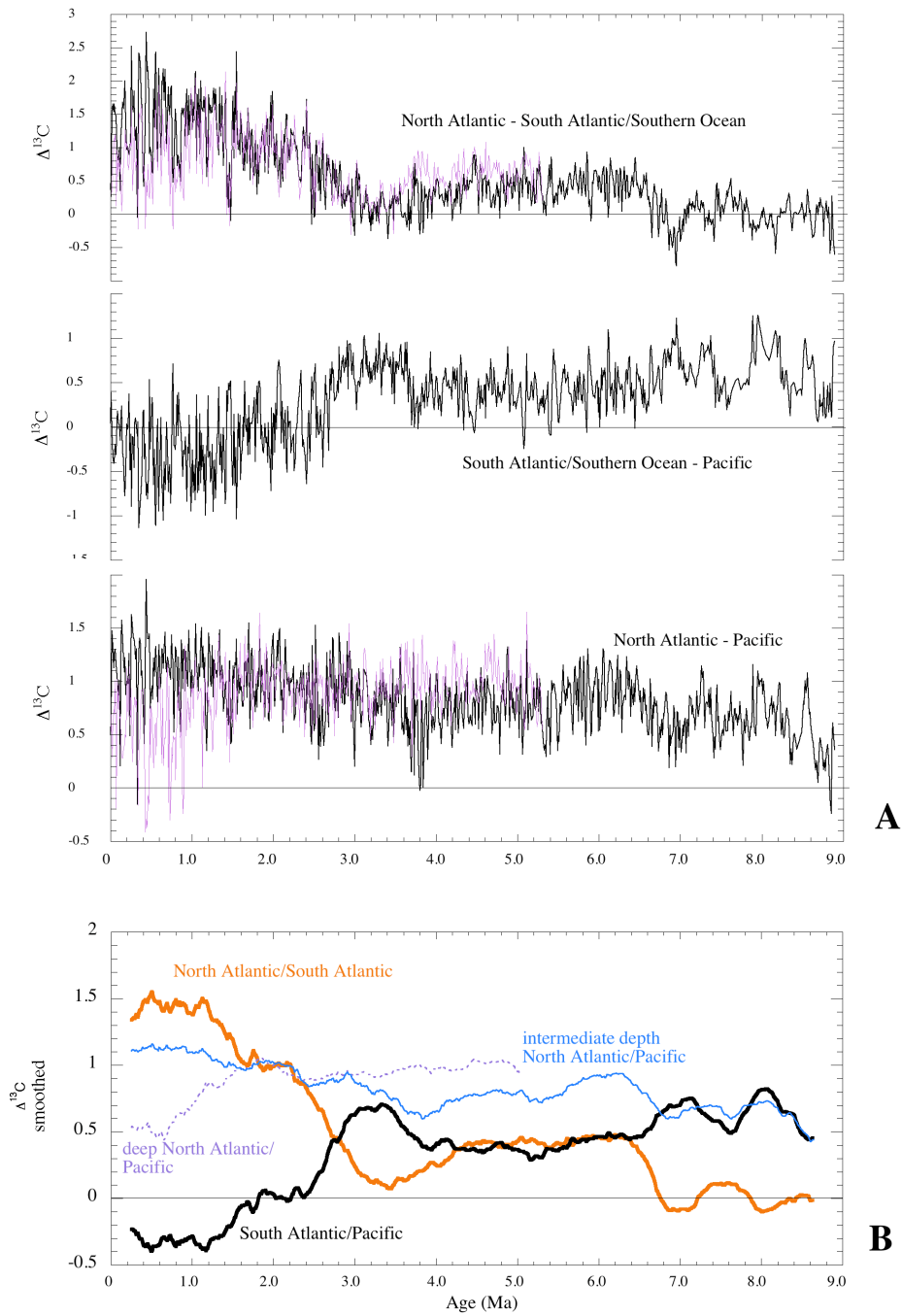


Figure 4-6. $\Delta^{13}\text{C}$ gradient calculated by resampling the data from sites 982, 1090/704, and 849 at a constant 10 kyr interval and subtracting $\Delta^{13}\text{C}_{982} - \Delta^{13}\text{C}_{1090} = \Delta^{13}\text{C}_{\text{North-South Atlantic}}$ (A) and $\Delta^{13}\text{C}_{1090/704} - \Delta^{13}\text{C}_{849} = \Delta^{13}\text{C}_{\text{South Atlantic-Pacific}}$ (B). Long-term variation in $\Delta^{13}\text{C}_{\text{North-South Atlantic}}$ and $\Delta^{13}\text{C}_{\text{South Atlantic-Pacific}}$ was highlighted by smoothing the records in 3A and 3B using a 50 point running mean (C).

(0.9‰ versus 0.7‰) [Muller et al., 1991] (Figure 4-6). Additionally, North Atlantic $\delta^{13}\text{C}$ values at site 982 increased by $\sim 0.3\text{‰}$ after the LMCS whereas South Atlantic values did not change.

The North-South Atlantic carbon isotopic gradient did not change between 6.6 and 3.6 Ma (Figure 4-6). At 3.6 Ma, carbon isotopic values in the South Atlantic increased and approached those of the North Atlantic, similar to the pattern observed between 9.2 and 6.65 Ma in the late Miocene (Figures 4-2 and 4-4). The $\delta^{13}\text{C}$ increase in the South Atlantic was temporary, however, and mean values decreased again after ~ 2.7 Ma, primarily due a decrease in glacial $\delta^{13}\text{C}$ values. Another marked decline in mean $\delta^{13}\text{C}$ values in the South Atlantic occurred at 1.55 Ma, which increased the carbon isotopic gradient between the North and South Atlantic to nearly 1.5‰ during glacial intervals (Figure 4-6).

The carbon isotopic gradient between the South Atlantic and the Pacific was relatively constant at $\sim 0.5\text{‰}$ between 8.5 and 3.6 Ma (Figure 4-6). Between 3.6 and 2.7 Ma, the gradient was greater ($\sim 0.7\text{‰}$) due to higher values in the South Atlantic. Mean carbon isotopic values in the South Atlantic decreased at ~ 2.7 Ma and were similar to those in the Pacific between 2.7 and 1.55 Ma (Figure 4-2), which brought the gradient to near zero (Figure 4-6). During this period, interglacial values in the South Atlantic were higher than those in the Pacific, whereas glacial values were lower. A marked decrease in glacial South Atlantic $\delta^{13}\text{C}$ values occurred at 1.55 Ma, which lowered mean values to considerably less than those in the Pacific [Venz and Hodell, 2002] (Figures 4-2 and 4-4). Glacial $\delta^{13}\text{C}$ values in the South Atlantic were commonly 1‰ lower than those in the

Pacific and interglacial values were generally equal to or slightly greater than those in the Pacific.

The North Atlantic-Pacific carbon isotopic gradient prior to 8.5 Ma fluctuated between 0 and 0.5‰ with most of the variation occurring in the deep Pacific record (Figure 4-6). From ~8.5 Ma to present, the intermediate North Atlantic and Pacific maintained a persistent $\delta^{13}\text{C}$ gradient of greater than 0.5‰ (Figure 4-6).

Oxygen Isotopic Records

Benthic oxygen isotopic records from the North Atlantic, South Atlantic, and deep Pacific generally show parallel trends. Most notably, $\delta^{18}\text{O}$ values increase from ~3.2 Ma to present, reflecting climate cooling and increased global ice volumes associated with the onset of Northern Hemispheric Glaciation (NHG) (Figure 4-3) [Raymo et al., 1992]. Oxygen isotopic values in the deep South Atlantic and deep Pacific were similar during the late Miocene (9 - ~5 Ma) (Figures 4-3 and 4-5). Pacific values decreased between ~7 and 6 Ma and became less than those in the South Atlantic at ~5.2 Ma. South Atlantic $\delta^{18}\text{O}$ values also decreased after ~4.3 Ma, but remained ~0.2 – 0.3‰ greater than the deep North Atlantic (site 607) and the Pacific (site 849) throughout the early and mid-Pliocene (5.2 - 2.6 Ma) (Figures 4-3 and 4-5). The range of glacial-to-interglacial isotopic variation in the South Atlantic, North Atlantic, and Pacific increased after ~3.6 Ma, primarily due to higher glacial values. Long-term mean values began to steadily increase after ~3.2 Ma. The difference in oxygen isotopic values between the South Atlantic and the other deep oceans lessened after ~2.6 Ma as values in the North Atlantic (site 607) and Pacific increased. Interglacial $\delta^{18}\text{O}$ values in the South Atlantic were generally similar to interglacial values in the deep Pacific after 2.6 Ma (Figures 4-3 and

4-5). However, $\delta^{18}\text{O}$ values in the glacial South Atlantic were greater than those in the deep Pacific until ~ 0.6 Ma (Figures 4-3 and 4-5). Mean $\delta^{18}\text{O}$ values in all three basins continued to increase into the late Pleistocene until ~ 0.6 Ma (Figure 4-3).

Correlation Between Benthic Carbon and Oxygen Isotopic Records

The correlation between benthic carbon and oxygen isotopic records from site 1090/704 is shown by creating scatter plots of $\delta^{13}\text{C}$ versus $\delta^{18}\text{O}$ for six specific time intervals (Figure 4-7). The intervals were chosen on the basis of changes in inter-ocean carbon isotopic gradients (see Figure 4-2). For each plot, a linear regression was applied noting the r^2 value and slope of each line (Table 4-4). No significant correlation (i.e., at 95% confidence) exists between $\delta^{18}\text{O}$ and $\delta^{13}\text{C}$ for the period between 9.2 and 3.6 Ma (Table 4-4). After ~ 3.6 Ma, oxygen and carbon isotopic records were negatively correlated at the 95% confidence level (Table 4-4). After 2.7 Ma, the records were negatively correlated at the 99% confidence level.

Discussion

The carbon isotopic gradient between the North and South Atlantic has been used to infer the relative proportion of high- $\delta^{13}\text{C}$ deep-water from the North Atlantic (NADW) present in the Southern Ocean [Oppo et al., 1987; Venz and Hodell, 2002]. The assumption implicit in this analysis is that $\delta^{13}\text{C}$ values in the South Atlantic are dependent only on mixing between NADW and PDW. If so, this implies that $\delta^{13}\text{C}$ values in the South Atlantic should never be higher than those in the North Atlantic or lower than those in the deep Pacific. During the Pleistocene, glacial benthic $\delta^{13}\text{C}$ values in the South Atlantic were often lower than values in the deep Pacific by a significant amount,

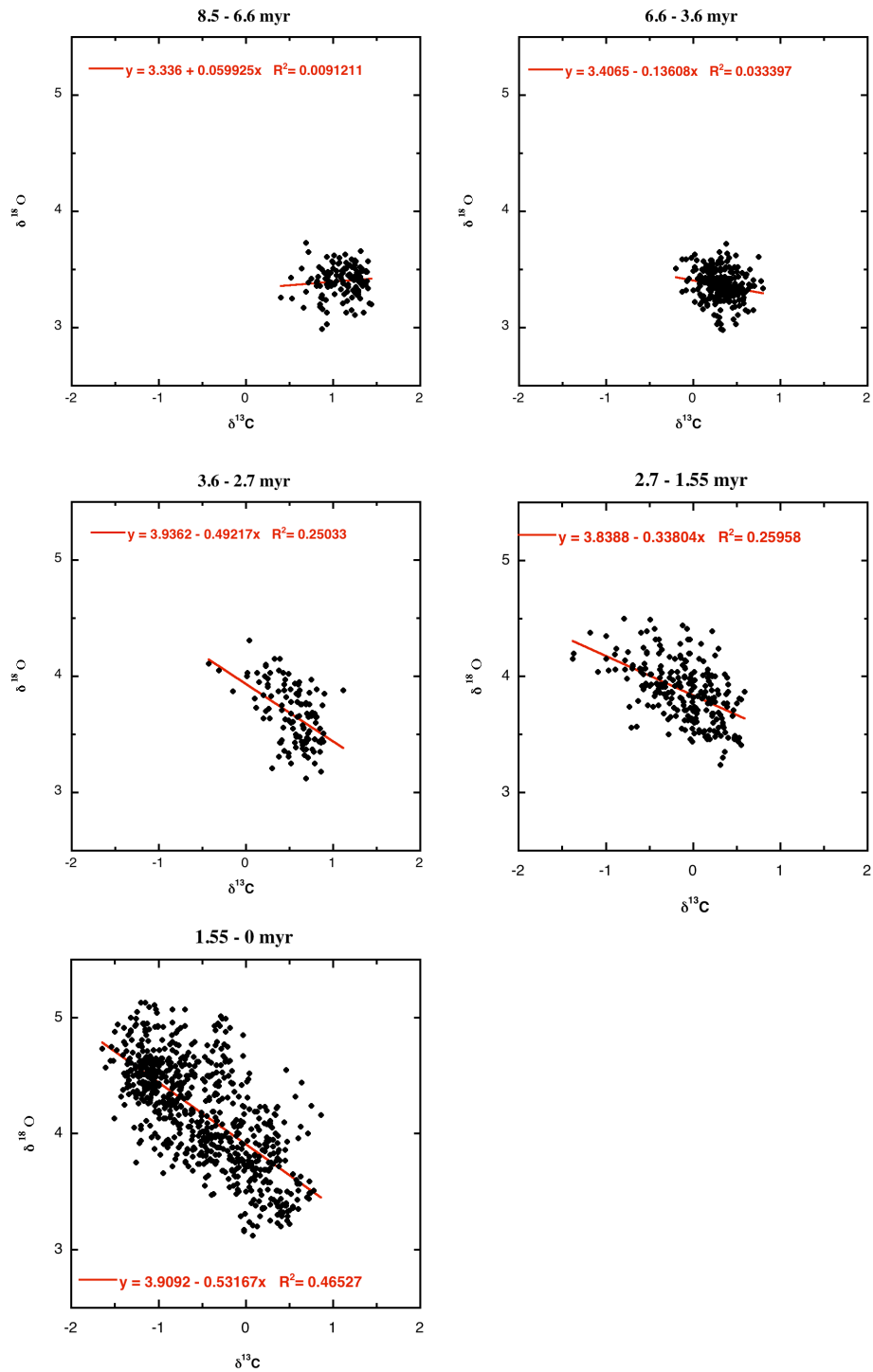


Figure 4-7. Scatter plots of the benthic carbon and oxygen isotopic data from site 1090/704 in the subantarctic South Atlantic for specific time intervals. Intervals were chosen based on changes in inter-ocean carbon isotopic gradients noted on Figure 4-2.

Table 4-4. Results of statistical analysis of benthic carbon and oxygen isotopic data from sites 704 and 1090 during different deep-water circulation modes.

	Mode D	Mode A	Mode D*	Mode C	Mode B	
	8.5 - 6.6 Ma	6.6 - 3.6 Ma	3.6 - 2.7 Ma	2.7 - 1.55 Ma	1.55 - 0 Ma	
$\delta^{13}\text{C}$	mean	1.07	0.31	0.58	-0.09	-0.53
	max	1.44	0.8	1.12	0.63	0.86
	min	0.25	-0.13	-0.15	-1.38	-1.65
	range	1.19	0.93	1.27	1.97	2.51
$\delta^{18}\text{O}$	mean	3.4	3.36	3.6	3.9	4.17
	max	3.73	3.72	4.03	4.5	5.13
	min	2.99	2.98	3.12	3.41	3.12
	range	0.74	0.74	0.91	1.09	2.01
linear curve fit	r^2	0.01	0.03	0.25	0.25	0.47
	slope	0.06	-0.14	-0.49	-0.33	-0.53
T-test	correlation	0.14	-0.17	-0.31	-0.42	-0.68
	correlation probability	0.1085	0.008	0.0017	<.0001	<.0001
significant correlation	at 95%	-	-	*	*	*
	at 99%	-	-	-	**	**
number of points	127	232	97	252	727	

suggesting the $\delta^{13}\text{C}$ value of CPDW was not simply the result of mixing of NADW and PDW, but rather due to changes in deep-water formation within the Southern Ocean that affect deep-water ventilation [Venz and Hodell, 2002].

On the basis of changes in oceanic carbon isotopic gradients, I define four different modes of deep-water circulation in the late Neogene (Figure 4-2). Mode A is similar to the modern ocean where $\delta^{13}\text{C}$ values of CPDW in the deep South Atlantic fall mid-way between high North Atlantic values and low Pacific values (i.e., North Atlantic $\delta^{13}\text{C} >$ South Atlantic $\delta^{13}\text{C} >$ Pacific $\delta^{13}\text{C}$), reflecting approximately equal proportions of NCW and PDW in the Southern Ocean. Mode B is represented by the last glacial period when a large gradient existed between the North Atlantic and South Atlantic and carbon isotopic values in the South Atlantic were less than those in the Pacific (North Atlantic $\delta^{13}\text{C} >$ Pacific $\delta^{13}\text{C} >$ South Atlantic $\delta^{13}\text{C}$). Such low benthic $\delta^{13}\text{C}$ values in the South Atlantic indicate that the Southern Ocean was poorly ventilated during glacial periods of the late Pleistocene. Mode C is marked by carbon isotopic values in the South Atlantic that were similar to those in the Pacific (North Atlantic $\delta^{13}\text{C} >$ South Atlantic $\delta^{13}\text{C} =$ Pacific $\delta^{13}\text{C}$). This configuration may reflect a lesser proportion of high $\delta^{13}\text{C}$ NCW and a greater proportion of low- $\delta^{13}\text{C}$ Pacific water within the Southern Ocean relative to today. Mode D occurs when $\delta^{13}\text{C}$ values are high in both the North and South Atlantic basins and values are low in the Pacific (North Atlantic $\delta^{13}\text{C} =$ South Atlantic $\delta^{13}\text{C} >$ Pacific $\delta^{13}\text{C}$). This pattern may indicate that either an exceptionally large volume of NCW was present in the South Atlantic or a high- $\delta^{13}\text{C}$ deep-water was formed in the Southern Ocean.

Deep-Water Circulation During the Late Miocene to Middle Pliocene

Carbon isotopic gradients were characterized by Mode D during the late Miocene between 8.5 and 6.6 Ma (Figure 4-2). One interpretation of carbon isotopic values in the Southern Ocean equal to North Atlantic values between 9.2 and 6.6 Ma is a larger contribution of NADW to the Southern Ocean than today [Wright et al., 1991]. However, ϵ_{Nd} data from the Southern Ocean suggest little change in the proportion of NADW present in the Southern Ocean during the late Miocene after ~9.2 Ma [Frank et al., 2002]. Alternatively, changes in Antarctic surface water processes and resultant changes in deep-water formation could have produced CPDW with a greater $\epsilon^{13}\text{C}$ value than today. For example, higher preformed $\epsilon^{13}\text{C}$ values of Antarctic surface waters may reflect increased nutrient utilization under generally warmer climatic conditions (relative to the modern) during the late Miocene between 9.2 - 6.6 Ma [Ciesielski et al., 1982]. The absence of Antarctic sea ice and a larger expanse of open water would have permitted more complete equilibration between surface water and the atmosphere through air/sea exchange, which would raise the $\epsilon^{13}\text{C}$ value of surface waters. The process of deep-water formation in the Southern Ocean may have been similar to that in the interglacial North Atlantic with evaporative cooling of relatively warm, high- $\epsilon^{13}\text{C}$ Antarctic surface waters and the inclusion of a large proportion of surface waters in newly formed deep-water. These processes would have resulted in a high- $\epsilon^{13}\text{C}$ deep-water in the Southern Ocean that was isotopically indistinguishable from NCW. Deep-water flow patterns may have been similar to today (as suggested by Nd isotopes), but the production of high- $\epsilon^{13}\text{C}$ deep-waters in both the high-latitude North Atlantic and

Southern Ocean would have resulted in a negligible carbon isotopic gradient between the North Atlantic and the Southern Ocean.

Low or non-existent $\delta^{13}\text{C}$ gradients between the North Atlantic and the Southern Ocean were not uncommon during the middle and late Miocene [Wright et al., 1991; 1992]. Based on a comparison of carbon isotopic gradients, Wright et al. [1991] also inferred the continued presence of a high- $\delta^{13}\text{C}$ water mass in the Atlantic since 8.5 Ma, which I refer to as Northern Component Water (NCW). This contrasts with the findings of Billups [2002] who reported a diminished contribution of a NCW in the Southern Ocean between \sim 8.5 and 6 Ma. This discrepancy likely results from the use of site 289 at 2000 m on the Ontong-Java Plateau as the Pacific endmember. Carbon isotopic values from deeper site 849 (3800 m) are distinctly lower (by \sim 0.5‰) than the values at site 289 in the late Miocene, suggesting that site 289 reflects an intermediate depth water mass and is not recording the $\delta^{13}\text{C}$ of PDW. If the record from site 849 is used to represent the deep Pacific, then the Atlantic-Pacific $\delta^{13}\text{C}$ gradient indicates the continual presence of NCW in the deep Atlantic during the late Miocene (8.5-6 Ma).

Production of a high- $\delta^{13}\text{C}$ CPDW ceased after \sim 6.6 Ma, which was signaled by a shift to Mode A in the Southern Ocean (Figure 4-2). The West Antarctic Ice Sheet (WAIS) developed in the late Miocene, which may have resulted in cooling of Antarctic surface waters, decreased nutrient utilization, expansion of sea ice, and northward migration of oceanic frontal zones [Ciesielski et al., 1982; Kennett and Barker, 1990]. These changes would have reduced nutrient utilization, air/sea exchange, and deep-water ventilation. The process of deep-water formation in the Southern Ocean probably changed at this time to become more like the modern; i.e., occurring near and/or under

ice shelves in the Weddell Sea. Residence time of water at the surface would have decreased and a smaller proportion of surface water would be entrained in deep-water formation [Broecker and Peng, 1982]. All of these changes would lower the $\delta^{13}\text{C}$ value of CPDW.

Pacific deep-water temperatures cooled slightly between ~ 7 and 6 Ma, which may have been related to Antarctic cooling and the associated changes in deep-water formation (i.e. bottom-water formed near/under ice shelved after 6.6 Ma was colder than bottom-water formed before 6.6 Ma). Deep-water did not cool at site 704 at this time, which suggests bottom water temperatures in the Pacific at site 849 may have been more affected by Antarctic cooling than mid-depth water in the South Atlantic.

The Southern Ocean remained in Mode A for an extended interval between 6.6 and 3.6 Ma (Figure 4-2). Mean $\delta^{13}\text{C}$ values in the Southern Ocean during this time were near the Holocene value of CPDW (0.4‰), which suggests the relative proportion of NCW present in the Southern Ocean was similar to, or slightly lower, than the modern (Holocene $\delta^{13}\text{C}$ value at site 1090 is 0.5‰). Based on benthic $\delta^{18}\text{O}$ and $\delta^{13}\text{C}$ gradients from the Ceara Rise, Billups et al. [1998] suggested a greater production of NCW than today during the mid-Pliocene between 4.2 and 3.7 Ma. The carbon isotopic records from South Atlantic at site 704 and nearby site 1092 [Andersson, 2002] do not support increased influence of NCW between 4.3 and 3.7 Ma, however. In fact, the Southern Ocean records indicate a greater proportion of NCW after 3.6 Ma than between 4.2 and 3.7 Ma. If NCW increased as interpreted from the Ceara Rise, then it was not great enough to influence CPDW in the Southern Ocean.

While the Southern Ocean was in circulation Mode A, oxygen isotopic values decreased in both the Southern Ocean and the deep Pacific at ~ 6 Ma. In the Southern

Ocean, the increase was relatively brief, lasting ~0.5 myrs. In the deep Pacific, however, the increase was the beginning of a long-term trend toward lower values. This may have been related to changes in oceanic circulation patterns associated with the uplift of the Isthmus of Panama during the early and middle Pliocene (between ~6 and 4 Ma) [Lear et al., 2003]. The Central American Seaway (CAS) was closed to deep-water flow since the middle to late Miocene [Droxler et al., 1998; Lyle, 1995]. However, continued shoaling reached a critical point between 4.7 and 4.2 Ma that changed both surface flow and deep-water formation in the North Atlantic [Haug et al., 2001]. By 4.6 Ma, deep-water ventilation in the North Atlantic began to increase, presumably due to increasing transport of warm, saline surface waters into the North Atlantic, which enhanced NCW production [Haug and Tiedemann, 1998; Haug et al., 2001]. The influx of heat brought by the transport of warm, saline surface waters into the North Atlantic after ~4.2 Ma may have contributed to boreal warmth during the middle Pliocene [Berger and Wefer, 1996], which led to deep-water warming in the North Atlantic. Oxygen isotopic values of deep water in the Pacific decreased as global ice volumes declined due to Northern Hemisphere warmth [Fronval and Jansen, 1996; Lear et al., 2003]. Oxygen isotopic values in the Southern Ocean did not change significantly because of the competing effects of decreased global ice volume (decreased $\delta^{18}\text{O}$) and cooling in the South Atlantic (increased $\delta^{18}\text{O}$). Enhanced transport of warm, saline surface and near surface water into the North Atlantic would have cooled the South Atlantic due to increased heat transport from the South Atlantic into the North Atlantic [so-called "heat piracy"; Berger and Wefer, 1996].

Since ~5.2 Ma, the deep Pacific has been warmer than the Southern Ocean (Figure 4-3). Mix et al. [1995] first noted higher $\delta^{18}\text{O}$ at site 704 relative to Pacific site 849

during the interval between ~4 and 2.6 Ma. Because of the difficulty in accounting for a more dense water mass at 2500 m in the South Atlantic than at 3850 m in the Pacific, Mix et al. [1995] attributed the high $\delta^{18}\text{O}$ values to a problem with the 704 data.

However, high benthic $\delta^{18}\text{O}$ values in the South Atlantic were confirmed by Andersson et al. [2002], who reported $\delta^{18}\text{O}$ values at subantarctic South Atlantic site 1092 (2000 m) were higher than at site 849 between ~2.6 and 4.4 Ma (Figures 4-3 and 4-5). The difference between $\delta^{18}\text{O}$ values in the Southern Ocean and the deep Pacific decreased after 2.6 Ma, but $\delta^{18}\text{O}$ values in the Southern Ocean continued to be higher than in the Pacific during glacial intervals until ~0.6 Ma (Figures 4-3 and 4-5).

Deep-Water Formation During the Middle Pliocene and Pleistocene

At 3.6 Ma, the Southern Ocean deep-water circulation abruptly switched back to a mode that resembled mode D, which is labeled D* (Figure 4-2). Higher $\delta^{13}\text{C}$ values in the Southern Ocean signaled a marked decrease in the nutrient content of this deep-water [Hodell and Venz, 1992; Andersson, 2002]. The carbon isotopic increase in the Southern Ocean occurred at the same time as increases in Caribbean $\delta^{13}\text{C}$ values and North Atlantic carbonate preservation, which led Haug and Tiedemann [1998] to suggest a maximum in NADW production. The interval between 3.6 and 2.7 Ma may represent the time of "optimal" NADW formation when the closure of the CAS promoted the retention of warm, saline surface waters in the North Atlantic while the continued overall climate cooling lowered the temperature of surface waters sufficiently for deep convection [Berger and Wefer, 1996]. An increase in the relative flux of NADW into the Southern Ocean could account for the increased $\delta^{13}\text{C}$ value of CPDW. Alternatively, a higher $\delta^{13}\text{C}$ value of CPDW at 3.6 Ma could have been due to a change in deep-water formation in

the Antarctic that resulted in higher preformed $\delta^{13}\text{C}$ values and greater ventilation of deep-water in the Southern Ocean. In this scenario, the Southern Ocean switched at 3.6 Ma to a late Miocene mode of deep-water formation at the end of a long interval of relative warmth during the mid-Pliocene between ~ 4.3 and 3.4 Ma (Figure 4-5b) [Dowsett and Cronin, 1990; Crowley, 1991]. Extended Pliocene warmth and reduced sea ice extent similar to the conditions between ~ 9 and 6.6 Ma may have resulted in higher $\delta^{13}\text{C}$ values for CPDW, as in the late Miocene. Benthic $\delta^{18}\text{O}$ values in the Atlantic and Pacific began to increase after ~ 3.0 Ma, indicating deep-water cooling and increases in global ice volume. The Southern Ocean, however, remained in deep-water circulation mode D* until 2.7 Ma. During this interval of the Pliocene (between 3.6 and 2.7 Ma), benthic $\delta^{13}\text{C}$ and $\delta^{18}\text{O}$ records from the Southern Ocean became negatively correlated, suggesting a stronger coupling between deep-water circulation and climate (Table 4-4, Figure 4-7).

Deep-water formation in the Southern Ocean changed from mode D* to C at 2.7 Ma with a marked decrease in glacial $\delta^{13}\text{C}$ at the same time as $\delta^{18}\text{O}$ values increased (Figures 4-2 and 4-4). The Southern Ocean, at this point, began to alternate between a nutrient-enriched, poorly-ventilated state during glacials and a nutrient-depleted, well-ventilated state during interglacials. Glacial intervals became more severe after 2.7 Ma with greater cooling, sea ice expansion, and northward migration of oceanic fronts [Hodell et al., 1991; Froelich et al., 1991; Hodell and Venz, 1992]. These changes would have reduced air/sea exchange (reduced ventilation to the atmosphere), increased deep-water CO_2 content, and reduced the $\delta^{13}\text{C}$ value of deep-water. The Southern Ocean also experienced reduced input of NADW during glacial periods beginning at 2.7 Ma [Hodell

and Venz, 1992; Venz and Hodell, 2002]. This may have been due to reduced NADW production during glacial periods as glacial severity increased after 2.7 Ma [Raymo et al., 1992].

Another change that occurred in the Southern Ocean at ~2.7 Ma was a shift toward stratification of the high latitude Antarctic surface ocean during glacial periods [Sigman et al., 2004]. In the modern Antarctic, the temperature distribution of cold surface waters over warmer deep waters promotes overturning, while the salinity distribution of fresher surface waters over saltier deep waters promotes stratification. The sensitivity of seawater density to temperature is reduced as temperature nears the freezing point, however. In the glacial Southern Ocean after ~2.7 Ma, temperature was no longer the dominant control on density and stratification became salinity controlled [Sigman et al. [2004]. Sigman et al. [2004] also suggested the switch to glacial stratification may have been a threshold event with gradual cooling of Antarctic surface waters over time and a sudden switch to stratification at 2.7 Ma. Only at 2.7 Ma when a critical temperature threshold was surpassed did glacial benthic $\delta^{13}\text{C}$ values in the Southern Ocean decrease to Pacific values indicating reduced ventilation.

The development of a stable salinity gradient in Antarctic surface or near surface water would have effectively isolated glacial deep-waters in the Southern Ocean from the surface. Today, the Southern Ocean is a source of CO_2 [Broecker and Peng, 1982]. The shift toward stratification of the polar ocean would have enhanced the Southern Ocean's ability to sequester CO_2 , which would have acted as a positive feedback to climate cooling. The strong correlation between benthic $\delta^{13}\text{C}$ and benthic $\delta^{18}\text{O}$ records from the Southern Ocean after 2.7 Ma supports a connection between changes in deep-water circulation and climate (i.e., deep-water ventilation and atmospheric CO_2) (Figure 4-7).

The Southern Ocean remained in Mode C until 1.55 Ma. At 1.55 Ma $\delta^{13}\text{C}$ values in the deep subantarctic South Atlantic decreased again and the Southern Ocean entered Mode B (Figures 4-2 and 4-4) [Hodell and Venz, 1992; Venz and Hodell, 2002]. The deep subantarctic South Atlantic after ~ 1.55 Ma was, except during full interglacial periods, the most nutrient enriched water mass in the deep ocean. Extremely depleted glacial benthic $\delta^{13}\text{C}$ values observed in the subantarctic South Atlantic have not been found in other sectors of the Southern Ocean. This change in glacial deep-water chemistry was likely due to continued Antarctic sea surface cooling, northward expansion of sea ice [Hodell and Venz, 1992; Venz and Hodell, 2002], and enhanced surface water stratification. Glacial reductions in deep-water ventilation after 1.55 Ma were as severe as those during late Pleistocene glacial intervals (Figure 4-4). Northward migration of the zone of maximum wind stress in the Southern Ocean (the westerlies) during glacial intervals may have acted to isolate deep-water circulation in the subantarctic South Atlantic by reducing the northward (wind driven) export of surface and near surface water out of the Southern Ocean [Toggweiler and Samuels, 1993, 1995; Klinck and Smith, 1993]. This, in turn, would have lessened the southward return flow of deep-water from the North Atlantic into the Atlantic sector of the Southern Ocean [Toggweiler and Samuels, 1995].

The changes in deep-water ventilation suggested by $\delta^{13}\text{C}$ records from the South Atlantic may be indicative of a significant increase in Antarctic sea ice extent at 1.55 Ma. An increase in Antarctic sea ice extent is also supported by increased biogenic silica fluxes and lower planktic $\delta^{13}\text{C}$ during glacials at site 704 beginning at 1.55 Ma [Froelich et al., 1991; Hodell and Venz, 1992]. These changes may signify increased cross-frontal

transport of dissolved silica and nutrients as diatoms south of the PFZ were unable to utilize these biolimiting elements due to expanded sea ice cover [Charles et al., 1991]. An expansion of sea ice to a northern limit similar to that of the Last Glacial Maximum would have reduced gas exchange between the deep ocean and the atmosphere [Stephens and Keeling, 2000]. Greater sea ice cover would have changed the vertical density gradient in the Southern Ocean by creating more saline deep-water (through brine rejection during ice formation) and fresher surface water (through melting of sea ice) [Sigman and Boyle, 2000; Stephens and Keeling, 2000; Sigman et al., 2004], and increased the volume of AABW formation [Shin et al., 2003]. The expansion of sea ice northward toward lower latitudes would make the Antarctic highly sensitive to insolation forcing [Shackleton, 2000; Shin et al., 2003]. The effects of ^{13}C -depleted deep-water of southern origin can be seen in the deep North Atlantic after 1.55 Ma as benthic carbon isotopic values at ODP site 607 also decrease during glacial periods after ~ 1.55 Ma [Raymo et al., 1992] (Figure 4-2).

Conclusions

The records from North Atlantic site 982, South Atlantic site 1090, and an extended record from the deep Pacific (site 849) were combined with existing records to create three composite carbon isotopic records that spanned the last 9 myr. Through the late Neogene, benthic $\delta^{13}\text{C}$ in Southern Ocean deep-water and inferred deep-water ventilation decreased as sea ice cover and stratification of Antarctic surface waters increased. Sea ice cover and stratification reduced the upwelling of deep-water to the surface, limited the equilibration of surface water with the atmosphere (i.e. CO_2 outgassing), and altered the process of deep-water formation. Changes in deep-water ventilation during the late Neogene occurred in abrupt steps that likely represented threshold events resulting from

gradual cooling of Antarctic surface waters. The first step occurred in the late Miocene at 6.6 Ma and was associated with late Miocene cooling and possibly the development of the West Antarctic Ice Sheet. The second step occurred at 2.7 Ma and was related to global cooling and the initiation of Northern Hemisphere glaciation. The third step occurred at 1.55 Ma, and was not associated with a large change in global ice volume, but instead likely represents further Antarctic cooling and an increase in the importance of the carbon cycle in the regulation of the climate system [Shackleton, 2000]. Each decrease in ventilation acted as a positive feedback to ongoing climate cooling by increasing deep-ocean CO₂ content and lowering atmospheric pCO₂.

CHAPTER 5 SUMMARY

The objective of this project was to reconstruct oceanic deep-water circulation during the late Neogene using inter-basinal carbon isotopic gradients. This was accomplished in three related studies. The first study focused on developing an improved record from the intermediate depth North Atlantic; the second involved producing a record of $\delta^{13}\text{C}$ variability in the Southern Ocean; the third combined the new records from the North Atlantic, Southern Ocean, and Pacific to examine deep-water circulation changes during the late Neogene and assess their relationship to climate change.

I first characterized the carbon isotopic history of intermediate waters in the northeast North Atlantic using ODP Site 982 (57°N) in 1100 meters of water. The new record from site 982 demonstrated that the intermediate depth North Atlantic was generally well ventilated during both interglacial (by North Atlantic Deep Water, NADW) and glacial periods (by upper NADW, also referred to as Glacial North Atlantic Intermediate Water (GNAIW)) of the late Pleistocene. This contrasts with the deep North Atlantic, which is well ventilated by lower NADW during interglacial intervals but poorly ventilated during glacial intervals owing to reduced production of lower NADW [Raymo et al., 1990b].

Beginning in the mid-Pleistocene, site 982 experienced brief intervals of carbon isotopic depletions during glacial termination and/or the earliest part of interglacial stages, suggesting short intervals of poorly ventilated intermediate waters. These brief isotopic depletions were accompanied by relatively large IRD events and by strong

isotopic depletions in bulk sediment $\delta^{18}\text{O}$ values. The similarity between the magnitude of the IRD events and benthic $\delta^{13}\text{C}$ minima at site 982 and glacial benthic $\delta^{13}\text{C}$ values at site 607 suggests a common mechanism relating variations in glacial production of lower NADW, the magnitude of IRD deposition, and the severity of the decrease in intermediate water ventilation during glacial terminations.

The second study involved reconstructing deep-water circulation history of the Southern Ocean. The benthic $\delta^{13}\text{C}$ record from site 1090 in the subantarctic South Atlantic provided a near-continuous record of changes in Southern Ocean deep-water circulation for the last 2.9 myr. Deep-water circulation patterns were reconstructed by comparing carbon isotopic gradients from site 1090 with other records from the deep North Atlantic and Pacific for the Plio-Pleistocene. The pattern of strongly depleted glacial $\delta^{13}\text{C}$ values in the Southern Ocean, which was typical of the late Pleistocene, began at 1.55 Ma. Glacial $\delta^{13}\text{C}$ values at site 1090 since this time (MIS 52) have been as much as 1‰ lower than those in the deep Pacific, consistent with previous results from site 704 [Hodell and Venz, 1992]. Such depleted $\delta^{13}\text{C}$ values in the Southern Ocean cannot be attributed solely to glacial reduction of NADW. Instead, low $\delta^{13}\text{C}$ values in the Southern Ocean after 1.55 Ma were related to sea ice expansion and enhanced surface water stratification, which limited air/sea exchange of CO_2 and reduced deep-water ventilation. Raymo et al. [1990b, 1997] attributed depleted $\delta^{13}\text{C}$ values at site 607 after 1.5 Ma to strong glacial suppression of Northern Component Water (deep-water originating in the North Atlantic); however, low $\delta^{13}\text{C}$ values at site 607 could also be explained by mixing with Southern Component Water (deep-water originating in the Southern Ocean) with reduced $\delta^{13}\text{C}$ values. Because deep-water composition in the

Atlantic falls on a mixing line between NCW and SCW, changes in the proportion of NCW present in the deep Atlantic at site 607 were recalculated using the carbon isotopic records from site 982 and site 1090 (rather than a deep Pacific record) [i.e., Raymo et al., 1990b]. The general pattern of glacial-to-interglacial change in %NCW in the deep Atlantic were still evident, however, the decreases were not as severe as those calculated previously and the trend toward reduced glacial suppression of NCW during the past 400 kyr, relative to the interval between 0.9 and 0.5 Ma is not evident in the new calculation.

The change in benthic $\delta^{13}\text{C}$ at site 1090 at 1.55 Ma is indicative of a fundamental change in Southern Ocean deep-water circulation. Northward migration of wind fields in the Southern Ocean during glacial intervals after 1.55 Ma may have limited the export of NCW out of the North Atlantic and into the deep Southern Ocean [Toggweiler and Samuels, 1993, 1995a]. Expansion of Antarctic sea ice potentially altered the salinity structure of Southern Ocean surface water, resulting in enhanced density stratification, reduced upwelling, and decreased CO_2 out-gassing from the deep ocean during glacials after 1.55 Ma [Keeling and Stephens, 2001]. These changes in the Southern Ocean provide potential mechanisms for the teleconnective linkage of deep-water circulation between the North and South Atlantic and may have led to tighter interhemispheric coupling observed between site 704 and North Atlantic records after 1.5 Ma [Hodell and Venz, 1992].

Between 1.2 Ma and the present, changes in deep-water circulation occurred that correlate with climatic events associated with the Mid-Pleistocene Transition (MPT) and dominance of the 100-kyr climate cycle of the late Pleistocene. The records from sites 982 and 1090 both contain evidence of change during the MPT. At 1.2 Ma, deep-water circulation changes occurred in the North Atlantic as recorded by an increase in the

carbon isotopic gradient between the intermediate (site 982) and the deep North Atlantic (site 607), indicating greater glacial suppression of NADW [Venz and Hodell, 2002]. At 0.9 Ma (MIS 22), a shift in dominance from the 41-kyr to 100-kyr frequency occurred in climate records accompanied by an increase in global ice volume that initiated "excess" ice growth of the late Pleistocene [Berger and Jansen, 1994; Mudelsee and Schulz, 1997]. The magnitude and pacing of variation in deep-water circulation changed throughout the Atlantic after 0.9 Ma in unison with increased ice volume and strength of the 100-kyr cycle. After 0.9 Ma, benthic $\delta^{13}\text{C}$ values in the Southern Ocean were marked by increased variability, signaling a change in deep-water circulation that included well-ventilated conditions during interglacials and poorly ventilated conditions during glacials.

The final study was designed to place long-term changes in intermediate and deep-water circulation in the North and Southern Ocean into the context of late Neogene climate evolution. This was accomplished using the new carbon isotopic records from the North Atlantic and the Southern Ocean as part of a longer composite record by combining additional data sets available from sites 982, 1090, 704, and 849. Comparison of $\delta^{13}\text{C}$ records from the North Atlantic, the Southern Ocean, and the Pacific revealed a trend toward decreasing deep-water ventilation during the past 9 myr. The Southern Ocean played a dominant role in these changes

Variation in deep-water circulation during the past 9 myr was divided into 4 different modes related to climate-controlled changes in deep-water formation in the Southern Ocean. The modes were based on changes in the inter-basinal carbon isotopic gradient. From 8.5 to 6.6 Ma (Mode D), deep-water in the Southern Ocean was well ventilated, likely by a high- $\delta^{13}\text{C}$ water mass formed in the Southern Ocean. Between 6.6 and 3.6 Ma (Mode A), deep-water in the Southern Ocean became less well ventilated

probably due to a change in the process of deep-water formation related to Antarctic cooling and growth of the West Antarctic Ice Sheet. From 3.6 to 2.7 Ma (Mode D*), ventilation of deep-water in the Southern Ocean again increased, contrary to the long-term trend, and was associated with the unusually warm climate of the mid-Pliocene. Alternatively, Mode D* may have been the result of changes in deep-water production in the North Atlantic at this time. The change to Mode C at 2.7 Ma signaled a marked reduction in deep-water ventilation and involved a threshold response to continued cooling, sea ice expansion, and enhanced glacial stratification of Antarctic surface waters. Another sharp reduction in deep-water ventilation occurred after 1.55 Ma and represents the shift to Mode B (1.55 Ma to present). Glacial deep-water ventilation was further reduced at this time as Antarctic sea surface temperatures continued to cool, permitting northward expansion of sea ice to limits similar to those of glacial maxima of the latest Pleistocene.

Changes in deep-water ventilation inferred from benthic $\delta^{13}\text{C}$ records were related to Antarctic sea surface conditions. As climate cooled during the late Neogene, Antarctic sea ice expanded, surface water stratification was enhanced, and deep-water ventilation decreased. Each step involved a decrease in deep-water ventilation, which sequestered CO_2 in the deep sea and acted as a positive feedback to further climate cooling. After ~2.7 Ma, a strong ocean/climate link developed as changes in deep-water circulation had become an important forcing mechanism for climate change via its role in the carbon cycle [i.e., Shackleton, 2000].

LIST OF REFERENCES

- Aksu, A. E., P. J. Mundie, S. A. Macko, and A. de Vernal, Upper Cenozoic history of the Labrador Sea, Baffin Bay, and the Arctic Ocean: a paleoclimatic and paleoceanographic summary, *Paleoceanography*, 3, 519-538, 1988.
- Allen, C. P., and D. A. Warnke, History of ice rafting at Leg 114 sites, Subantarctic/South Atlantic, *Proc. Ocean Drill. Program, Sci. Results*, 114, 599-607, 1991.
- Andersson, C., D. A. Warnke, J. E. T. Channell, J. Stoner, and E. Jansen, The mid-Pliocene (4.3-2.6) benthic stable isotope record of the Southern Ocean: ODP sites 1092 and 704, Meteor Rise. *Palaeogeogr. Palaeoclimatol. Palaeoecol.*, 182, 165-181, 2002.
- Becquey, S., and R. Gersonde, Past hydrographic and climatic change in the Subantarctic Zone- A 1.8 M.Y. Record from ODP Site 1090, *Palaeogeogr. Palaeoclimatol. Palaeoecol.*, 182, 221-239, 2002.
- Berger, W. H., and E. Jansen, Mid-Pleistocene climate shift—The Nansen connection, in *The Polar Oceans and Their Role in Shaping the Global Environment*, Geophys. Monogr. Ser. Vol. 85, edited by M. Johannessen, R. D. Muench, and J. E. Overland, pp. 295-311, American Geophysical Union, Washington, DC, 1994.
- Berger, W. H., and G. Wefer, Expeditions into the past, in *The South Atlantic: Present and Past Circulation*, edited by G. Wefer, W. H. Berger, G. Siedler, D. J. Webb, pp. 363-410, Sringer-Verlag, Berlin, Heidelberg, 1996.
- Bertram, C. J., H. Elderfield, N. J. Shackleton, and J. A. MacDonald, Cadmium/calcium and carbon isotope reconstructions of the glacial northeast Atlantic Ocean, *Paleoceanography*, 10, 563-578, 1995.
- Bickert, T., W. B. Curry, and G. Wefer, Late Pliocene to Holocene (2.6 - 0 Ma) western equatorial Atlantic deep-water circulation: Inferences from benthic stable isotopes, *Proc. Ocean Drill. Program, Sci. Result*, 154, 239-253, 1997.
- Billups, K., Late Miocene through early Pliocene deep-water circulation and climate change viewed from the subantarctic South Atlantic, *Palaeogeogr. Palaeoclimatol. Palaeoecol.*, 185, 287-307, 2002.

- Billups, K., A.C. Ravelo, and J. C. Zachos, Early Pliocene Deep Water Circulation in the Western Equatorial Atlantic: Implications for High Latitude Climate Change, *Paleoceanography*, 13, 84-95, 1998.
- Bischof, J. F., The decay of the Barents ice sheet as documented in Nordic seas ice-rafted debris, *Mar. Geol.* 117, 35-55, 1994.
- Bloemendal, J., X. M. Liu, and T. C. Rolph, Correlation of the magnetic susceptibility stratigraphy of Chinese loess and the marine oxygen isotope record: chronological and palaeoclimatic implications, *Earth Planet. Sci. Lett.*, 131, 371-380, 1995.
- Boyle, E. A., The role of vertical nutrient fractionation in controlling late Quaternary atmospheric carbon dioxide, *J. Geophys. Res.*, 93, 15701-15714, 1988.
- Boyle, E. A., and L. Keigwin, North Atlantic thermohaline circulation during the last 20,000 years linked to high-latitude surface temperature, *Nature*, 330, 35-40, 1987.
- Broecker, W. S., The Great Ocean Conveyor, *Oceanography*, 4, 79-89, 1991.
- Broecker, W. S., An oceanographic explanation for the apparent carbon isotope-cadmium discordancy in the glacial Antarctic? *Paleoceanography*, 8, 137-139, 1993.
- Broecker, W. S., and T. H. Peng, *Tracers in the Sea*, Eldigio, Palisades, NY, 1982.
- Broecker, W. S., T. Takahashi, and T. Takahashi, Sources and flow patterns of deep-ocean waters as deduced from potential temperature, salinity, and initial phosphate concentration, *J. Geophys. Res.*, 90, 6925-6939, 1985.
- Broecker, W. S., and G. H. Denton, The role of ocean-atmosphere reorganizations in glacial cycles, *Geochim. Cosmochim. Acta*, 53, 2465-2501, 1989.
- Channell, J. E. T., and B. Lehman, Magnetic stratigraphy of North Atlantic sites 980-984, *Proc. Ocean Drill. Program, Sci. Results*, 162, 113-130, 1999.
- Charles, C. D., and R. G. Fairbanks, Glacial to interglacial changes in the isotopic gradients of Southern Ocean surface water, in *Geological History of the Polar Oceans: Arctic Versus Antarctic*, edited by U. Bleil and J. Thiede, pp. 519-538, Kluwer, Netherlands, 1990.
- Charles, C. D., P. N. Froelich, M. A. Zibello, R. A. Mortlock, and J. J. Morley, Biogenic opal in Southern Ocean sediments over the last 450,000 years: Implications for surface water chemistry and circulation, *Paleoceanography*, 6, 697-728, 1991.
- Charles, C. D., and R. G. Fairbanks, Evidence from Southern Ocean sediments for the effect of North Atlantic deep-water flux on climate, *Nature*, 355, 416-419, 1992.

- Chen, T., J. W. Farrell, D. W. Murray, and W. L. Prell, Timescale and paleoceanographic implications of a 3.6 m.y. oxygen isotope record from the northeast Indian Ocean (Ocean Drilling Program site 758), *Paleoceanography*, *10*, 21-47, 1995.
- Ciesielski, P. F., M. T. Ledbetter, and B. B. Elliot, The development of Antarctic glaciation and the Neogene paleo-environment of the Maurice Ewing Bank, *Mar. Geol.*, *46*, 1-51, 1982.
- Clemens, S. C., D. W. Murray, and W. L. Prell, Nonstationary phase of the Plio-Pleistocene Asian monsoon, *Science*, *274*, 943-948, 1996.
- CLIMAP, The surface of the Ice-Age Earth, *Science*, *191*, 1131-1137, 1976.
- Coplen, T. B., More uncertainty than necessary, *Paleoceanography*, *11*, 369-370, 1996.
- Crowley, T. C., Modeling Pliocene warmth, *Quat. Sci. Rev.*, *10*, 275-282, 1991.
- Crowley, T. J., North Atlantic deep-water cools the southern hemisphere, *Paleoceanography*, *7*, 489-497, 1992.
- Curry, W. B., J. C. Duplessy, L. D. Labeyrie, and N. J. Shackleton, Quaternary deep-water circulation changes in the distribution of $\delta^{13}\text{C}$ of deep-water CO_2 between the last glaciation and the Holocene, *Paleoceanography*, *3*, 317-342, 1988.
- deMenocal, P. B., Plio-Pleistocene African climate, *Science*, *270*, 53-59, 1995.
- deMenocal, P. B., D. W. Oppo, W. L. Prell, Pleistocene $\delta^{13}\text{C}$ variability of North Atlantic Intermediate Waters, *Paleoceanography*, *7*, 229-250, 1992.
- Diekmann, B., and G. Kuhn, Sedimentary record of the mid-Pleistocene climate transition in the southeastern South Atlantic (ODP Site 1090), *Palaeogeogr. Palaeoclimatol. Palaeoecol.*, *182*, 241-258, 2002.
- Dowsett H. J., and T. M. Cronin, High eustatic sea level during the middle Pliocene: Evidence from the southeastern U.S. Atlantic Coastal Plain, *Geology*, *18*, 435-438, 1990.
- Droxler, A. W., K. Burke, A. D. Cunningham, A. C. Hine, E. Rosencrantz, D. S. Duncan, P. Hallock, and E. Robinson, Caribbean constraints on circulation between Atlantic and Pacific Oceans over the past 40 million years, in *Tectonic Boundary Conditions for Climate Reconstructions*, edited by T. J. Crowley and K. C. Burke, pp 169-191, Oxford University Press, New York, 1998.
- Duplessy, J. C., N. J. Shackleton, R. G. Fairbanks, L. Labeyrie, D. W. Oppo, and N. Kallel, Deepwater source variations during the last climatic cycle and their impact on the global deepwater circulation, *Paleoceanography*, *7*, 343-360, 1988.

- Duplessy, J.C., L. Labeyrie, A. Juillet-Leclerc, F. Maitre, J. Duprat, and M. Sarnthein, Surface salinity reconstruction of the North Atlantic Ocean during the last glacial maximum, *Oceanol. Acta*, 14, 311-324, 1991.
- Elderfield, H., and E. M. Rickaby, Oceanic Cd/P ratio and nutrient utilization in the glacial Southern Ocean, *Nature*, 405, 305-310, 2000.
- Engleman, E. E., L. L. Jackson, and D. R. Norton, Determination of carbonate carbon in geological materials by coulometric titration, *Chem. Geol.*, 53, 125-128, 1985.
- Fillon, R. H., Northwest Labrador Sea stratigraphy, sand input and paleoceanography during the last 160,000 years, in *Quaternary Environments: Eastern Canadian Arctic, Baffin Bay, and Western Greenland*, edited by J. T. Andrews, pp. 211-247, Allen and Unwin, Boston, 1985.
- Fillon, R. H., and J. C. Duplessy, Labrador Sea bio-, tephro, oxygen isotopic stratigraphy and Late Quaternary paleoceanographic trends, *Can. J. Earth Sci.*, 17, 831-854, 1980.
- Flower, B. P., D. W. Oppo, K. A. Venz, D. A. Hodell, J. F. McManus, and J. Cullen, North Atlantic intermediate- to deep water circulation and nutrient redistribution during the past 1 m.y., *Paleoceanography*, 15, 388-403, 2000.
- Francois, R., M. A. Altabet, E. F. Yu, D. M. Sigman, M. P. Bacon, M. Frank, G. Bohrmann, G. Bareille, and L. D. Labeyrie, Contributions of Southern Ocean surface water stratification to low atmospheric CO₂ concentrations during the last glacial period, *Nature*, 389, 929-935, 1997.
- Frank, M., Whiteley, N., Kasten, S., Hein, J., and O'Nions, K., North Atlantic Deep Water export to the Southern Ocean over the past 14 myr: Evidence from Nd and Pb isotopes in ferromanganese crusts, *Paleoceanography*, 17, 10.1029/2000PA00606, 2002.
- Froelich, P. N., P. N. Malone, D. A. Hodell, P. F. Cielski, D. A. Warnke, F. Westall, E. A. Hailwood, D.C. Nobes, J. Fenner, J. Mienert, C. J. Mwenifumbo, and D. W. Muller, Biogenic opal and carbonate accumulation rates in the subantarctic South Atlantic: The late Neogene of Meteor Rise site 704, *Proc. Ocean Drill. Program, Sci. Results*, 114, 515-550, 1991.
- Fronval, T., and E. Jansen, Late Neogene paleoclimate and paleoceanography in the Iceland-Norwegian Sea: Evidence from the Iceland and Voring Plateaus, *Proc. Ocean Drill. Program, Sci. Results*, 151, 455-468, 1996.
- Gersonde, R., D. A. Hodell, P. Blum, and Leg 177 Scientific Shipboard Party, Site 1090, *Proc. Ocean Drill. Prog., Initial Rep.*, 177, 1-101, 1999.

- Gordon, A. L., Oceanography of Antarctic Waters, in *Antarctic Oceanology*, Antarctic Research Series v15, edited by J. T. Andrews, pp. 169-203, American Geophysical Union, Washington, DC, 1971.
- Gordon, A.L., Comment on the South Atlantic role in the global circulation, in *The South Atlantic: Present and Past Circulation*, edited by G. Wefer, W. H. Berger, G. Siedler, D. J. Webb, pp. 50-65, Springer-Verlag, Berlin, Heidelberg, 1996.
- Gordon, A. L., and J. C. Comiso, Polynyas in the Southern Ocean, *Sci. Am.*, 257, 90-97, 1988.
- Grousset, F. E., L. Labeyrie, J. A. Sinko, M. Cremer, G. Bond, J. Duprat, E. Cortijo, and S. Huon, Patterns of ice rafted debris in the glacial North Atlantic (40° - 55°N), *Paleoceanography*, 8, 175-192, 1993.
- Graham, D., B.H. Corliss, M.L. Bender, and L.D. Keigwin, Carbon and oxygen isotopic disequilibria of recent deep-sea benthic foraminifera, *Marine Micropaleontology*, 6, 483-497, 1981.
- Haug, G. H., and R. Tiedemann, Effect of the formation of the Isthmus of Panama on Atlantic Ocean thermohaline circulation, *Nature*, 393, 673-676, 1998.
- Haug, G. H., R. Tiedemann, R. Zahn, and A. C. Ravelo, Role of Panama uplift on oceanic freshwater balance, *Geology*, 29, 207-210, 2001.
- Hebbeln, D., T. Dokken, E. S. Andersen, M. Hald, and A. Elverhoi, Moisture supply for northern ice-sheet growth during the Last Glacial Maximum, *Nature*, 370, 357-359, 1994.
- Henrich, R., Glacial/Interglacial cycles in the Norwegian Sea: Sedimentology, paleoceanography, and evolution of late Pliocene to Quaternary Northern Hemisphere climate, *Proc. Ocean Drill. Program, Sci. Results*, 104, 189-216. 1989.
- Henrich, R., K.-H. Baumann, R. Huber, and H. Meggers, Carbonate preservation records of the past 3 myr in the Norwegian-Greenland Sea and the northern North Atlantic: implications for the history of NADW production, *Marine Geology*, 184, 17-39, 2002.
- Hillare-Marcel, C., A. de Vernal, G. Bilodeau, and G. Wu, Isotope stratigraphy, sedimentation rates, deep circulation, and carbonate events in the Labrador Sea during the last ~200 ka, *Can. J. Earth Sci.*, 31, 63-89, 1994.
- Hodell, D. A., Late Pleistocene paleoceanography of the South Atlantic sector of the Southern Ocean: Ocean Drilling Program Hole 704A, *Paleoceanography*, 8, 47-67, 1993.

- Hodell, D. A. and K. A. Venz, Toward a high-resolution stable isotopic record of the Southern Ocean during the Plio-Pleistocene (4.8 to 0.8 Ma), in *The Antarctic Paleoenvironment: A Perspective on Global Change, Part I*, *Antarc. Res. Ser.* 56, edited by J. P. Kennett and D. A. Warnke, pp. 265-310, American Geophysical Union, Washington, DC, 1992.
- Hodell, D. A., C. D. Charles, and U. S. Ninnemann, Comparison of interglacial stages in the South Atlantic sector of the southern ocean for the past 450 kyr: implications for Marine Isotope Stage (MIS) 11, *Global Planet. Change*, 24, 7-26. 2000.
- Hodell, D. A., J. H. Curtis, F. J. Sierro, and M. E. Raymo, Correlation of late Miocene to early Pliocene sequences between the Mediterranean and North Atlantic, *Paleoceanography*, 16, 164-178, 2001.
- Hodell, D. A., C. D. Charles, and F. J. Sierro, Late Pleistocene evolution of the ocean's carbonate system, *Earth Planet. Sci. Letters*, 192, 109-124, 2002.
- Hodell, D. A., K. A. Venz, C. D. Charles, and U. S. Ninnemann, Pleistocene vertical carbon isotopic gradients in the South Atlantic sector of the Southern Ocean, *Geochem. Geophys. Geosyst.*, 4(1). 1004. doi:10.1029/2002GC000367.2003., 2003a.
- Hodell, D. A., K. A. Venz, C. D. Charles, and F. J. Sierro, The mid-Brunhes transition in ODP sites 1089 and 1090, in *Earth's Climate and Orbital Eccentricity: The Marine Isotope Stage 11 Question*, edited by A. W. Droxler, R. Z. Poore, and L. H. Burckle, pp. 113-129, AGU Geophysical Monograph 137, American Geophysical Union, Washington, DC, 2003b.
- Hulbe, C. L., An ice shelf mechanism for Heinrich layer production, *Paleoceanography*, 12, 711-717. 1997.
- Imbrie, J., J. D. Hays, D. G. Martison, A. McIntyre, A. C. Mix, J. J. Morley, N. G. Pisias, W. L. Prell, and N. J. Shackleton, The orbital theory of Pleistocene climate: Support from a revised chronology of marine $\delta^{18}\text{O}$ record, in *Milankovitch and Climate*, edited by A. L. Berger, J. Imbrie, J. Hays, G. Kukla, and B. Saltzman, pp. 269-305, NATO ASI Series 126 D. Riedel, Hingham, Mass., 1984.
- Imbrie, J., E. A. Boyle, S. C. Clemens, A. Duffy, W. R. Howard, G. Kukla, J. Kutzbach, D. G. Martinson, A. McIntyre, A. C. Mix, B. Molino, J. J. Morley, L. C. Peterson, N. G. Pisias, W. L. Prell, M. E. Raymo, N. J. Shackleton, and J. R. Toggweiler, On the structure and origin of major glacial cycles 1: linear response to Milankovitch forcing, *Paleoceanography*, 7, 701-738, 1992.
- Jansen, E., M. E. Raymo, P. Blum, and Leg 162 Scientific Shipboard Party, Site 982. *Proc. Ocean Drill. Prog., Initial Rep.*, 162, 91-138, 1996.

- Jansen, E., T. Fronval, F. Rack, and J. E. T. Channell, Pliocene-Pleistocene ice rafting history and cyclicity in the Nordic Seas during the last 3.5 myr, *Paleoceanography*, *15*, 709-721, 2000.
- Jones, G. A., and L. D. Keigwin, Evidence from Fram Strait (78°N) for early deglaciation, *Nature*, *336*, 56-59, 1988.
- Kawase, M, and J. L. Sarmiento, Circulation and nutrients in middepth Atlantic waters, *J. Geophys. Res.* *91*, 9748-9770, 1986.
- Keeling, R., and B. Stephens, Antarctic sea ice and the control of Pleistocene climate instability, *Paleoceanography*, *16*, 112-131, 2001.
- Keigwin, L. D., Late Cenozoic stable isotope stratigraphy and paleoceanography of DSDP sites from the east equatorial and central north Pacific Ocean. *Earth Planet. Sci. Lett.*, *45*, 361-382, 1979.
- Keigwin, L. D., North Pacific deep-water formation during the latest glaciation, *Nature*, *330*, 362-364, 1987.
- Keigwin, L. D., Glacial-age hydrography of the far northwest Pacific Ocean, *Paleoceanography*, *13*, 323-339, 1998.
- Kellogg, T. B., Paleoclimatology and paleo-oceanography of the Norwegian and Greenland seas: glacial-interglacial contrasts, *Boreas*, *9*, 115-136, 1980.
- Kennett, J. P., and P. F. Barker, Latest Cretaceous to Cenozoic climate and oceanographic developments in the Weddell Sea, Antarctica: An ocean-drilling perspective. *Proc. Ocean Drill. Program, Sci. Results*, *113*, 937-960, 1990.
- Kroopnick, P. M., The distribution of ^{13}C of $\square\text{CO}_2$ in the world oceans, *Deep-Sea Res.*, *32*, 57-84, 1985.
- Lackschewitz, K. S, and Wallrabe-Adams, H.-J., Composition and origin of volcanic ash zones in late Quaternary sediments from the Reyjanes Ridge: evidence for ash fallout and ice-rafting, *Mar. Geol.*, *136*, 209-224, 1997.
- Lea, D. W., A trace metal perspective on the evolution of Antarctic Circumpolar Deep-water chemistry, *Paleoceanography*, *10*, 733-747, 1995.
- Lear, C. H., Y. Rosenthal, and J. D. Wright, The closing of a seaway: ocean water masses and global climate change, *Earth Planet. Sci. Lett.*, *210*, 425-436, 2003.
- Lehman, S. J., G. A. Jones, L. D. Keigwin, E. S. Anderson, G. Butenko, and S.-R. Ostmo, Initiation of Fennoscandian ice-sheet retreat during the last deglaciation, *Nature*, *349*, 513-516, 1991.

- Lund, D. C., and A. C. Mix, Millennial-scale deep-water oscillations: reflections of the North Atlantic in the deep Pacific from 10 to 60 ka, *Paleoceanography*, 13, 10-19, 1998.
- Lyle, M., K. Dadey, and J. W. Farrel, The late Miocene (11-8 myr) eastern Pacific carbonate crash: Evidence for reorganization of deep-water circulation by the closure of the Panama gateway, *Proc. Ocean Drill. Program, Sci. Results*, 138, 821-838, 1995.
- Mackensen, A., H. W. Hubberten, T. Bickert, G. Fischer, and D. K. Fütterer, The $\delta^{13}\text{C}$ in benthic foraminiferal tests of *Fontbotia Wuellerstorfi* (Schwager) relative to the $\delta^{13}\text{C}$ of dissolved inorganic carbon in Southern Ocean deep-water: Implications for glacial ocean circulation models, *Paleoceanography*, 8, 587-610, 1993.
- Mackensen, A., and T. Bickert, Stable carbon isotopes in benthic foraminifera: Proxies for deep and bottom water circulation and new production, in *Use of Proxies in Paleooceanography: examples from the South Atlantic*, edited by G. Fischer, and G. Wefer, pp. 229-254, Springer-Verlag, New York, 1999.
- Mackensen A., M. Rudolph, and G. Kuhn, Late Pleistocene deep-water circulation in the subantarctic eastern Atlantic, *Global Planet. Change*, 30, 197-229, 2001.
- Manighetti, B., and I. N. McCave, Late glacial and Holocene palaeocurrents around Rockall Bank, NE Atlantic Ocean, *Paleoceanography*, 10, 611-626, 1995.
- Manighetti, B., I. N. McCave, M. Maslin, and N. J. Shackleton, Chronology for climate change: developing age models for the Biogeochemical Ocean Flux Study cores, *Paleoceanography* 10, 513-525, 1995.
- Mantyla, A. W. and J. L. Reid, Abyssal characteristics of the World Ocean waters, *Deep-Sea Res.*, 30, 805-833, 1983.
- Martinson, D. G., N. G. Pisias, J. D. Hays, J. Imbrie, T. C. Moore, and N. J. Shackleton, Age dating and the orbital theory of the ice ages: development of a high-resolution 0 to 300,000-year chronology, *Quat. Res.*, 27, 1-27, 1987.
- McCorkle, D. C., P. A. Martin, D. W. Lea, and G. P. Klinkhammer, Evidence of a dissolution effect on benthic foraminiferal shell chemistry: $\delta^{13}\text{C}$, Cd/Ca, Ba/Ca, Sr/Ca results from the Ontong Java Plateau, *Paleoceanography*, 10, 699-714, 1995.
- McManus, J.F., G.C. Bond, W.S. Broecker, S.M. Higgins, and M.Q. Fleischer, Heinrich events associated with glacial terminations, *EOS Trans. AGU* 75 (16), Spring Meet. Suppl., 57, 1994.
- Mix, A. C., N. G. Pisias, W. Rugh, J. Wilson, A. Morey, and T. K. Hagelberg, Benthic foraminifer stable isotope record from site 849 (0-5 Ma): local and global climate changes, *Proc. Ocean Drill. Program, Sci. Result*, 138, 371-412, 1995.

- Mudelsee, M., and M. Schultz, The Mid-Pleistocene climate transition: onset of 100 ka cycle lags ice volume build-up by 280 ka, *Earth Planet. Sci. Lett.*, 151, 117-123, 1997.
- Muller, D. W., D. A. Hodell, and P. F. Ciesielski, Late Miocene to earliest Pliocene (9.8-4.5 Ma) paleoceanography of the subantarctic southeast Atlantic: Stable isotopic, sedimentologic, and microfossil evidence. *Proc. Ocean Drill. Program, Sci. Results*, 114, 459-474, 1991.
- Oppo, D. W., and R. G. Fairbanks, Variability in the deep and intermediate water circulation of the Atlantic Ocean: Northern Hemisphere modulation of the Southern Ocean, *Earth Planet. Sci. Lett.*, 86, 1-15, 1987.
- Oppo, D. W., R. G. Fairbanks, A. L. Gordan, and N. J. Shackleton, Late Pleistocene Southern Ocean $\delta^{13}\text{C}$ variability, *Paleoceanography*, 5, 43-54, 1990.
- Oppo, D. W., and S. J. Lehman, Mid-depth circulation of the subpolar North Atlantic during the last glacial maximum, *Science*, 259, 1148-1152, 1993.
- Oppo, D. W., and Y. Rosenthal, Cd/Ca changes in a deep Cape Basin core over the past 730,000 years: Response of circumpolar deep-water variability to northern hemisphere ice sheet melting? *Paleoceanography*, 9, 661-675, 1994.
- Oppo, D. W., M. E. Raymo, G. P. Lohmann, A. C. Mix, J. D. Wright, and W. L. Prell, A $\delta^{13}\text{C}$ record of Upper North Atlantic Deep-water during the past 2.6 million years, *Paleoceanography* 10, 373-394, 1995.
- Oppo, D. W., M. Horowitz, and S. J. Lehman, Marine core evidence for reduced deep-water production during Termination II followed by a relatively stable substage 5e (Eemian), *Paleoceanography*, 12, 51-63, 1997.
- Oppo, D.W., J.F. McManus, and J.L. Cullen, Abrupt climate events 500,000 to 340,000 years ago: Evidence from subpolar North Atlantic sediments, *Science*, 279, 1335-1338, 1998.
- Paillard, D., L. Labeyrie, and P. Yiou, Macintosh program performs time-series analysis, *Eos*, 77, 379, 1996.
- Poore, R. Z., and W. K. Berggen, Late Cenozoic planktonic foraminiferal biostratigraphy and paleoclimatology of Hatton-Rockall Basin: DSDP Site 116, *J. Foramin. Res.*, 5, 270-293, 1975.
- Rasmussen, T. L., T. C. E. van Weering, and L. Labeyrie, High resolution stratigraphy of the Faeroe-Shetland Channel and its relation to North Atlantic paleoceanography: the last 87 kyr, *Mar. Geol.*, 131, 75-88, 1996.
- Raymo, M.E., The Himalayas, organic carbon burial, and climate in the Miocene, *Paleoceanography*, 9, 399-404, 1994.

- Raymo, M. E., The timing of major climate terminations, *Paleoceanography*, 12, 577-585, 1997.
- Raymo, M. E., W. F. Ruddiman, J. Backman, B. M. Clement, and D. G. Martinson, Late Pliocene variation in northern hemisphere ice sheets and North Atlantic deep-water circulation, *Paleoceanography*, 4, 413-446, 1989.
- Raymo, M. E., D. Rind, and W. F. Ruddiman, Climatic effects of reduced Arctic sea ice limits in the GISS II general circulation model, *Paleoceanography*, 5, 367-382, 1990a.
- Raymo, M. E., W. F. Ruddiman, N. J. Shackleton, and D. W. Oppo, Evolution of Atlantic-Pacific $\delta^{13}\text{C}$ gradients over the last 2.5 m.y, *Earth Planet. Sci. Lett.*, 97, 353-368, 1990b.
- Raymo, M. E., D. A. Hodell, and E. Jansen, Response of deepwater circulation to initiation of Northern Hemisphere glaciation (3-2 Ma), *Paleoceanography*, 7, 645-672, 1992.
- Raymo, M. E., D. W. Oppo, and W. Curry, The mid-Pleistocene climate transition: A deep sea carbon isotopic prospective, *Paleoceanography*, 12, 546-559, 1997.
- Rhamstorf, S., and M. England, Influence of Southern Hemisphere winds on North Atlantic deep-water flow, *J. Phys. Oceanogr.*, 27, 2040-2054, 1997.
- Robinson, S. G., M. A. Maslin, and I. N. McCave, Magnetic susceptibility variations in Upper Pleistocene deep-sea sediments of the NE Atlantic: implications for ice rafting and paleocirculation at the last glacial maximum, *Paleoceanography*, 10, 221-250, 1995.
- Rosenthal, Y., E. A. Boyle, and L. Labeyrie, Last glacial maximum paleochemistry and deepwater circulation in the Southern Ocean: Evidence from foraminiferal cadmium, *Paleoceanography*, 12, 787-796, 1997.
- Ruddiman, W. F., Late Quaternary deposition of ice-rafted sand in the subpolar North Atlantic (lat. 40° to 65°N), *Geol. Soc. Am. Bull.*, 88, 1813-1827, 1977.
- Ruddiman, W. F., M. E. Raymo, D. Martinson, B. Clement, and J. Backman, Pleistocene evolution: Northern Hemisphere ice sheets and North Atlantic ocean, *Paleoceanography*, 4, 353-412, 1989.
- Rutherford, S., and S. D'Hondt, Early onset and tropical forcing of 100,000-year Pleistocene glacial cycles, *Nature*, 408, 72-75, 2000.
- Sarnthein, M., and R. Tiedemann, Younger Dryas-style cooling events at glacial terminations I-VI at ODP site 658: associated benthic $\delta^{13}\text{C}$ anomalies constrain meltwater hypothesis, *Paleoceanography*, 5, 1041-1055, 1990.

- Sarnthein, M., K. Winn, S. Jung, J. C. Duplessy, L. Labeyrie, H. Erlenkeuser, and G. Ganssen, Changes in east Atlantic deepwater circulation over the last 30,000 years: eight time slice reconstructions, *Paleoceanography*, 9, 209-267, 1994.
- Shackleton, N. J., The 100,000-year ice-age cycle identified and found to lag temperature, carbon dioxide, and orbital eccentricity, *Science*, 289, 1897-1902, 2000.
- Shackleton, N. J., and M. A. Hall, Oxygen and carbon isotope stratigraphy of Deep Sea Drilling Project Hole 552A: Plio-Pleistocene glacial history. *Proc. Ocean Drill. Prog., Initial Rep.*, 81, 599-609, 1984.
- Shackleton, N.J., and N.G., Pisias, Atmospheric carbon dioxide, orbital forcing, and climate, in *The Carbon Cycle and Atmospheric CO₂: Natural Variations Archean to Present*, *Geophys. Monogr. Ser. vol. 32*, edited by E. Sundquist and W. Broecker, pp.412-417, AGU, Washinton, D.C., 1985.
- Shackleton, N., A. Berger, and W. Peltier, An alternative astronomical calibration of the lower Pleistocene timescale based on ODP site 677, *T. Roy. Soc. Edin.-Earth.*, 81, 251-261, 1990.
- Shackleton, N. J., S. Crowhurst, T. Hagelberg, N. G. Pisias, and D. A. Schneider, A new late Neogene time scale: Application to Leg 138 sites, *Proc. ODP, Sci. Res. 138*, College Station, TX, 73-101, 1995.
- Shin, S.-I., Liu, Z., Otto-Bliesner, B. L., Kutzbach, J. E., and Vavrus, S. J., Southern Ocean sea-ice control of the glacial North Atlantic thermohaline circulation, *Geophys. Res. Lett.*, 30, 1096, doi:10.1029/2002GL015513, 2003.
- Sigman, D., and E. Boyle, Glacial/interglacial variations in atmospheric carbon dioxide, *Nature*, 407, 859-869, 2000.
- Sigman, D. M., S. L. Jaccard, and G. Haug, Polar ocean stratification in a cold climate, *Nature*, 428, 59-63, 2004.
- Sikes, E. L., L. D. Keigwin, and W. B. Curry, Pliocene paleoceanography: Circulation and oceanographic changes associated with the 2.4 Ma glacial event, *Paleoceanography*, 6, 245-257, 1991.
- Stanton, C. L., History of ice-rafted debris at ODP Leg 162, Site 982 in the North Atlantic for the past 2 million years, Unpublished M.S. Thesis, California State University, Hayward, 1997.
- Stephens, B., and R. Keeling, The influence of Antarctic sea ice on glacial-interglacial CO₂ variations, *Nature*, 404, 171-174, 2000.

- Thiede, J., A. Winkler, T. Wolf-Welling, O. Eldholm, A. M. Myhre, K.-H. Baumann, R. Henrich, R. Stein, Late Ceneozoic history of the polar North Atlantic: Results from ocean drilling, *Quaternary Sci. Rev.*, *17*, 185-208, 1998.
- Toggweiler, J. R., Variation of atmospheric CO₂ by ventilation of the ocean's deepest water, *Paleoceanography*, *14*, 571-588, 1999.
- Toggweiler, J. R., and B. Samuels, Is the magnitude of the deep outflow from the Atlantic Ocean actually governed by southern hemisphere winds? in *The Global Carbon Cycle*, edited by M. Heimann, pp. 303-331, Springer-Verlag, Berlin, 1993a.
- Toggweiler, J. R., and B. Samuels, New radiocarbon constraints on the upwelling of abyssal water to the ocean's surface, in *The Global Carbon Cycle*, edited by M. Heimann, pp. 333-366, Springer-Verlag, Berlin, 1993b.
- Toggweiler, J. R., and B. Samuels, Effect of the Drake Passage on the global thermohaline circulation, *Deep-Sea Res.*, *42*, 477-500, 1995.
- Venz, K. A., D. A. Hodell, C. Stanton, and D. Warnke, A 1.0 Myr record of Glacial North Atlantic Intermediate Water variability from ODP site 982 in the northeast Atlantic, *Paleoceanography*, *14*, 42-52, 1999.
- Venz, K. A., and D. A. Hodell, New evidence for changes in Plio-Pleistocene deep-water circulation from Southern Ocean ODP Leg 177 site 1090, *Palaeogeogr. Palaeoclimatol. Palaeoecol.*, *182*, 197-220, 2002.
- Veum, T., E. Jansen, M. Arnold, I. Beyer, and J.-C. Duplessy, Water mass exchange between the North Atlantic and the Norwegian Sea during the past 28,000 years, *Nature*, *356*, 783-785, 1992.
- Vidal, L., L. Labeyrie, E. Cortijo, M. Arnold, J.C. Duplessy, E. Michel, S. Becque, and T.C. van Weering, Evidence for changes in the North Atlantic Deep Water linked to meltwater surges during the Heinrich events, *Earth Planet. Sci. Lett.*, *146*, 13-27, 1997.
- Weber, M., and N. Pisias, Spatial and temporal distribution of biogenic carbonate and opal in deep sea sediments from the eastern equatorial Pacific: implications for ocean history since 1.3 Ma, *Earth Planet. Sci. Lett.*, *174*, 59-73, 1999.
- Weinelt, M., M. Sarnthein, U. Pflaumann, H. Schulz, S. Jung, and H. Erlenkeuser, Ice-free Nordic seas during the Last Glacial Maximum? Potential sites of deepwater formation, *Paleoclimates*, *1*, 283-309, 1996.
- Weyl, P. K., The role of the oceans in climatic change: A theory of the ice ages, *Meteorological Monographs*, *8*, 37-62, 1968.

- Williams, D. F., M. A. Sommer, and M.L. Bender, Carbon isotopic composition of Recent planktic foraminifera of the Indian Ocean, *Earth Planet. Sci. Lett.*, 36, 391-403, 1977.
- Wright, J. D., K. G. Miller, and R. G. Fairbanks, Evolution of modern deepwater circulation: Evidence from the late Miocene Southern Ocean, *Paleoceanography*, 6, 275-290, 1991.
- Wright, J. D., K. G. Miller, and R. G. Fairbanks, Early and middle Miocene stable isotopes: implications for deepwater circulation and climate, *Paleoceanography*, 7, 357-389, 1992.
- Zahn, R., M. Sarnthein, and H. Erlenkeuser, Benthic isotope evidence for changes of the Mediterranean outflow during the late Quaternary, *Paleoceanography*, 2, 543-559, 1987.
- Zahn, R., J. Schönfeld, H.-R. Kudrass, M.-H. Park, H. Erlenkeuser, and P. Grootes, Thermohaline instability in the North Atlantic during meltwater events: stable isotope and ice-rafted detritus records from core SO75-26KL, Portuguese margin, *Paleoceanography*, 12, 696-710, 1997.

BIOGRAPHICAL SKETCH

Kathryn Venz Curtis was born on April 28, 1968, in Hamilton, Bermuda. She graduated from Columbia High School in Lake City, Florida, in 1986 and attended the University of Florida where she received her Bachelor of Science in geology in 1990. For graduate work she continued at the University of Florida where her research interests focused on the paleoclimatology and paleoceanography of the Southern Ocean during the Pliocene. She received her Master of Science in 1992 from the Department of Geological Sciences.